



저작자표시-비영리-변경금지 2.0 대한민국

이용자는 아래의 조건을 따르는 경우에 한하여 자유롭게

- 이 저작물을 복제, 배포, 전송, 전시, 공연 및 방송할 수 있습니다.

다음과 같은 조건을 따라야 합니다:



저작자표시. 귀하는 원저작자를 표시하여야 합니다.



비영리. 귀하는 이 저작물을 영리 목적으로 이용할 수 없습니다.



변경금지. 귀하는 이 저작물을 개작, 변형 또는 가공할 수 없습니다.

- 귀하는, 이 저작물의 재이용이나 배포의 경우, 이 저작물에 적용된 이용허락조건을 명확하게 나타내어야 합니다.
- 저작권자로부터 별도의 허가를 받으면 이러한 조건들은 적용되지 않습니다.

저작권법에 따른 이용자의 권리는 위의 내용에 의하여 영향을 받지 않습니다.

이것은 [이용허락규약\(Legal Code\)](#)을 이해하기 쉽게 요약한 것입니다.

[Disclaimer](#)

**A THESIS
FOR THE DEGREE OF DOCTOR OF PHILOSOPHY**

**Modelling distribution and dispersal phenology of
Metcalfa pruinosa (Hemiptera: Flatidae)**

미국선녀벌레의 분포 및 분산 이동 시기 모델링

**BY
Min-Jung Kim**

**ENTOMOLOGY PROGRAM
DEPARTMENT OF AGRICULTURAL BIOTECHNOLOGY
SEOUL NATIONAL UNIVERSITY**

August 2020

**Modelling distribution and dispersal phenology of
Metcalfa pruinosa (Hemiptera: Flatidae)**

**UNDER THE DIRECTION OF ADVISER JOON-HO LEE
SUBMITTED TO THE FACULTY OF THE GRADUATE SCHOOL
OF SEOUL NATIONAL UNIVERSITY**

**BY
Min-Jung Kim**

**ENTOMOLOGY PROGRAM
DEPARTMENT OF AGRICULTURAL BIOTECHNOLOGY
SEOUL NATIONAL UNIVERSITY**

August, 2020

**APPROVED AS A QUALIFIED THESIS OF MIN-JUNG KIM
FOR THE DEGREE OF DOCTOR OF PHILOSOPHY
BY THE COMMITTEE MEMBERS**

| | | |
|----------------------|-----------------------|-------|
| Chairman | Seunghwan Lee | _____ |
| Vice Chairman | Joon-Ho Lee | _____ |
| Member | Chang-Gyu Park | _____ |
| Member | Chuleui Jung | _____ |
| Member | Jun-Hyung Tak | _____ |

ABSTRACT

Modelling distribution and dispersal phenology of *Metcalfa pruinosa* (Hemiptera: Flatidae)

Min-Jung Kim

Department of Agricultural Biotechnology

Seoul National University

The citrus flatid planthopper, *Metcalfa pruinosa* (Say) has showed rapid establishment and spread through Korea since its first detection in 2009, causing serious economic damage to various crops and wild plants. Thus, the necessity for management of *M. pruinosa* has been increasing in Korea. This study was conducted to provide the ecological information that could help efficient management for *M. pruinosa*. The objectives of this study were (1) to determine the factors responsible for the fast expansion of *M. pruinosa* in Korea and identify its spreading process, (2) to predict the current potential distribution and future habitat suitability of *M. pruinosa* in Korea, (3) to predict

phenology of young nymphs of *M. pruinosa* (4) to understand population dynamics of *M. pruinosa* nymphs within crop fields.

In order to verify cause of fast spreading of *M. pruinosa*, and predict its current potential distribution, several statistical modelling methods and MaxEnt software were used with spatio-temporal occurrence information in Korea. Results showed that range expansion of *M. pruinosa* in Korea were significantly different from a pattern of continuous spreading mechanism. In early spread phase in 2013, traffic volume, one of human mediated factors, was the most important in explaining *M. pruinosa* distribution. Traffic volume of the relative pre-occupied habitat in 2013 was also significantly higher than the one lately occupied in 2017. According to these results, traffic volume was strongly proposed as a main reason of rapid spreading of *M. pruinosa* in Korea, causing long-distance dispersal in stratified spread mechanism. However, the mean temperature in the warmest quarter became the most important environmental factor in current phase in 2017, and rather the distribution could be better explained without traffic factor. The current distribution model was finally developed using three bioclimatic variables, except for traffic variable. This final model was used to predict future habitat suitability under

climate change scenario (RCP 8.5.) In 2030s and 2050s, most parts of Korea except for mountainous area and southern parts were estimated to be suitable for *M. pruinosa* to be established.

The distribution models of egg hatching time and first instar falling time of *M. pruinosa* from host trees were developed based on degree-days with a lower development threshold of 10.1 °C. January 1, commonly used in degree-day models, and March 18, an empirical date estimated in this study were examined as starting points for degree-day accumulation. As a result, the egg hatching and first instar falling models both used January 1 because the starting point performed better. From simulation result projected by these two models, the optimal time range for chemical sprays targeting the tree hosts of *M. pruinosa* were deduced as 423 DD to 474 DD. The control time for nymphs around the trees was suggested by the first instar falling model, along with observations of population density on the ground plants.

The model of nymphal immigration time into crop fields was developed based on degree-days with a lower development threshold of 10.1 °C. In addition, survival rate of the nymphs until adult emergence was observed in field cages, and proportions of stage

transition from the nymphs to the adults were modelled based on degree-days. Finally, a population simulation model for *M. pruinosa* nymphs in crop fields was constructed by integrating following factors: (1) beginning time of plants growing, (2) amount of immigrant nymphs, (3) survival rate in the crop fields, and (4) proportion of stage transition to the adults. There was a good agreement between the population model output and the nymphal abundance in various crop cultivation conditions. After 205.5 DD, the beginning time of plants growing was important in determining nymphal density in crop fields. However, even with the delayed beginning of crop cultivation, the times of peak density did not change as much as delayed time. After 800 DD, the population of *M. pruinosa* within crop fields was predicted to gradually decrease due to emigration of the adults.

Key words: *Metcalfa pruinosa*, Habitat suitability, Stratified spread, egg hatching, first instar falling, immigration risk, population simulation, optimal control timing

Student number: 2017-24294

List of Contents

| | |
|--|----|
| Abstract | i |
| List of Contents | v |
| List of Tables | ix |
| List of Figures | xi |
| | |
| Chapter I . General introduction | 1 |
| 1-1. Distribution and invasion history | 3 |
| 1-2. Life cycle and seasonal occurrence | 8 |
| 1-3. Symptoms of damage and economic impact | 13 |
| 1-4. Invasion stage and management in Korea | 15 |
| 1-5. Objectives of this study | 20 |
| | |
| Chapter II. Current and future distribution of <i>Metcalfa pruinosa</i> in Korea: Reasoning of fast spreading | 23 |
| 2-1. Abstract | 25 |
| 2-2. Introduction | 27 |
| 2-3. Materials and methods | 30 |

| | |
|---|----|
| 2-3-1. Species occurrence data ----- | 30 |
| 2-3-2. Spreading rate and pattern ----- | 31 |
| 2-3-3. Preparation of environmental variables ----- | 33 |
| 2-3-4. Modelling procedure ----- | 35 |
| 2-3-5. Model selection and projection ----- | 38 |
| 2-3-6. Comparison of traffic factor for <i>M. pruinosa</i> occurrence in 2013 and 2017 ----- | 39 |
| 2-4. Results ----- | 42 |
| 2-4-1. Spreading rate and pattern ----- | 42 |
| 2-4-2. Distribution model in 2013 (early spreading phase) --- | 45 |
| 2-4-3. Distribution model in 2017 (current phase) ----- | 45 |
| 2-4-4. Future habitat suitability ----- | 52 |
| 2-4-5. Comparison of traffic factor for <i>M. pruinosa</i> occurrence in 2013 and 2017 ----- | 54 |
| 2-5. Discussion ----- | 55 |

Chapter III. Phenology modelling of egg hatching and first instar

| | |
|--|-----------|
| falling of <i>Metcalfa pruinosa</i> ----- | 65 |
| 3-1. Abstract ----- | 67 |
| 3-2. Introduction ----- | 69 |

| | |
|---|----|
| 3-3. Materials and methods ----- | 73 |
| 3-3-1. Data collection for model development ----- | 73 |
| 3-3-2. Starting point of degree-day models ----- | 78 |
| 3-3-3. Estimation of model parameters ----- | 81 |
| 3-3-4. Validation and accuracy of models ----- | 82 |
| 3-3-5. Change of nymphal density ----- | 84 |
| 3-4. Results ----- | 86 |
| 3-4-1. Starting date of degree-day models ----- | 86 |
| 3-4-2. Egg hatching and first instar falling models ----- | 88 |
| 3-4-3. Change in nymphal density ----- | 94 |
| 3-5. Discussion ----- | 97 |

Chapter IV. Immigration risk and population simulation models

| | |
|--|------------|
| for <i>Metcalfa pruinosa</i> within crop fields ----- | 103 |
| 4-1. Abstract ----- | 105 |
| 4-2. Introduction ----- | 107 |
| 4-3. Materials and methods ----- | 110 |
| 4-3-1. Nymphal immigration model ----- | 110 |
| 4-3-2. Immigration risk of nymphs in crop fields ----- | 115 |
| 4-3-3. Survival rate and development time of the nymphs -- | 119 |

| | |
|---|------------|
| 4-3-4. Stage transition model from the nymph to adult ----- | 122 |
| 4-3-5. Population simulation model for the nymphs within the crop fields ----- | 124 |
| 4-4. Results ----- | 127 |
| 4-4-1. Nymphal immigration model ----- | 127 |
| 4-4-2. Immigration risk of nymphs in crop fields ----- | 129 |
| 4-4-3. Survival rate and development time of the nymphs -- | 132 |
| 4-4-4. Stage transition model from the nymph to adult ----- | 133 |
| 4-4-5. Population simulation model for the nymphs within the crop fields ----- | 136 |
| 4-5. Discussion ----- | 140 |
| Chapter V. General conclusion ----- | 147 |
| 5-1. National management plan ----- | 149 |
| 5-2. Optimal control timing in various landscape ----- | 151 |
| 5-3. Management in crop fields ----- | 152 |
| Literatures Cited ----- | 153 |
| Abstract in Korean ----- | 171 |

List of Tables

Chapter II.

| | |
|---|----|
| Table 1. Summary of developed four models in MaxEnt and values of average AUC and AICc of 2013 and 2017 ----- | 47 |
| Table 2. Table 2. Contribution (%) of environmental variables for each model in 2013 and 2017 ----- | 48 |

Chapter III.

| | |
|--|----|
| Table 1. Description of the study sites and sampling information for model development ----- | 76 |
| Table 2. Estimated parameter values for the distribution model of egg hatching time and first instar falling time of <i>Metcalfa pruinosa</i> - | 89 |
| Table 3. Parameter values of the regression line between the Julian dates predicted by the two groups of models with different starting points, and the accuracy of each group ----- | 90 |
| Table 4. Predicted time (DD) of egg hatching and first instar falling of <i>Metcalfa pruinosa</i> ----- | 93 |

Chapter IV.

| | |
|---|-----|
| Table 1. Description of the study sites and sampling information for the development of a nymphal immigration model of <i>Metcalfa pruinosa</i> in open fields and adult transition model ----- | 113 |
| Table 2. Description of the crop fields and sampling information for validation of immigration risk model for the nymphs ----- | 118 |
| Table 3. Developmental time and emergence rate of <i>Metcalfa pruinosa</i> nymphs in semi-field condition ----- | 121 |
| Table 4. Estimated parameter values used by each sub-model for population model for <i>Metcalfa pruinosa</i> nymphs within crop fields ----- | 135 |

List of Figures

Chapter I.

- Fig. 1. Current global distribution of *Metcalfa pruinosa*. ----- 6
- Fig. 2. Changes in the distribution of *Metcalfa pruinosa* in Korea represented by the first reported year in each administrative area (-Si and -Gun). ----- 7
- Fig. 3. Schematic of *Metcalfa pruinosa* life cycle, change of host plant and behavior according to its developmental stages. ----- 11
- Fig. 4. Photos of *Metcalfa pruinosa* development stages. (a) egg; (b) new-born nymphs; (c) nymphs on herbaceous plants (*Hosta* sp.); (d) exuvia (→) wax filaments and droplets of honeydew (→) produced by the third-instar nymphs; (e) adults gathering on a tree (*Robinia pseudoacacia*) (photo by Kim et al., 2011). ----- 12
- Fig. 5. A series of biological invasion stages, generalized invasion curve, and according phase of management strategies (adapted from Blackburn et al., 2011; Lockwood et al., 2013). ----- 19

Chapter II.

- Fig. 1. (a) Occurrence points of *Metcalfa pruinosa* in Korea in 2009 (●) and 2013 (●) reported in other papers (Kim et al., 2011; Kim and Kim, 2014). Convex hull (■) was drawn by 2013 distribution; (b) Rarefied discovered points of *Metcalfa pruinosa* in 2017 (▲ and ▲) surveyed in this paper. Traffic volume was extracted from points in convex hull and out of convex hull for comparison. --- 41
- Fig. 2. Nearest distances between newly discovered administrative areas in each year from the first invaded administrative areas. Solid line was regression line. The spreading rate of *Metcalfa pruinosa* in Korea was estimated 5.19 ± 1.742 km (Mean \pm SEM) from the slope of regression line. ----- 43
- Fig. 3. Mean distance of all pairs of nearest five administrative areas from one administrative area. Dashed line was calculated in condition of hypothetical continuous spread. ----- 44
- Fig. 4. Potential distribution of *Metcalfa pruinosa* estimated by MaxEnt models in Korea (a) 2013 Climate+Traffic model; (b) 2017 Climate only model. ----- 49
- Fig. 5. Jackknife test for relative importance of selected variables in each model (a) Relative importance of four variables in the 2013

Climate+Traffic model; (b) Relative importance of three variables in the 2017 Climate only model. ----- 50

Fig. 6. Response curve of presence probability of *Metcalfa pruinosa* to environmental variables (a) Mean Traffic Volume per day (2013 Climate+Traffic model); (b) Mean Traffic Volume per day (unselected 2017 Climate+Traffic model); (c) Mean Temperature of Warmest Quarter (2017 Climate only model); (d) Mean Temperature of Coldest Quarter (2017 Climate only model); (e) Annual Precipitation (2017 Climate only model). ----- 51

Fig. 7. Future habitat suitability of *Metcalfa pruinosa* in Korea predicted using RCP 8.5 scenario and 2017 Climate only model. (a) 2030s; (b) 2050s; (c) 2070s; (d) 2090s. ----- 53

Chapter III.

Fig. 1. Installation of clear sticky panel trap to capture the first instar nymphs falling from the trees (a) Front view; (b) Side view; (c) Connector to maintain the width of two rods as the trap width. ----
----- 77

Fig. 2. Estimation of first egg hatching date in (a) Yeoncheon, (b) Seoul, (c) Suwon, and (d) Yesan in 2018, and (e) Yeoncheon, (f)

| | |
|--|----|
| Chuncheon, (g) Seocheon, and (h) Paju in 2019 (●, Observed points; ---, Extrapolation line). ----- | 80 |
| Fig. 3. Coefficient of variation (CV) of the cumulative degree-days (DD) from the potential starting date to the first hatch of <i>Metcalfa pruinosa</i> ; March 18 (◆) produced the lowest CV. ----- | 87 |
| Fig. 4. Distribution model of <i>Metcalfa pruinosa</i> egg hatching time, (DD) from January 1. ----- | 91 |
| Fig. 5. Distribution model of falling time of the first instar nymphs of <i>Metcalfa pruinosa</i> from the trees, (DD) from January 1. The dashed line represents the egg hatching model of <i>Metcalfa pruinosa</i> . ----- | 92 |
| Fig. 6. Simulation model for estimating the relative population density of <i>Metcalfa pruinosa</i> on the trees. The population on the trees was calculated with different moving parameters (p) of the first instar nymph falling from the tree to the ground. The maximum density on the trees was estimated at 423 DD to 474 DD. ----- | 95 |
| Fig. 7. Changes of <i>Metcalfa pruinosa</i> nymph densities on 30 leaves of ground plants relative to the degree days in Chuncheon and Yeoncheon. ----- | 96 |

Chapter IV.

- Fig. 1. Sets of traps with top and bottom heights to capture the immigrant nymphs of *Metcalfa pruinosa* in open fields and on the border of crop fields. (a) Front view; (b) Side view; (c) Photo of a set of traps installed in open field. ----- 114
- Fig. 2. Distribution model of *Metcalfa pruinosa* nymph immigration time (DD) ----- 128
- Fig. 3. Validation of *Metcalfa pruinosa* nymph immigration risk (%) in crop field. The regression line was created to compare 1:1 line, using observed proportions and predicted proportions of field specific immigration risk model. ----- 130
- Fig. 4. Normalized immigration risk (%) models for *Metcalfa pruinosa* nymphs with field specific starting point. Each nymph immigration risk model was created with different parameters t_0 representing the time of the start of plant growing. ----- 131
- Fig. 5. Stage transition model from nymphs to adults of *Metcalfa pruinosa*. The ratio of trap catch rates between nymphs and adults was reflected as a weight for obtaining observed points. ----- 134
- Fig. 6. Population simulation model for estimating relative population density of *Metcalfa pruinosa* nymphs within crop fields. Each

population model was created with different parameters t_0 representing the time of the start of plant growing. ----- 137

Fig. 7. Variations of *Metcalfa pruinosa* nymphal density predicted by population simulation model and observed density in soybean fields in (a) Yenchon in 2017, (b) Jinchon in 2017, (c) Anseong in 2017, (d) Yeoncheon in 2018, (e) Yesan in 2018, (f) Paju in 2019, and in a sesame field in (g) Paju in 2019. The predicted and observed values were scaled against respective peak density of each crop field. In the case of insecticide treatment (✓), the survival rate of the immigrant nymphs until the treatment in the fields was assumed to be zero at this time. ----- 138

Chapter I .
General introduction

1-1. Distribution and invasion history

The citrus flatid planthopper, *Metcalfa pruinosa* (Say, 1830) (Hemiptera: Flatidae), is native to North America (Mead, 2004), but has now invaded non-native countries. In its native regions, *M. pruinosa* has a wide distribution, being found in the East of North America, from Ontario to Florida, and in the Southwest from Texas to Mexico (Mead, 2004) (Fig. 1). *M. pruinosa* was first identified outside of its native regions, in Treviso province, Italy in 1979 (Zangheri and Donadini, 1980) and then, its distribution has expanded out to neighboring countries (Preda and Skolka, 2011). *M. pruinosa* has now successfully established itself in about twenty European countries including Italy, France, Spain, Slovenia, Switzerland, Croatia, Austria, Czech Republic, Greece, Turkey, Hungary, Bulgaria, Serbia, Montenegro, Bosnia Herzegovina, Netherlands, Romania and Russia (Zangheri and Donadini, 1980; Lauterer and Malenovsky, 2002; Mikhajlovic, 2007; Strauss, 2009; Grozea et al., 2011; Preda and Skolka, 2011; Balakhnina et al., 2014; Popova et al., 2019) (Fig. 1). Outside of Europe, this planthopper was first reported in Korea in 2009, the only record of this pest in the Eastern part of the Palearctic regions

(Lee and Wilson, 2010; Kim et al., 2011) (Fig. 1). The introduction of this planthopper into Korea was most likely owing to accidental transportation of horticultural nursery stock infested with *M. pruinosa* eggs from its already established regions (Lauterer, 2002; Kim et al., 2011). A recent study considering the genetic divergence of *M. pruinosa* suggested that the Korean founder population of *M. pruinosa* was most likely introduced via Europe and not directly from its native region, North America (Kwon et al., 2015).

It is unclear precisely when *M. pruinosa* was introduced into each of the non-native countries because invasive insects are, in general, highly undetected at the arrival point of time due to their low population size (Liebhold et al., 2016). Nonetheless, shortly after *M. pruinosa* populations were detected in non-native countries, the planthopper underwent a rapid range expansion and was frequently reported across new regions. In just a few decades, *M. pruinosa* has spread to a national scale in many European countries (Girolami and Conte, 1999; Péntzes and Hári, 2016). This rapid spread of *M. pruinosa* was also observed in Korea, where it was discovered in almost all regions of Korea within 10 years of its initial detection in 2009 (Kim et al., 2011; Kim and Kil, 2014; Kim et al., 2019) (Fig. 2). These

phenomena are speculated to be related to human-mediated activities for several reasons. Firstly, active dispersal of *M. pruinosa* is only applicable across small spatial scales (Strauss, 2010; Preda and Skolka, 2011) as the estimated natural rate of spread of *M. pruinosa* is just 0.2 - 0.5 km/year (Kahrer et al., 2009). Secondly, it is strongly believed that the introduction of *M. pruinosa* into some European countries was a result of the transport of woody plants infested with *M. pruinosa* eggs (Lauterer, 2002; Strauss, 2009). Finally, *M. pruinosa* populations have been commonly found along roadsides, parking sites, and rest areas (Strauss, 2010; Kim and Kil, 2014; Lee et al., 2019a), suggesting that the long distance spread of this insect may have been facilitated by vehicle traffic. In addition, the broad host range (Souliotis et al., 2008; Seo et al., 2019), high environmental adaptability (Strauss, 2010; Byun et al., 2017), lack of natural enemies (Keane and Crawley, 2002), and/or high susceptibility of host plants (Rebek et al., 2008) to *M. pruinosa* may have aided its spread into new regions. A combination of these factors would have influenced the successful establishment of this invasive insect in newly arrived areas. Thus, the introduction and establishment of *M. pruinosa* have persisted as a result of rapid range expansion.

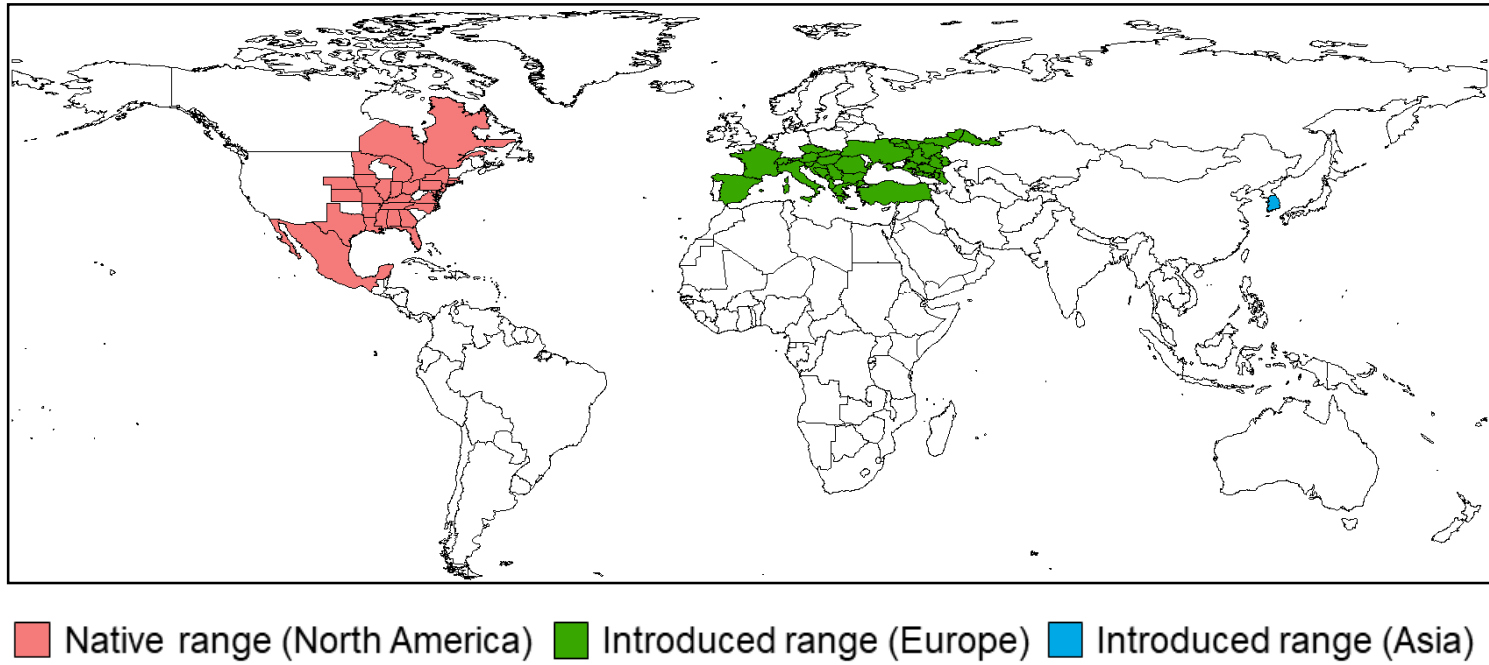


Fig. 1. Current global distribution of *Metcalfa pruinosa*.

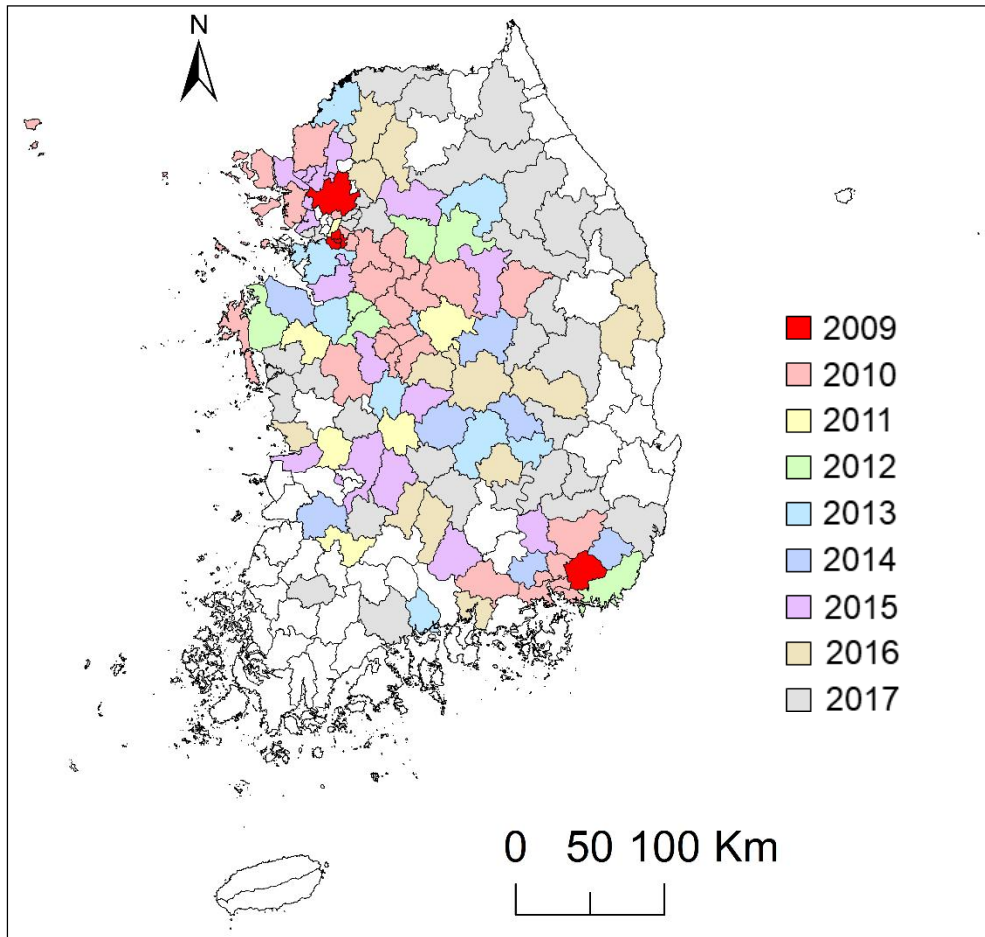


Fig. 2. Changes in the distribution of *Metcalfa pruinosa* in Korea represented by the first reported year in each administrative area (-Si and -Gun).

1-2. Life cycle and seasonal occurrence

The life history of *M. pruinosa* is shown in Fig. 3. *M. pruinosa* is a univoltine species which overwinters as eggs (Dean and Baily, 1961). Eggs are laid from mid-August to September (Yoon et al., 2012) and scattered singly beneath the bark and/or in the cracks of tree branches (Dean and Baily, 1961; Choi et al., 2018). Eggs are approximately 0.8 mm in length (Dean and Baily, 1961; Wilson and McPherson, 1981) (Fig. 4), and are laid on a variety of deciduous tree species in Korea, including, *Acer palmatum*, *Cerasus* spp., *Cornus kousa*, *Cornus officinalis*, *Morus alba*, *Robinia pseudoacacia*, *Zelkova serrata*, and *Ziziphus jujube* (unpublished personal observation). In temperate regions, *M. pruinosa* remains as an egg for over 200 days of the year. Overwintered eggs start to hatch in mid-May (Lucchi, 1994; Lee et al., 2016; Kim et al., 2020).

After eggs hatched in the spring, substantial numbers of nymphs fall from the tree branches and move to nearby herbaceous plants or shrubs (Park et al., 2019; Seo et al., 2019) (Fig. 4). The fallen nymphs disperse into surrounding vegetation around the host trees from which they hatched (Ciampolini et al., 1987). Nymphs have at

least 200 host plant species, including various agricultural and horticultural plant species (Wilson and Lucchi, 2001; Seo et al., 2019). Nymphs suck the xylem and phloem of hosts (Seo et al., 2016), producing copious amounts of honeydew due to a lack of a filter chamber (Wilson and Lucchi, 2007). Growing nymphs produce whitish wax filaments, which cover their bodies as protection from biotic and abiotic stressors and to prevent self-contamination from the honeydew (Lucchi and Mazzoni, 2004). Nymphs develop rapidly in comparison to the long period spent as an egg and emerge into adults approximately two months after hatching (Dean and Bailey, 1961; Wilson and McPherson, 1981; Wilson and Lucchi, 2001; Mead, 2004). After their fifth instar stage, the first adults appear in early July in Korea (Park et al., 2016; Park et al., 2019).

Adults of *M. pruinosa* return to trees for mating and oviposition soon after their emergence (Santini and Lucchi., 1994; Park et al., 2019; Seo et al., 2019) (Fig. 4). Adults mature sexually approximately 25-30 days after emergence (Santini and Lucchi, 1994) and demonstrate calling behavior via substrate vibration for copulation (Virant-Doberlet and Žežlina, 2007). Female fecundity is estimated to be maximum 90 eggs per individual (Bozsik, 2012). Like the nymph

stages, *M. pruinosa* adults produce honeydew during sap feeding, however, they secrete relatively small amounts of wax in comparison to the nymphs (Lucchi and Mazzoni, 2004). Adults of *M. pruinosa* are observed until mid-October in most temperate regions (Dean and Bailey, 1961; Wilson and McPherson, 1981; Wilson and Lucchi, 2001) (Fig. 3).

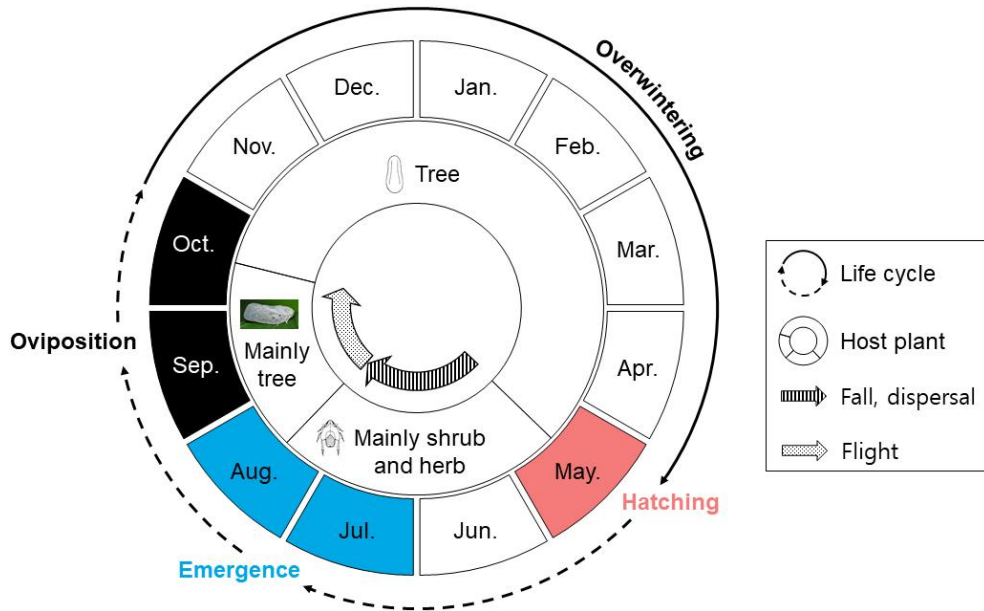


Fig. 3. Schematic of *Metcalfa pruinosa* life cycle, change of host plant and behavior according to its developmental stages.

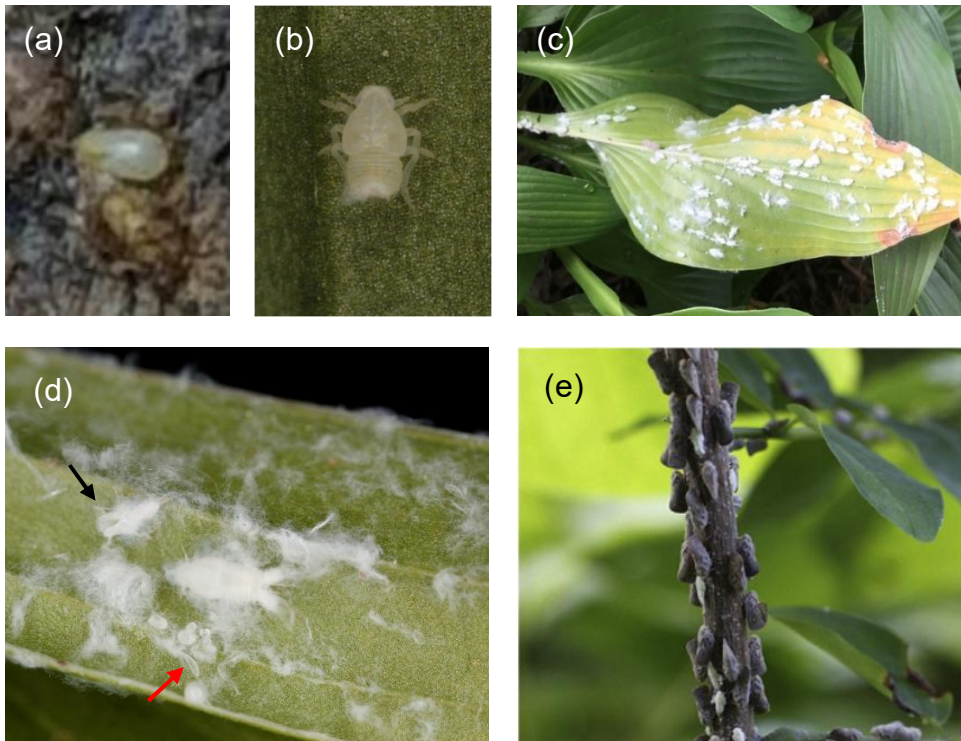


Fig. 4. Photos of *Metcalfa pruinosa* development stages. (a) egg; (b) new-born nymphs; (c) nymphs on herbaceous plants (*Hosta* sp.); (d) exuvia (→), wax filaments, and droplets of honeydew (→) produced by the third-instar nymphs; (e) adults gathering on a tree (*Robinia pseudoacacia*) (photo by Kim et al., 2011).

1-3. Symptoms of damage and economic impact

M. pruinosa is not considered an economic pest in its native region (Alma et al., 2005). However, it has caused serious economic impacts in its non-native invaded region, due to its substantial population buildup and subsequent plant damage (Wilson and Lucchi, 2001). In Europe, crop impacts including a reduction in the sugar content and acidity of grapes, and yield losses of 30 - 40% in soybean crops have been reported (Ciampolini et al., 1987; Strauss, 2010). In Korea, *M. pruinosa* is a problem for a wide range of agricultural crops and fruit trees including, ginseng, sesame, perilla, grape, peach, pear, persimmon, apple, and mulberry (Kim et al., 2011; Kim and Kil, 2014; Seo et al., 2019). Furthermore, extensive damage has been reported across various other landscapes (e.g., forests, urban parks, private gardens, and plant nurseries), as well as in agricultural fields (Kim et al., 2011).

M. pruinosa causes damage directly via its feeding mechanism of sucking plant sap, leading to shoot stunting, a reduction in plant vitality and plant wilting (Wilson and Lucchi, 2007; Strauss, 2010). In particular, herbaceous plants near overwintering habitats are most at

risk of sucking damage due to the high density of nymphs around the trees (Ciampolini et al., 1987; Strauss, 2010). *M. pruinosa* also causes indirect plant damage through its excretion of honeydew and wax filaments. Honeydew residues left on plants can induce the growth of sooty molds, which negatively affect plant photosynthesis or the aesthetic quality (Della Giustina and Navarro, 1993). The wax produced by nymphs remains on plants and can be a nuisance in a nursery of ornamental trees or in public parks. However, perhaps the largest concern regarding *M. pruinosa* in the future may be the potential transmission of plant diseases. Although no specific cases of damages caused by disease transmission have been reported yet, it has been proved that *M. pruinosa* can serve as a vector for *Pseudomonas syringae* pv. *actinidiae* (Psa) and *Candidatus Phytoplasma asteris* (Aster yellows phytoplasma) (Donati et al., 2017; Mergenthaler et al., 2020). Thus, the necessity for management of *M. pruinosa* is increasing in invaded regions.

1-4. Invasion stage and management in Korea

In general, the process of biological invasion comprises a series of stages i.e., introduction, establishment, spread, and impact (Lockwood et al., 2013) (Fig. 5). During the introduction stage, individuals of non-native species are transported to a new area by overcoming geographical barrier. In the next two stages, some species achieve successful establishment, by escaping extinction risk and spreading to large area. In the impact stage, they cause ecological or economic harm across their newly wide distribution range, and become 'invasive species' (Blackburn et al., 2011). In Korea, *M. pruinosa* already reached the impact stage of the biological invasion process, with the fast range expansion and population buildup of *M. pruinosa*. At present, plant damage and consequent economic impacts have been reported nationwide (Fig. 2). Therefore, the management of *M. pruinosa* in Korea needs to be focused on the mitigation of its economic and ecological impacts through the management of the current established population (Lockwood et al., 2013; Liebhold et al., 2008) (Fig. 5). The mitigation is the most feasible strategy, as eradication of *M. pruinosa* from the entire of Korea or containment of

its spread to unreached areas are now unlikely to be realized due to its wide distributed range, and the severe damage already have been occurring at present.

As damages caused by *M. pruinosa* are persistently reported each year nationwide, the demand for geographic distribution information is increasing across Korea. In line with these demands, Byeon et al. (2017) predicted the current and future distribution of *M. pruinosa* in Korea using CLIMEX software, which adopts a deterministic modelling approach (except for 'Climate matching' function) using physiological parameters (Strauss, 2010). However, the actual distribution of *M. pruinosa* does not match with their prediction, because Byeon et al. (2017) uses predetermined parameters without including non-climatic constraints (Colwell and Rangel, 2009). Thus, the results are close to prediction of fundamental niche constructed with climate conditions (Sutherst and Maywald, 1985; Elith, 2016). These models would be very useful for the evaluation of establishment risk or surveillance of non-native species before they reached the spread stage (Liebhold et al., 2016), but have less demanded once a species has reached the impact stage (Fig. 5).

A viable management option for widespread *M. pruinosa* might

be the intentional introduction of *Neodryinus typhlocybae* (Ashmead) (Hymenoptera: Dryinidae), a specialist natural enemy which attacks nymphs (Dean and baily, 1961; Alma et al., 2005). This parasitoid wasp has become established in several European countries after its introduction from North America (Alama et al., 2005; Véték et al., 2019). Recently, introduction and release programs of *N. typhlocybae* have been considered in Korea at a government level (<http://www.rda.go.kr/>). However, environmental adaptability of *N. typhlocybae* and its risk of attack for non-target insects in the Korean environment have not been fully studied yet. Moreover, it is hard to imagine that the introduction of this natural enemy will have an immediate effect of density reduction on *M. pruinosa* populations. Therefore, the introduction of *N. typhlocybae* may be a necessary, long term solution, but emergency control options are more important for an immediate effect in the short term.

To control the abundance of *M. pruinosa*, chemical sprays have been a major tactic in its non-native countries including Korea. Several commercial insecticides and plant extracts such as Derris, Citronella, and Cinnamon have been screened and applied as efficient control methods to date (Ahn et al., 2011; Lee et al., 2019b). Managers

and farmers generally have treated insecticide depending on observed densities of *M. pruinosa*, because there is very little information related to control timing and occurrence pattern of *M. pruinosa* in local habitats (Lee et al., 2016; Park et al., 2019). However, young nymphs of *M. pruinosa* are hard to be detected due to their very small body size and low wax secretion. Thus, when the *M. pruinosa* nymphs is detected by the managers, the nymphs could have already damaged the plants. In addition, this conventional manner of control would decrease control efficiency along with side effects caused by widespread treatment against the various potential hosts (Lauterer, 2002).

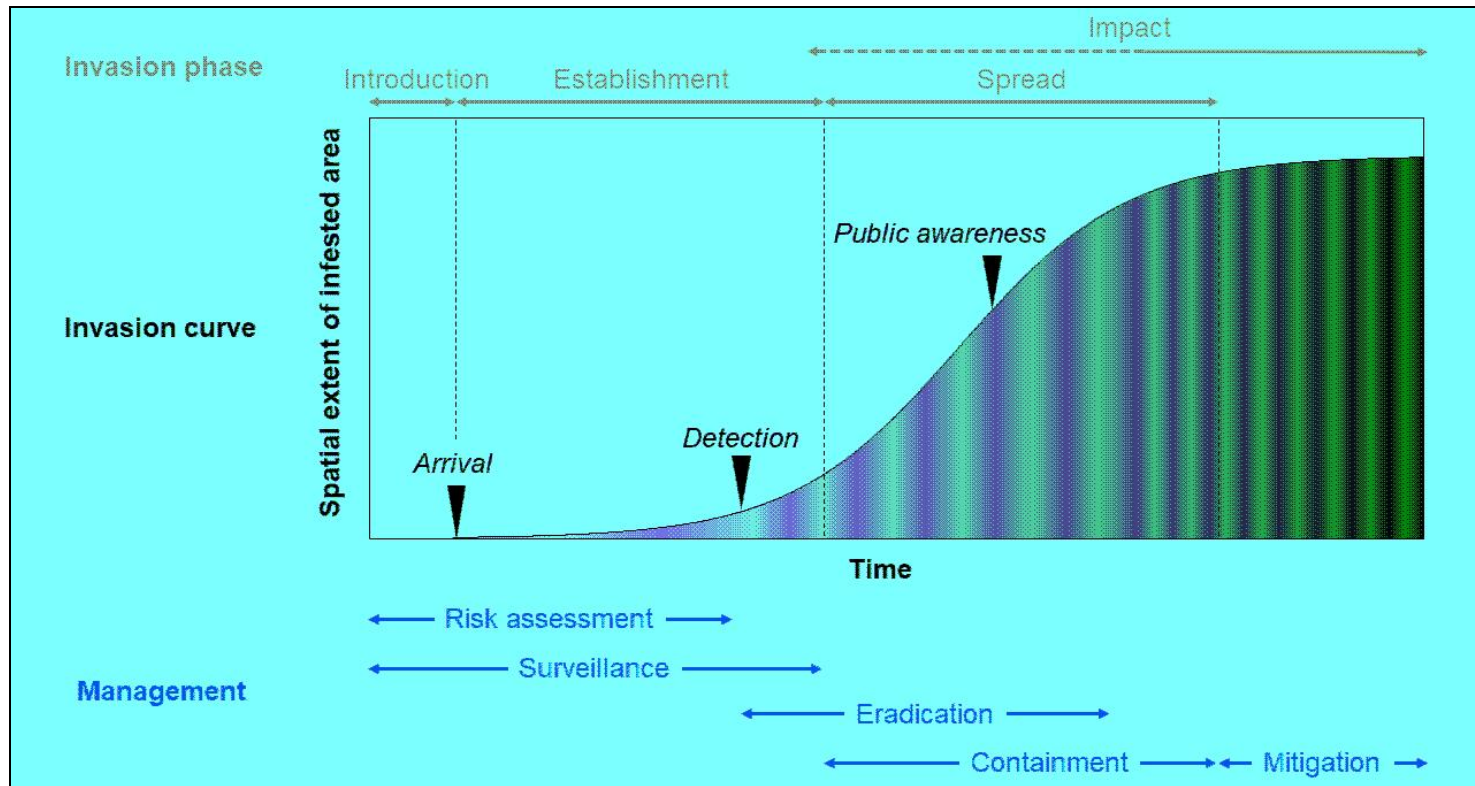


Fig. 5. A series of biological invasion stages, generalized invasion curve, and according phase of management strategies (adapted from Blackburn et al., 2011; Lockwood et al., 2013).

1-5. Objectives of this study

To delineate the distribution of *M. pruinosa* in the impact stage, a correlative modelling approach within concerned geographical area (i.e., Korea) would be more useful than a deterministic model. This is because sufficient information related to the specific occurrence point of *M. pruinosa* throughout Korea can be constructed. Using environmental variables, geographically referenced to the occurrence points, the presence possibility of *M. pruinosa* could be modelled, reflecting non-climatic constraints implicitly (Colewell and Rangel, 2009). This approach would be close to explanation of realized niche of *M. pruinosa* for why this pest is abundant or absent in certain areas (Elith and Leathwick, 2009; Lockwood et al., 2013). Therefore, the model output could contribute to establishing a national management policy for controlling *M. pruinosa* density. Moreover, multiple circumstantial evidence of fast and long-distance dispersal via traffic vehicles has been proposed (Lauterer, 2002; Strauss, 2010), but this speculation has not been proven yet. To test this hypothesis, quantitative evaluation of the traffic factor using statistical models with distribution information might be viable. This will provide a better

understanding of the process of spread and distribution changes of this invasive species.

Although studies on *M. pruinosa* distribution are clearly important for national and long-term management plans, it is also urgent to establish strategies for efficient management of *M. pruinosa* causing economic impacts. As previously mentioned, *M. pruinosa* overwinters as eggs in trees, with the distribution of nymphs thus formed around trees after they hatch (Fig. 3). This density gradient becomes gentler over time, as the nymphs disperse to surrounding vegetation (Ciampolini et al., 1987). Therefore, an effective target for the chemical control of *M. pruinosa* is the young nymphs clumping around the trees. In this respect, knowing times for egg hatching and falling of young nymphs from trees is key for the management of *M. pruinosa* in various landscapes. Predictive models, which are applicable to field conditions, would be useful for determining the optimal timing to control this pest, because young nymphs of *M. pruinosa* are difficult to detect, despite being the main proposed target for effective control (Fig. 4).

In Korea, *M. pruinosa* damage in agricultural fields are mainly caused by its nymphs immigrating into the fields. The nymphs that

invade crop fields originate entirely from trees close to those fields (Fig. 3). The nymphal immigration from source trees to nearby crop fields continues from mid-May to late July (personal observation), but adults emerging on crop plants soon leave to find tree hosts for mating and oviposition (Fig. 3 and 4). Therefore, clarifying the immigration pattern of nymphs into crop fields is important to reduce nymphal damage in field crops. In addition, the application scope of existing control options for the nymphs in crop fields could be extended by considering factors related to their population change, such as the survivorship of nymphs and adult emigration along with nymphal immigration.

Therefore, this study was conducted to (1) estimate the current potential distribution of *M. pruinosa* in Korea, (2) predict future distribution of *M. pruinosa* in Korea under the RCP 8.5 climate change scenario, (3) determine whether traffic factors were responsible for the rapid spread of *M. pruinosa* in Korea, (4) develop an egg hatching model of *M. pruinosa*, (5) develop a falling time model of *M. pruinosa* first instar nymphs from trees, (6) develop and validate an immigration model of *M. pruinosa* nymphs in crop fields, and (7) construct a population model for *M. pruinosa* nymphs within the crop fields.

Chapter II.

Current and future distribution of *Metcalfa pruinosa* in Korea: Reasoning of fast spreading

2-1. Abstract

Metcalfa pruinosa (Say) is an invaded species in Korea and has showed rapid establishment and spread through Korea since its first detection in 2009. To identify spreading pattern of *M. pruinosa* in Korea, expansion rate and inter-colonies distance of established areas were analyzed with spatio-temporal occurrence information. In addition, distribution models for *M. pruinosa* were developed by Maximum Entropy method (MaxEnt), using environmental variables including a traffic volume variable, in order to verify whether traffic factor was responsible for the rapid spread of *M. pruinosa*, and estimate its potential distribution in Korea. Results showed that range expansion of *M. pruinosa* has been facilitated by long-distance passive transportation rather than dispersal of itself. In early spread phase in 2013, the traffic volume was the most important factor in explaining *M. pruinosa* distribution. Traffic volume of the relative pre-occupied habitat in 2013 was also significantly ($P < 0.05$) higher than the one lately occupied in 2017. Therefore, this factor was strongly proposed as a main factor responsible for long-distance dispersal and consequent rapid spreading of *M. pruinosa* in Korea. However, contribution of the traffic factor was significantly decreased in current

distribution model in 2017, and rather the distribution could be better explained without traffic factor. The current distribution model was finally developed using selected three bioclimatic variables, mean temperature in the warmest quarter, mean temperature of coldest quarter, and annual precipitation, except for traffic variable. This final model was used to predict future habitat suitability under RCP 8.5 climate change scenario. In near future, in 2030s and 2050s, most parts of Korea except for mountainous area and southern parts were estimated to be suitable for *M. pruinosa* to be established.

Key words: *Metcalfa pruinosa*, stratified spread, biological invasion, species distribution model, human mediated factor, traffic volume, MaxEnt

2-2. Introduction

Metcalfa pruinosa has quickly spread out throughout Korea in less than 10 years. Because *M. pruinosa* has more than 300 host plant species (Seo et al., 2019), it is highly likely to establish in all suitable areas in Korea. In addition, *M. pruinosa* can serve a vector for *Pseudomonas syringae* pv. *actinidiae* (Psa) that can cause severe bacterial canker in plants (Donati et al., 2017). Thus, the economic importance of *M. pruinosa* as an agricultural pest is increasing in Korea. With fast range expansion and population growth of *M. pruinosa* in Korea, demands for current and future distribution of *M. pruinosa* and determinants of its distribution and spreading are increasing for its efficient management. However, most studies have been focused on development of management techniques (Wilson and Lucchi, 2007; Ahn et al, 2011; Lee et al., 2016; Donati et al, 2017).

One previous study (Byeon et al., 2017) has predicted current and future distribution of *M. pruinosa* in Korea with CLIMEX software. That study (Byeon et al., 2017) is valuable in that it has evaluated establishment risk of *M. pruinosa* in Korea. However, the current distribution of *M. pruinosa* does not match with their prediction.

Moreover, it is more important to delineate *M. pruinosa* distribution precisely and find environmental factors related to its distribution than to assess potential risk of establishment because this invasive pest has been causing economic impacts (Lockwood et al., 2013).

There have been also multiple studies (Lauterer, 2002; Strauss, 2010; Kim and Kil, 2014) supporting the contribution of human related activities to the rapid spread and distribution of *M. pruinosa*. Kim and Kil (2014) reported that *M. pruinosa* was found more on trees of roadsides (53.3 %) than that in forests (33.3 %) or orchards (20.0 %). In addition, in Europe, high spread chance by human-mediated pathways was proposed for *M. pruinosa* and infested trees with *M. pruinosa* eggs (Lauterer, 2002; Strauss, 2009). Although multiple circumstantial evidences of fast and long distance dispersal via vehicles have been proposed, this speculation has not been proven yet. To test this hypothesis, quantitative evaluation of the impact of human mediated activities using distribution information might be one useful method.

Therefore, the objectives of this study were (1) to estimate spread rate and pattern of *M. pruinosa* in Korea, (2) to determine environmental factors mainly affecting the distribution of *M. pruinosa*

in Korea, (3) to predict the current potential distribution of *M. pruinosa* in Korea, (4) to forecast future habitat suitability for *M. pruinosa* in Korea, and (5) to verify the hypothesis of spread of *M. pruinosa* via traffic factor using species distribution modelling approach and several statistical models.

2-3. Materials and methods

2-3-1. Species occurrence data

In this study, three kinds of presence-only distribution data of *M. pruinosa* in Korea were collected: (1) data from previous studies (Lee and Wilson, 2010; Kim et al., 2011; Lee et al., 2011; Lee et al., 2013a; Park et al., 2013; Choi et al., 2013; Lee et al., 2013b; Lee et al., 2014; Kim and Kil, 2014; Choi et al., 2014; Jung et al., 2015; Lee et al., 2017) and collection records of specimens (<https://species.nibr.go.kr>) for the analysis of spreading rate and pattern of *M. pruinosa* (2) data of 30 occurrence points with GPS coordinates in 2013 (Fig. 1a) from a previous study (Kim and Kil, 2014) for a distribution model of the early spreading phase; (3) distribution data from occurrence survey results in 2017 in this study, representing the current phase. For survey of *M. pruinosa* in 2017, South Korea was divided with grids of 30 km by 30 km (128 grids total). At least one point per grid was surveyed for the occurrence of *M. pruinosa* from June to August. Five host plant trees were examined by naked eyes for two shoots and their leaves per plant. Observed trees were mainly false acacia. When acacia trees were not enough for survey, other host plants (e.g., mulberry, king cherry, cornus, and so on) were examined to determine the presence or

absence of *M. pruinosa*. A total of 399 presence point data were obtained for distribution modelling.

2-3-2. Spreading rate and pattern

Presence data of *M. pruinosa* in Korea was reconstructed for exploiting all available distribution information. Because data from the previous studies and collection records of specimens of *M. pruinosa* (i.e., data 1 in the previous description) had only administrative area (e.g., -Si and -Gun in Korea) without specific geo-coordinates for the collection location, the central point for each administrative area reported for *M. pruinosa* was assumed as a discovered location, and its geo-coordinates were used. Occurrence data (i.e., data 2 and 3 in the previous description) for 2013 and 2017 distribution modelling were also used here. In case that at least one occurrence of *M. pruinosa* was present, the administrative area was considered as a presence area and central geo-coordinate was obtained. From these process, total 108 geo-coordinates of administrative areas were obtained as presence points among 159 areas until 2017. These central points were used for following analysis of spreading rate and pattern of *M. pruinosa* in Korea. All distances in this part were

calculated using central points of administrative areas.

To estimate spreading rate, regression analysis, using distance and year of newly infested locations from first invaded locations in Korea, was conducted (Tobin et al., 2007). The minimum linear distances of newly discovered central points in each year from the first introduced points in Korea in 2009 were then measured. Minimum spreading distance per year from 2010 to 2017 was estimated by linear regression in R 3.4.3 to estimate the spreading rate of *M. pruinosa* in Korea (R core team).

Nearest neighbor distances of presence points were also analyzed to show spreading pattern of *M. pruinosa* for 159 administrative areas of Korea. In this analysis, the hypothetical expected distance under condition of continuous spread was postulated for comparison of colonies distance in each year. This hypothetical distances were calculated from the center of an administrative area to center of all directly abutting areas. The calculated total 802 pairs of distances were averaged and postulated as expected distance in continuous spread. This is because if *M. pruinosa* had spread continuously, it should have been discovered only in surrounding of the founder population. The nearest neighbor

distances of presence points in each year was estimated by cumulative presence points including previous presence points after 2009. Because one area was adjacent to five areas on average in total 159 administrative areas, the nearest neighbor distance calculated by nearest five presence areas from one presence area. This pairs of nearest 5 neighbor distance in each year were averaged and compared to hypothetical distance. If spread of *M. pruinosa* is close to the continuous spread, the average neighbor distance of each year will be similar to the hypothetical expected distance.

2-3-3. Preparation of environmental variables

Numerical climate data in Korea were generated using 77 synoptic observation station data from Korea Meteorological Administration (KMA). Because *M. pruinosa* is a relatively recent invading species, only last decade climatic data were used. Interpolation of 2010s (2001-2010) climate data was estimated by IDW (Inverse Distance Weighting) from observation data. Among estimated values, temperature and precipitation data were used to create 19 bioclimatic variables (Ramirez-Villegas and Bueno-Cabrera, 2009) by using DIVA-GIS 7.5 (Hijmans et al., 2012). Created 19 bioclimatic

variables were converted to ASCII (American Standard Code for Information Interchange) files using Raster to ASCII of SDMs tool in ArcGIS by 1km grid resolution. Next, to project future distribution of *M. pruinosa*, RCP (Representative concentration pathway) 8.5 scenario based on historical data (1986-2005) from KMA was used. From the scenario, 2030s (2031-2040), 2050s (2051-2060), 2070s (2071-2080) and 2090s (2091-2100) climate data were used to forecast future habitat suitability. Like 2010s, 19 bioclimatic variables were created with the same extent and resolution.

To evaluate the hypothesis that dispersal of *M. pruinosa* was accelerated via vehicles, traffic volume data were collected because traffic-heavy points could have high probabilities for *M. pruinosa* to arrive at these points according to the hypothesis. Traffic information of Korea was downloaded from Traffic Monitoring System (TMS) website (<http://www.road.re.kr>) which included road types, addresses of surveyed points, measurement scheme (i.e., regular or occasional survey), length of section, number of measurement (in occasional survey), and traffic volume per car type. Addresses of surveyed 3,477 points in this information were translated to GPS coordinates using google map (<https://www.google.com/maps>). Traffic volume and

number of measurements were transformed to average daily traffic volume of the last ten years (2007-2016). These data were then projected and interpolated using the ordinary kriging method in ArcGIS 10.1. The layer created by these procedures was converted to a raster file with the same resolution of climate variables. The raster file was then converted and stored in ASCII file format.

2-3-4. Modelling procedure

To avoid overfitting due to sampling bias (Veloz, 2009), the average nearest neighbor test was conducted using ArcGIS 10.1 (ESRI, 2012). According to this test, data in 2013 had random pattern ($p = 0.909$) while, data in 2017 showed clumped pattern ($p < 0.001$). Based on expected mean distance (0.079683 decimal degrees) which was the average distance of nearest points at hypothetical random distribution, points in 2017 were rarified by the method of Rarefy Occurrence Data of SDMs tool in ArcGIS (Brown, 2014). A total of 128 points of presence finally remained (Fig. 1b).

To eliminate highly correlated variables which would cause unstable results in SDMs (Dormann et al., 2013), correlation test was evaluated with calculation of Pearson correlation coefficient, r . One

environmental variable among correlated variables ($r > 0.85$) was selected to analyze biological relevance with *M. pruinosa* while the others were not analyzed anymore (Elith et al., 2006). A total of eight among 20 variables (i.e. 19 bioclimatic variables and traffic volume variable) remained. They were analyzed to predict the distribution of *M. pruinosa* in Korea.

MaxEnt (Maximum Entropy Modelling) is one of the most commonly used software for the correlative model for species distribution modellings (i.e., SDMs) and needs presence-only data. Thus, MaxEnt 3.4.0 software (Phillips et al., 2017) was used for modelling. The modelling processes of MaxEnt were run with default settings except for the feature, machine learning term, which was a function for transformation of original environmental variables (Elith et al., 2010). Selected features were linear, quadratic, and hinge features. This feature combination showed interpretable response curves in preliminary execution.

Among eight environmental variables, variables showing multimodal response were removed from preliminary execution. Because response curves of population to environment factors generally could have unimodal curves (Austin, 2007). Also, variables

for which response curves showed opposite pattern between 2013 and 2017 were eliminated because an environmental factor should affect the distribution of *M. pruinosa* with similar ways even though each environmental factor might have different weight on its distribution at different time frame. Through these procedures, four variables, Bio 10 (Mean Temperature of Warmest Quarter), Bio 11 (Mean Temperature of Coldest Quarter), Bio 12 (Annual Precipitation), and Traffic_av (Mean Traffic Volume per day), were selected.

In this study, environmental variables could be divided into two categories; climate related variables and anthropogenic variables. Thus, two different models (with or without traffic factor) were developed for 2013 and 2017. A total of four models were created: using climatic variables with 2013 occurrence data (2013 Climate only), using climatic and traffic variables with 2013 occurrence data (2013 Climate+Traffic), using climatic variables with 2017 occurrence data (2017 Climate only), and using climatic and traffic variables with 2017 occurrence data (2017 Climate+Traffic). In this study, because there is no independent test data set to evaluate predictive performance of developed models, the trained models were evaluated by average AUC scores of 10-folds cross validation. At the same time, variable

importance among all environmental factors was compared through jackknife test. To compare estimated distribution of early spreading (2013) and current (2017), output format was set to logistic output (Phillips and Dudík, 2008).

2-3-5. Model selection and projection

In MaxEnt, AUC (area under the curve) score can be an indicator of the model performance describing the discrimination power (Hanley and McNeil, 1982). In general, model of AUC score greater than 0.75 was considered reliable while a score of 0.5 indicated that the discrimination was the same as random (Elith, 2002). Although AUC scores were popularly used for model selection and predictability, the calculation of AUC scores necessarily uses pseudo-absence data (background data, not true absence) in presence-only modelling, like that in MaxEnt (Phillips et al., 2006). This could cause over- or under-estimation of prediction ability. AIC (Akaike's Information Criteria) is also popularly used to determine the most suitable model among available models. Smaller value of AIC represents a better model that has small information loss (Johnson and Omland, 2004). In this study, AIC was used to determine whether

traffic factor should be included when predicting *M. pruinosa* distribution. AICc (corrected AIC) was calculated using ENM Tools (Warren et al., 2010) and raw output of MaxEnt (Warren and Seifert, 2011). Models that had smaller score were selected from competing models of each year. Finally, selected models of 2013 and 2017 were expressed by probability of presence in geographic maps. Habitat suitability of 2030s, 2050s, 2070s and 2090s were mapped by using Maximum training sensitivity plus specificity threshold for generating binary prediction (Pearson, 2010).

2-3-6. Comparison of traffic factor for *M. pruinosa* occurrence in 2013 and 2017

To compare values of traffic factor in occurrence points of *M. pruinosa* between two data sets, a convex hull (Fig. 1a; b) was drawn using the 2013 data set. Among the 2017 data set, 32 newly occurred points outside of the convex hull were extracted from the rarefied 2017 data (Fig. 1b). Traffic volume per each point was extracted from the layer, Traffic_av. The extracted two data sets did not show normal distribution according to the shapiro-wilk normality test in R 3.4.3 ($p < 0.05$). Thus, both sets of traffic data were transformed as $\lambda = 0.13$ by

using the box-cox power transformation in R 3.4.3 to meet assumption of normality, the requirement of parametric analysis. These values of traffic factor in *M. pruinosa* occurred points in both 2013 and 2017 were then statistically compared using Tukey student *t*-test in R 3.4.3 (R core team).

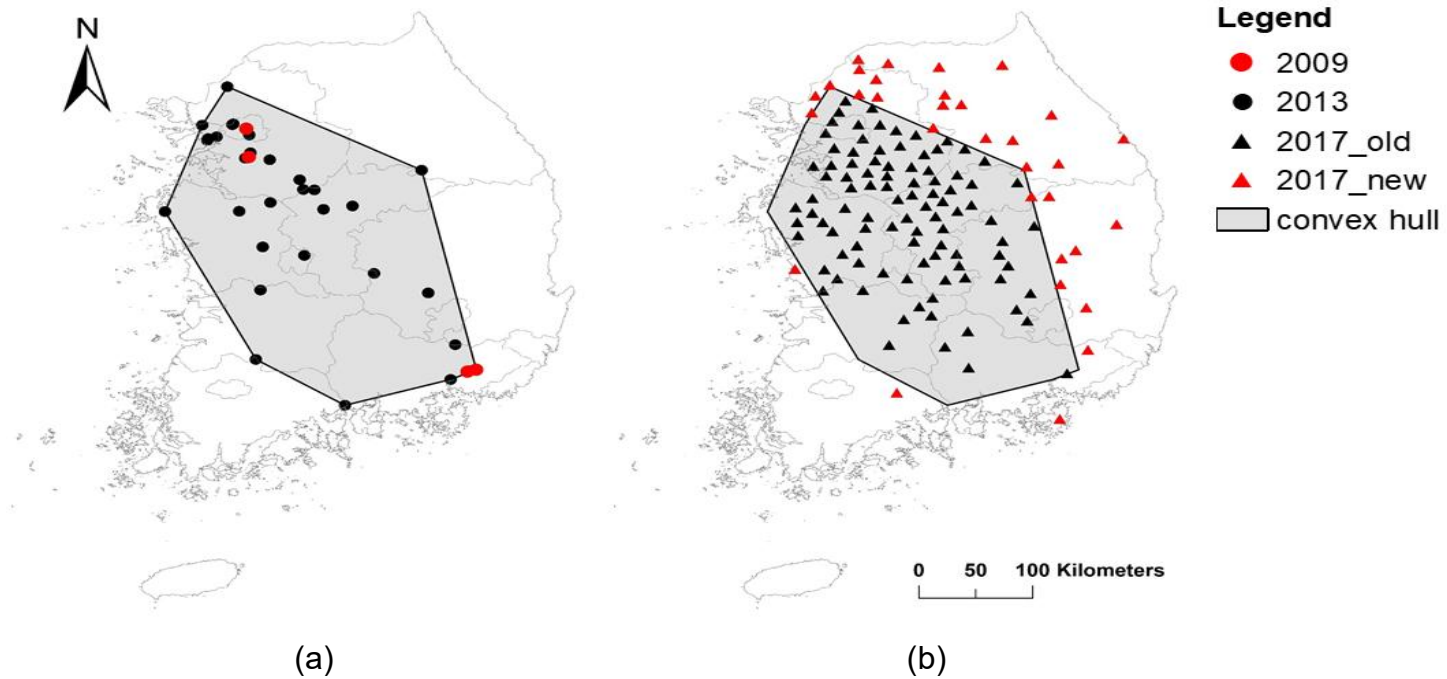


Fig. 1. (a) Occurrence points of *Metcalfa pruinosa* in Korea in 2009 (●) and 2013 (●) reported in other papers (Kim et al., 2011; Kim and Kim, 2014). Convex hull (■) was drawn by 2013 distribution; (b) Rarefied discovered points of *Metcalfa pruinosa* in 2017 (▲ and ▲) surveyed in this paper. Traffic volume was extracted from points in convex hull and out of convex hull for comparison.

2-4. Results

2-4-1. Spreading rate and pattern

The spreading rate of *M. pruinosa* (Fig. 2) was estimated to 5.19 ± 1.742 km (Mean \pm SEM) from the slope of linear equation ($F = 8.862$; $df = 1, 103$; $P < 0.05$). Mean distances of nearest five points in each year were much higher than the mean neighbor distance of central point of all administrative areas (i.e. hypothetical expected distance) of *M. pruinosa* in Korea. However, the mean distance was steadily decreased as time went by (Fig. 3). This distance became very close to the hypothetically expected distance in 2017 (Fig. 3).

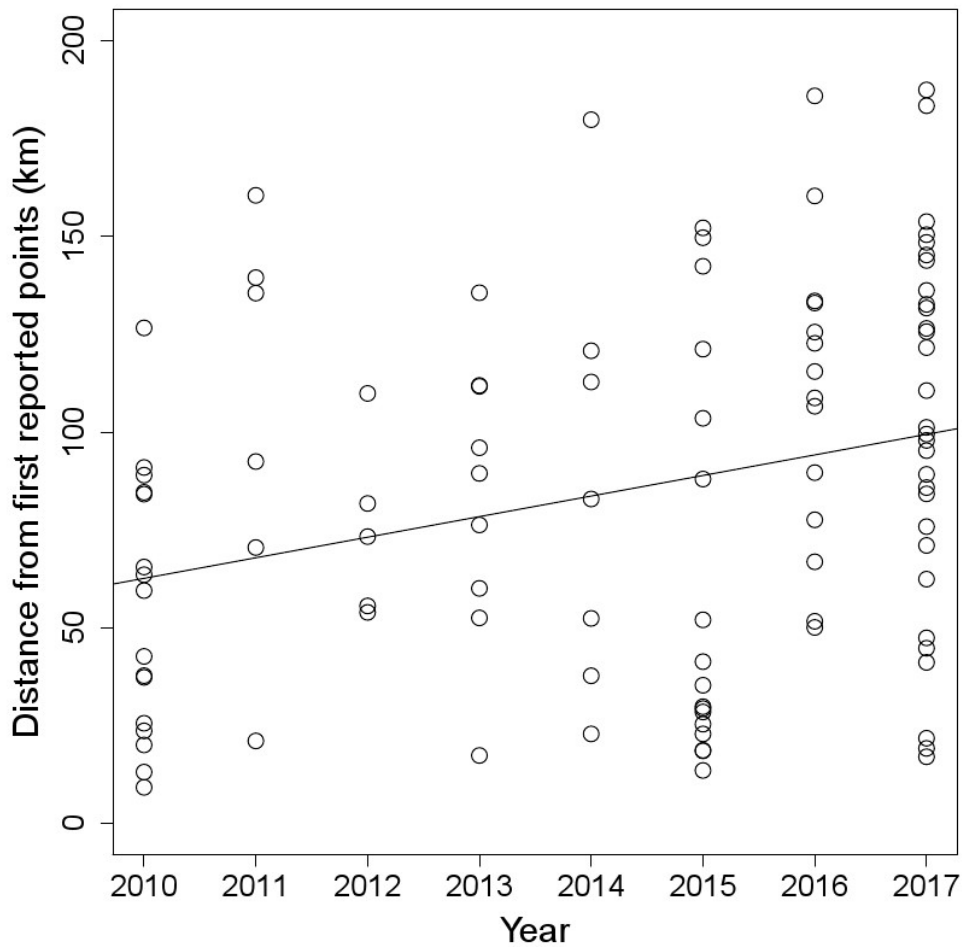


Fig. 2. Nearest distances between newly discovered administrative areas in each year from the first invaded administrative areas. Solid line was regression line. The spreading rate of *Metcalfa pruinosa* in Korea was estimated 5.19 ± 1.742 km (Mean \pm SEM) from the slope of regression line.

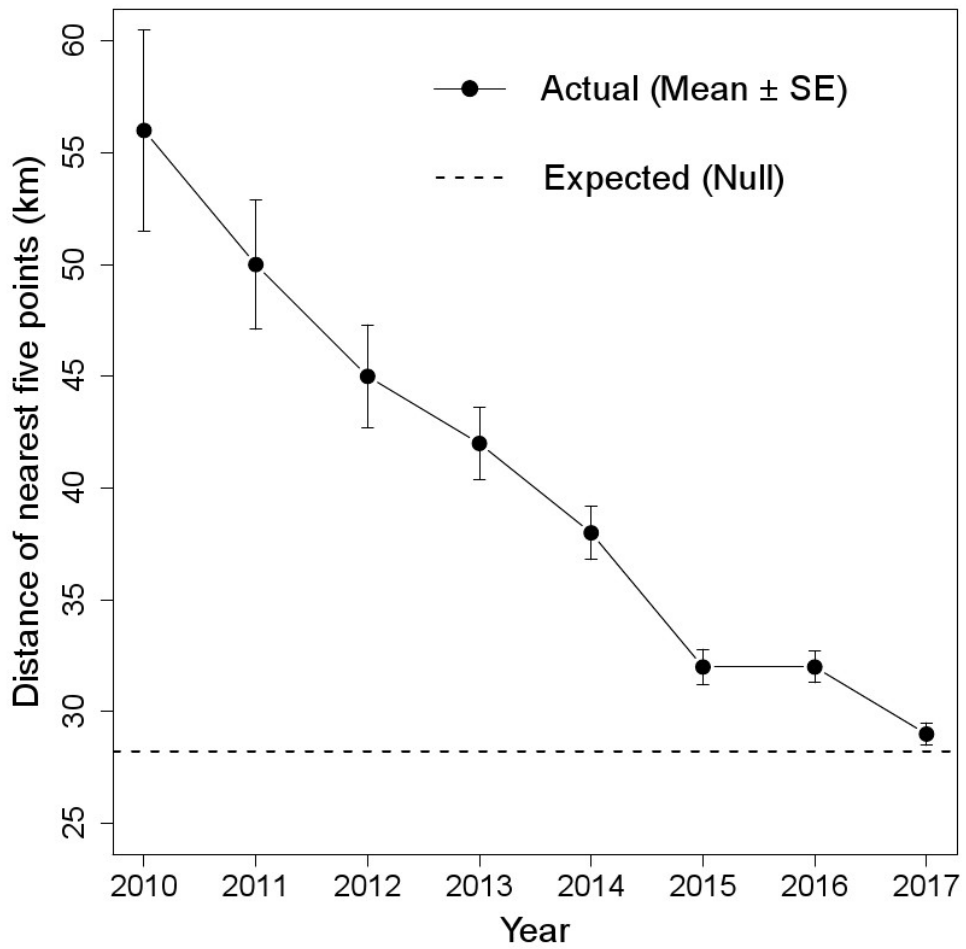


Fig. 3. Mean distance of all pairs of nearest five administrative areas from one administrative area. Dashed line was calculated in condition of hypothetical continuous spread.

2-4-2. Distribution model in 2013 (early spreading phase)

All average AUC scores of 2013 models (with or without traffic factor) were larger than 0.75, indicating significant predictive ability (Table 1). AICc values for both 2013 Climate only and Climate+Traffic models were 764.5 and 751.6, respectively. The AICc comparison indicated that the model including the traffic factor explained the distribution of *M. pruinosa* in 2013 much better than the model without the traffic factor (Table 1; Fig. 4a). Traffic factor occupied approximately 86% contribution in the 2013 Climate+Traffic model. Moreover, the order of variable importance for this model was also traffic factor, Bio10, Bio11, and Bio 12 (Table 2; Fig. 5a).

2-4-3. Distribution model in 2017 (current phase)

All average AUC scores of 2017 models (with or without traffic factor) were larger than 0.75, showing significant predictive ability (Table 1). AICc values of both 2017 Climate only and 2017 Climate+Traffic models were 2837.1 and 2847.2, respectively. AICc comparison of 2017 models evaluated that the model excluding the traffic factor described the distribution of *M. pruinosa* in 2017 better than the model including the traffic factor (Table 1). Therefore, the

model without traffic factor was finally selected for describing *M. pruinosa* distribution in 2017, contrary to the model of 2013 (Fig. 4b). The highest contribution among environmental variables in the selected model was Bio 10 (53.4%), followed by Bio11 (45%) and Bio 12 (1.6%) (Table 2). In jackknife test, Bio 10 and Bio 11 were found to be important variables in model development (Fig. 5b). Although not selected, the contribution of traffic volume in the 2017 Climate+Traffic model decreased significantly from 88% to 16% compared to the selected 2013 Climate+Traffic model (Table 2).

In response curve of the selected model, Bio 10 showed that the logistic output was increased exponentially until optimal temperature, but rapidly decreased soon after the optimal temperature (Fig. 6c). Response curves of Bio 11 and Bio12 showed that adequate temperature was needed during overwinter while annual precipitation affected to distribution (Fig. 6d; e).

Table 1. Summary of developed four models in MaxEnt and values of average AUC and AICc of 2013 and 2017

| Year | Model | Description | | Evaluation | Selection | | Final selection |
|------|------------------|--------------------------------------|----------------|-----------------------|-----------|--------|-----------------|
| | | Variables | No. parameters | Average AUC (Mean±SD) | AICc | Δ AICc | |
| 2013 | Climate only | Bio 10, Bio 11 Bio 12 | 9 | 0.756±0.118 | 764.5 | 12.9 | |
| | Climate +Traffic | Bio 10, Bio 11 Bio 12, Traffic_av | 14 | 0.831±0.085 | 751.6 | 0 | Selected |
| 2017 | Climate only | Bio 10, Bio 11 Bio 12 | 18 | 0.778±0.050 | 2837.1 | 0 | Selected |
| | Climate +Traffic | Bio 10, Bio 11 Bio 12, Traffic_av | 23 | 0.771±0.050 | 2847.2 | 10.1 | |

Table 2. Contribution (%) of environmental variables for each model in 2013 and 2017

| Variables | 2013 | | 2017 | |
|------------|--------------|-----------------|--------------|-----------------|
| | Climate only | Climate+Traffic | Climate only | Climate+Traffic |
| Bio 10 | 77.4 | 8.5 | 53.4 | 41.2 |
| Bio 11 | 16.3 | 2 | 45 | 41.3 |
| Bio 12 | 6.3 | 3.8 | 1.6 | 1.2 |
| Traffic_av | - | 85.8 | - | 16.3 |

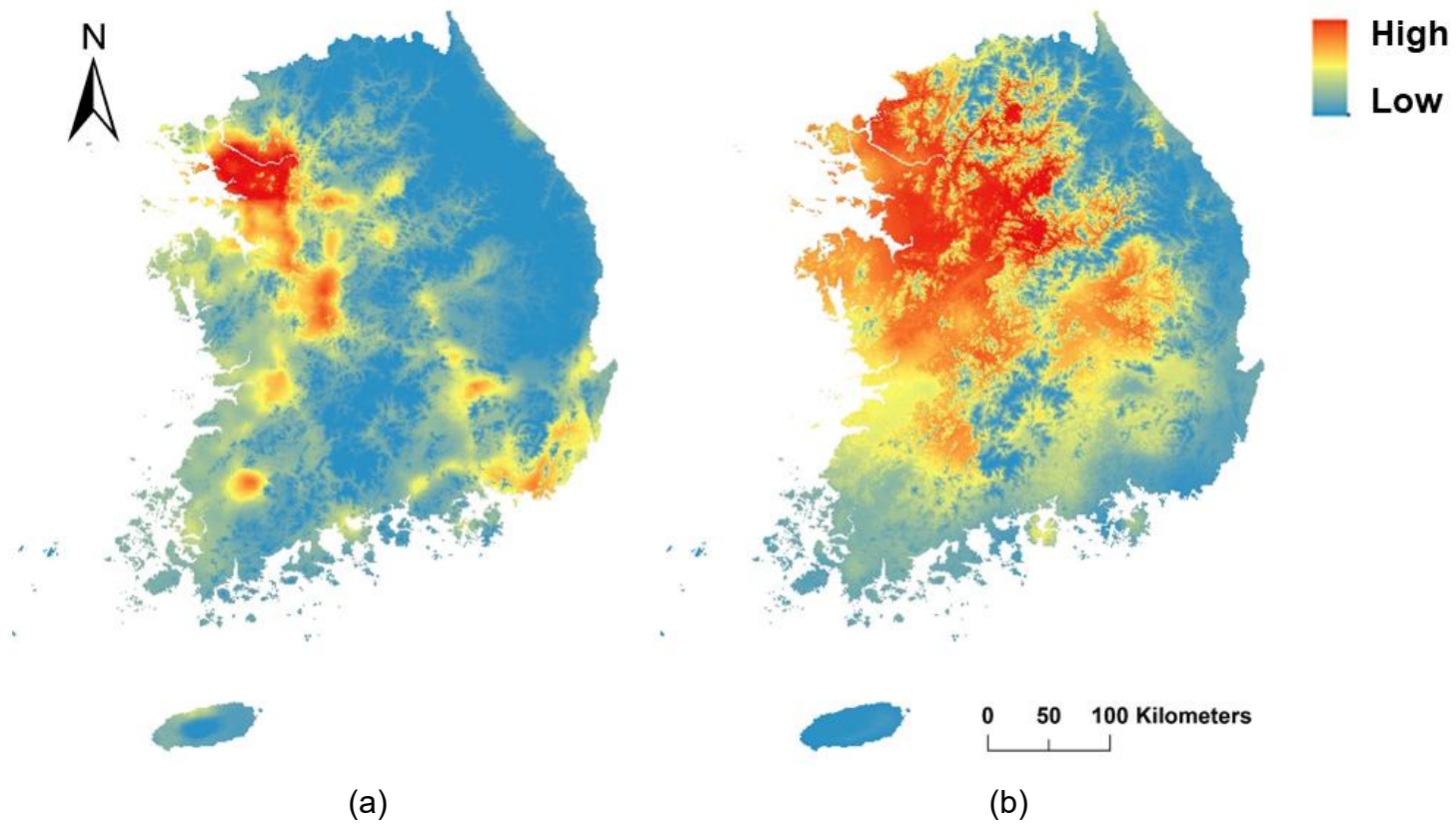


Fig. 4. Potential distribution of *Metcalfa pruinosa* estimated by MaxEnt models in Korea (a) 2013 Climate+Traffic model; (b) 2017 Climate only model.

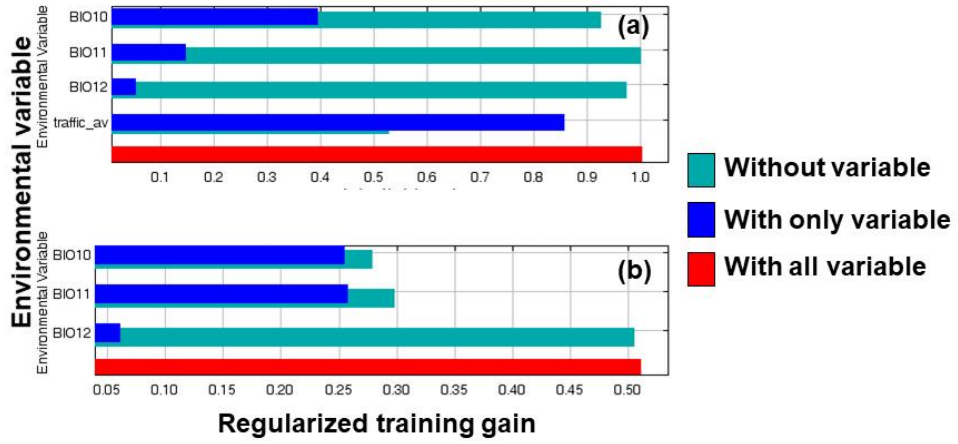


Fig. 5. Jackknife test for relative importance of selected variables in each model (a) Relative importance of four variables in the 2013 Climate+Traffic model; (b) Relative importance of three variables in the 2017 Climate only model.

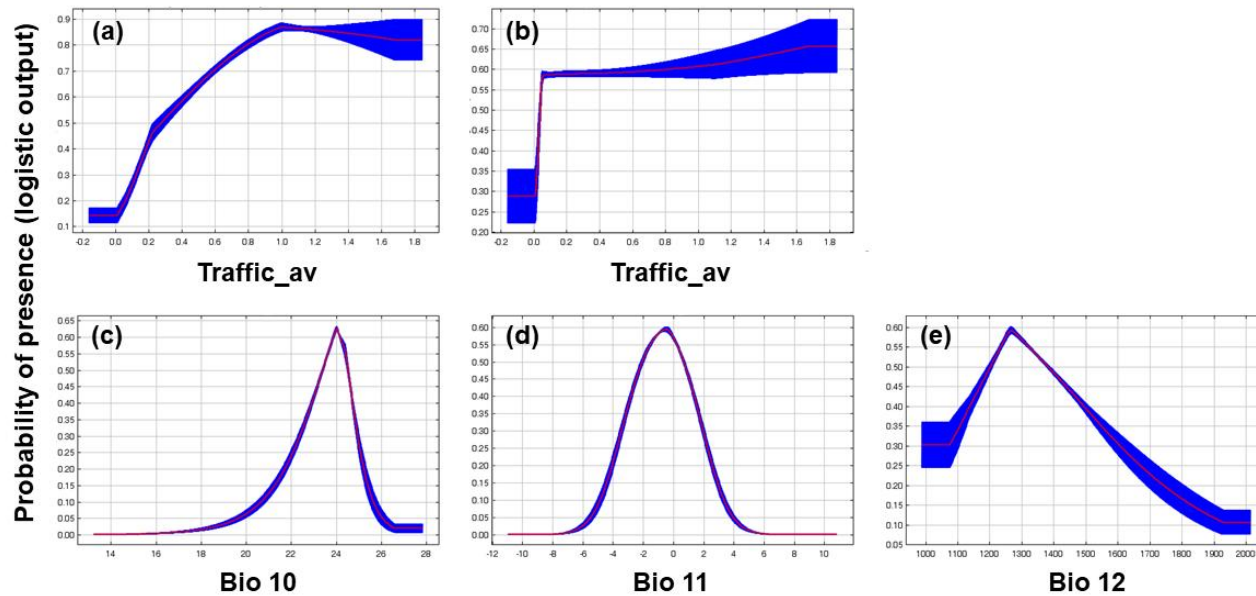


Fig. 6. Response curve of presence probability of *Metcalfa pruinosa* to environmental variables (a) Mean Traffic Volume per day (2013 Climate+Traffic model); (b) Mean Traffic Volume per day (unselected 2017 Climate +Traffic model); (c) Mean Temperature of Warmest Quarter (2017 Climate only model); (d) Mean Temperature of Coldest Quarter (2017 Climate only model); (e) Annual Precipitation (2017 Climate only model)

2-4-4. Future habitat suitability

Using 2017 Climate only model that represented the current distribution, future habitat suitability according to climate change scenario was expressed as a binary map. Threshold value for binary prediction was 0.4623, which was the maximum training sensitivity plus specificity threshold value. Logistic output value above threshold represented a suitable habitat while below threshold indicated unsuitable (Fig. 7). As a result, in 2030s and 2050s, most parts of Korea except for mountainous area and southern parts were estimated to be suitable for *M. pruinosa* to be established. In further future, 2070s and 2090s, dimension of suitable habitat would be decreased, and establishment might be possible mainly in northern parts of Korea.

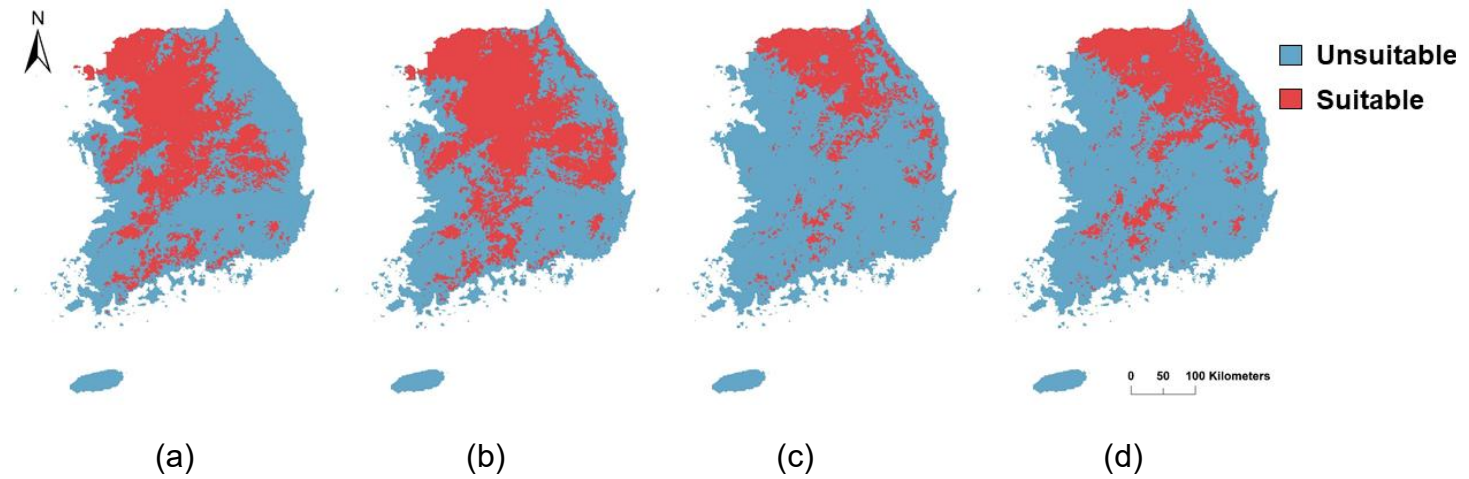


Fig. 7. Future habitat suitability of *Metcalfa pruinosa* in Korea predicted using RCP 8.5 scenario and 2017_climate model. (a) 2030s; (b) 2050s; (c) 2070s; (d) 2090s.

2-4-5. Comparison of traffic factor for *M. pruinosa* occurrence in 2013 and 2017

The traffic volume of *M. pruinosa* occurred points in 2013 was significantly higher than the one in 2017 (t value = 5.24, $p < 0.001$). Newly occurred points after 2013 had significantly ($p < 0.05$) lower traffic volume than early occurred points (i.e., 2013).

2-5. Discussion

Current and future distribution of *M. pruinosa* have already been proposed by Byeon et al. (2017). Byeon et al. (2017) modelled potential distribution composed by physiological parameters against environmental conditions using CLIMEX software. They predicted that the habitat suitability of *M. pruinosa* is mainly high along coastline, but the current distribution turns out to be the opposite from their prediction. Such discrepancy would be caused that they used a deterministic modelling approach with predetermined parameters without including non-climatic constraints (Colwell and Rangel, 2009). The results of deterministic models are close to prediction of fundamental niche constructed with inputted environmental variables (Sutherst and Maywald, 1985; Elith, 2016), and do not explain occupied habitat. In other words, it is inevitable for distribution prediction based on only predetermined physiological parameters for a species to show discrepancy with actual distribution, because it cannot consider factors that may affect the establishment of a species, such as interspecific competition (Sutherst and Maywald, 1985; Elith, 2016). These models would be very useful for the evaluation of establishment risk or

surveillance of non-native species before they spread out (Liebhold et al., 2016), but have less demanded after that (Fig. 5). At present, delineating the distribution of *M. pruinosa* is more needed for management this pest in Korea. To delineate the potential distribution of *M. pruinosa* in Korea, correlative modelling methods using sufficient information related to occupied habitats would be better than deterministic methods. In addition, the correlative modelling approach would give why this pest is abundant or absent within concerned area (Elith and Leathwick, 2009; Lockwood et al., 2013).

In this study, MaxEnt, one of popular methods among correlative methods for species distribution models, was applied. Correlative methods including MaxEnt require a key precondition that species are equilibrium with its surrounding environments (Elith and Leathwick, 2009). Thus, the reliability of the modelling results could be acquired by proving that the distribution of the target species has almost reached as stable status (Elith and Leathwick, 2009). The result of this study showed that the colonies distance of *M. pruinosa* became stable to expected distance and it was verified its populations spread out whole territory of Korea recently (Fig. 1b and Fig. 2). By using these methods, the reliability of the MaxEnt modelling could be

improved and granted.

It is showed that the spreading of *M. pruinosa* in Korea was not a continuous spread, but a stratified spread in which stochastic long-range dispersals and natural diffusions were mixed (Liebhold and Tobin, 2008). This is because average distances between established areas which *M. pruinosa* were present further than average distances of the contagiously neighboring administrative units. Thus, this invasive pest might have moved long distances using mechanisms such as wind, stream, wild animals, anthropogenic factors, and so on. Especially, in case of *M. pruinosa* in Korea, super long-distance dispersal events (more than 50km apart from founder population) were frequently occurred in the spreading phase in spite of extinction risks in new regions due to Allee effect (Liebhold and Bascompte, 2003). In other words, population size over Allee threshold has been successfully supplied to new regions in just a few years or 1 year. This phenomenon implies that there have been efficient mechanisms for carrying *M. pruinosa* in Korea. These mechanisms might have facilitated long-distance transportation and triggered consequent fast expansion of *M. pruinosa*. Shigesada and Kawasaki (2002) have also suggested and mathematically proven that the larger the Allee radius

(r_A), the distance that satellite population able to establish itself from neighbor colonies, the faster spreading rate in stratified spread model. This would be main reason that the spread rate of *M. pruinosa* in Korea was much faster than natural spread rate of 0.2 - 0.5 km/year (Kahrer et al., 2009).

In general, traffic volume itself may be unimportant than temperature and precipitation, among factors affecting habitat suitability of insects (Bradie and Leung, 2016). However, traffic factor that might relate to human mediated long-distance transportation of *M. pruinosa* was found to be the most important variable showing great contribution in the early spreading model (i.e., 2013 Climate+Traffic). From results of this study and previous studies, human related factors could strongly affect the distribution of *M. pruinosa* at the early spreading phase. Whereas, the contribution of traffic factor in 2017 was sharply decreased and performance of the model with this factor was poor. It appears that once *M. pruinosa* dispersed across the country at a certain level which difference is not found in the traffic factor between occupied and unoccupied areas, the traffic factor would be less important for determining its distribution. This is same meaning of result that the traffic volume at newly *M. pruinosa* occurrence points

in 2017 was lower than the 2013 occurrence points. Because *M. pruinosa* already occupied the areas of low traffic in 2017, so its occurrence could not be explained by traffic factor anymore.

The current distribution model for *M. pruinosa* in Korea (i.e. 2017 Climate only) well described its observed occurrence with only three environmental variables (i.e., Bio 10, Bio 11, and Bio 12) except for traffic variable (i.e. Traffic_av). It is interpretable that the mean temperature of the warmest quarter (i.e., Bio 10) positively affects *M. pruinosa* development and survival until the optimal temperature. Temperature higher than the optimal range negatively affected to occurrence of *M. pruinosa*, perhaps due to its ectodermal characteristics (Chapman, 1982). Higher the mean temperature of the warmest quarter (i.e., Bio11) is expected to be helpful for the establishment of *M. pruinosa*. However, high temperature after the optimal temperature, around 0 °C, was expected to negatively affect its occurrence in this study. Lee et al. (2016) reported that *M. pruinosa* required a certain amount of cooling periods to break its overwintering diapause state. Thus, higher temperature above a certain temperature might negatively affect the occurrence of *M. pruinosa* in Korea. Annual precipitation (i.e., Bio 12) has also optimal condition as the

temperature-related factors because too low and high humidity could decrease its development and survival, and increase disease occurrence (Chapman, 1982).

Among these three important environmental factors (i.e., Bio 10, Bio 11, and Bio 12), the mean temperature of the warmest quarter (i.e., Bio 10) was the most important factor, contributing to 53.4 % of the occurrence of *M. pruinosa*. The developmental stage of *M. pruinosa* is the adult stage in Korea at the warmest quarter. Adults of *M. pruinosa* need relatively long pre-oviposition period (i.e., over one month) considering its body size (Yoon et al., 2012). They should also move from herbaceous plants to arboreal plants for oviposition (Santini and Lucchi., 1994). Moreover, oviposition itself needs a lot of energies (Chapman, 1982). Results of this study and previous studies indicate that successful oviposition of *M. pruinosa* might determine its establishment. It might be highly affected by temperature in newly invaded areas.

The mean temperature of coldest quarter (i.e., Bio 11) as another environmental factor was found to be as important as the mean temperature of the warmest quarter by contributing to 45 % of the occurrence of *M. pruinosa* in the model in this study. This period is

related to overwintering of *M. pruinosa* (Lee et al., 2016). This indicates that optimal temperature during overwintering would be important for the occurrence of *M. pruinosa*. The other environmental factor, annual precipitation (i.e., Bio 12), affected the occurrence of *M. pruinosa* although effects were expected to be inappreciable (i.e., 1.6 %).

It is generally believed that propagule pressures (i.e., invasion amount, frequency, and quality) would be as important as its surrounding environmental conditions for alien species to successfully establish its populations in newly invaded areas (Lockwood et al., 2013). After successfully establishing its populations, population growth, disperse, and impact are more affected by surrounding environmental conditions than by propagule pressures. Therefore, the 2017 model excluding traffic factor should be used to predict future distributions or habitat suitability of *M. pruinosa* according to RCP 8.5 scenarios.

Results of this study predicted that *M. pruinosa* would increase its distribution until 2030s. Thus, managements for *M. pruinosa* would be required to stop or slow its spreading into unreached area along with density control in established area. Management efficiency could

be increased by choosing appropriate timing (from around adults to first instar) because temperature during these developmental stages affected its distribution in this study. It is difficult to manage them during other stages due to its high activities and polyphagous characteristics (Ciampolini et al., 1987). Therefore, studies related to these periods such as using trap plants to attract just hatched adults, chemical or natural pesticides for overwintering eggs, and the occurrence model of the first instar should help to manage *M. pruinosa* populations in Korea.

In conclusion, this study proved that human-related factor (i.e., traffic volume) affected the rapid spreading of *M. pruinosa* in Korea in early spreading phase. It is estimated that the traffic factor aid to long-distance transportation of *M. pruinosa*. After this phase, its effects were decreased and it cannot explain *M. pruinosa* distribution anymore. This study also predicted the current and future distribution of *M. pruinosa* in Korea with MaxEnt. The predicted probability of *M. pruinosa* presence well matched with the observed current occurrence (Average AUC = 0.778 ± 0.050). Temperatures during adult and egg stages affected the distribution of *M. pruinosa* indicating that the success of reproduction could determine its occurrence in most

occurred areas. Finally, the current distribution model was used to predict future habitat suitability for *M. pruinosa* under climate change scenario (RCP 8.5.) In 2030s and 2050s, most parts of Korea except for mountainous area and southern parts were estimated to be suitable for *M. pruinosa* to be established. The predicted current and future distribution of *M. pruinosa* should be helpful for preparing management plans and increasing management efficiency for *M. pruinosa* in Korea.

Chapter III.

Phenology modelling of egg hatching and first instar falling of *Metcalfa pruinosa*

3-1. Abstract

Metcalfa pruinosa (Say) hibernates as eggs beneath bark and/or in cracks of tree branches, and then substantial numbers of first instar nymphs fall from the trees and move to other host plants. Knowing the timing of egg hatching and falling of the first instar nymphs would be key for controlling *M. pruinosa*. In this study, the hatching of overwintered *M. pruinosa* eggs and falling of the first instar nymphs from trees were monitored in several areas of Korea. The distribution models of egg hatching time and first instar falling time of *M. pruinosa* from host trees were then developed based on degree-days with a lower development threshold of 10.1 °C. January 1, commonly used in degree-day models, and March 18, an empirical date estimated in this study were examined as starting points for degree-day accumulation. The egg hatching and first instar falling models both used January 1 because the starting point performed better. The 50% appearance and falling times of the first instar nymphs were predicted to be 360.50 DD and 452.23 DD from January 1, respectively, indicating that newly hatched nymphs stayed on the trees for about a week (i.e., 91.74 DD). Using these models, changes in the

population density of the first instar nymphs of *M. pruinosa* on the trees were simulated, and the optimal control time range targeting the nymphs on the trees was deduced. The control time for nymphs on ground plants bordering the trees was suggested by the first instar falling model, along with observations of population density on the ground plants.

Keywords: *Metcalfa pruinosa*; Overwintered eggs; egg hatching; nymph falling; degree-day model

3-2. Introduction

The citrus flatid planthopper, *Metcalfa pruinosa* (Say) (Hemiptera: Flatidae), originating in eastern North America (Metcalfa and Bruner, 1948), has caused serious economic damage in many European countries and Korea (Preda and Skolka, 2011; Kim et al., 2019). Although *M. pruinosa* is not problematic in its native regions (Alma et al., 2005), it has caused serious economic impacts in invaded countries because of its mass occurrence (Wilson and Lucchi, 2001). In Italy, a yield loss of 30 – 40% of the soybean crop was reported (Ciampolini et al., 1987). In Korea, *M. pruinosa* has been a problem in various agricultural crops and fruit trees, such as ginseng, sesame, perilla, grape, peach, pear, persimmon, apple, and mulberry. (Kim and Kil, 2014; Seo et al., 2019). *M. pruinosa* directly causes shoot stunting, plant vitality reduction, and plant wilting (Strauss, 2010), and indirectly causes sooty molds on plants by excretion honeydews, which have been also considered a nuisance problem in urban areas (Kim et al., 2011).

M. pruinosa is univoltine, and hibernates as eggs beneath the bark and/or in the cracks of tree branches (Dean and Baily, 1961;

Strauss, 2010). In spring, after the eggs are hatched, substantial numbers of first instar nymphs fall from the tree branches and move to herbaceous plants nearby (Park et al., 2019; Seo et al., 2019). The fallen nymphs persistently disperse to surrounding vegetation or crop fields, and this characteristic makes controlling *M. pruinosa* difficult. Adults return to the trees for oviposition soon after emergence (Park et al., 2019), but are not proper targets for control because the sucking damage caused by the adults is less concerning than the nymphs (Lauterer and Malenovsky, 2002) and the adults can easily escape chemical sprays by flight (Duso, 1984). The effective target for the chemical control of *M. pruinosa* is probably the first instar nymphs clumping around the trees. In Korea, chemical spraying for the control of *M. pruinosa* has been implemented, targeting nymphs present in orchards, crop fields, and urban parks; and managers usually spray based on the observed nymph density. Wax filaments produced by growing nymphs could be a good indicator of the abundance of *M. pruinosa* nymphs (Strauss, 2010), but they are hard to detect in newly hatched young nymphs due to their very small body size and low wax secretion. Thus, when the white wax of nymphs is detected, the nymphs could have already damaged the plants. Predictive studies for

timing the appearance and movement of the first instar nymphs of *M. pruinosa* would be useful for deciding the optimal timing to control this pest in various landscapes because, despite being the main target of effective control, the first instar is most invisible.

Several studies have addressed the seasonal occurrence of *M. pruinosa* in temperate regions (Wilson and McPherson, 1981; Duso, 1984; Wilson and Lucchi, 2001; Souliotis et al, 2008; Balakhnina et al., 2014; Lee et al., 2016; Park et al., 2019). Lee et al. (2016) reported the lower developmental threshold (LDT) of overwintered eggs to be 10.1 °C in laboratory conditions. They also proposed an egg hatching model of *M. pruinosa* with a starting degree-day accumulation date of April 1, for which no explanation was given but is needed. *M. pruinosa* nymphs moved from their overwintering trees to other host plants mainly from the end of May to the middle of June in a persimmon orchard (Park et al., 2019). However, no predictive model has been developed yet. Therefore, this study was conducted to (1) determine a proper starting degree-day accumulation point for models for the phenology of *M. pruinosa*, (2) develop an egg hatching model of *M. pruinosa* based on degree-days, (3) develop a falling model of the *M. pruinosa* first instar nymphs from the trees to the ground based on

degree-days, and (4) discuss control options for *M. pruinosa* based on the simulation results using the developed models.

3-3. Materials and methods

3-3-1. Data collection for model development

The hatching of *M. pruinosa* overwintered eggs was monitored in Yeoncheon, Seoul, Suwon, and Yesan in Korea in 2018, and in Yeoncheon, Chuncheon, Seocheon, and Paju in Korea in 2019 to develop an egg hatching model (Table 1). The monitoring was carried out by observing appearance of first instar nymphs from samples of tree branches infested with *M. pruinosa* eggs. Because *M. pruinosa* adults prefer the trees with rough surface of branches (Choi et al., 2018), this characteristic was considered for efficient sampling when the branch samples were collected. In each site, ten trees (e.g., *Robinia pseudoacacia*, *Zelkova serrata*, and *Cornus officinalis*) were selected and five branches per tree were cut in late April. The excised branches were 10 cm in length from the base and > 1 cm in thickness because *M. pruinosa* adults prefer to lay eggs on thicker branches (Choi et al., 2018). Then, five branches from the same tree were put into a nylon mesh pouch (30 cm × 20 cm, 104 × 94 mesh, BugDorm, Talchung, Taiwan). Thus, ten pouches of branches were prepared in each site. These pouches were put into a meshed fabric bag (90 × 90 cm, Eggthirty, Namyangju, Korea) to protect the nylon pouches. The

bag was hung on a tree randomly selected in each site. The pouches were checked at one-week intervals for the appearance of *M. pruinosa* nymphs, except for the monitoring in Seoul in 2018, which was conducted every two days, from late April until no further egg hatching occurred. At each observation, the nymphs were counted and removed from the pouches.

The falling of *M. pruinosa* first instar nymphs from the trees to the ground was monitored in the same sites as the egg hatching monitoring in 2018 and 2019 (Table 1). Clear, sticky panel traps (25 cm × 15 cm, Greenagrotech, Gyeongsan, Korea) were used for capturing the nymphs falling from the trees. The traps were installed 1 m above the ground around the trees in which the *M. pruinosa* eggs were found. In each site, three to six trees were randomly selected. Two rods (5.2 mm diameter × 160 cm height, Eden Plant Support, Gimhae, Korea) were embedded 40 cm vertically into the ground at a position 1 m away from each selected tree to fix the sticky traps. The distance between the two rods was the trap width, and the rods were fixed with connectors and metal sticks to maintain the width (Fig. 1c). Then, the 50 cm tips of the rods were bent at 45° angles in the opposite direction of the trees, and a sticky trap was fixed on the tilted parts of

two rods (Fig. 1a; b). The reason for the tilted trap installation was to increase the capture capacity of the traps. The traps were changed on the same date as the egg hatching monitoring. The nymphs caught on the traps were counted under a microscope in the laboratory.

Air temperature data from the weather station closest to each monitoring site were obtained from the Korea Meteorological Administration website (<http://web.kma.go.kr/>). The temperature data were paired with field observation data of *M. pruinosa* egg hatching and nymphal falling taken at each monitoring site. The daily maximum and minimum temperature data were used for degree-day calculations using the sine wave method.

Table 1. Description of the study sites and sampling information for model development.

| Site | Year | Latitude and longitude (°, min, sec.) | Egg hatching | | First instar falling | |
|-----------|------|--|------------------|---------------------|----------------------|----------------|
| | | | No. hatchings | First appearance | No. trap catches | First catch |
| Yeoncheon | 2018 | 38°04'59.0" N, 127°04'36.7" E | 194 | 5/16 | 85 | 5/29 |
| Seoul | 2018 | 37°27'27.4" N, 126°56'54.4" E | 188 | 5/18 | 93 | 5/27 |
| Suwon | 2018 | 37°15'57.8" N, 126°59'11.1" E | 24 | 5/21 | 15 | 5/28 |
| Yesan | 2018 | 36°44'11.9" N, 126°49'17.9" E | 58 | 5/24 | 16 | 5/28 |
| Yeoncheon | 2019 | 38°04'59.0" N, 127°04'36.7" E | 92 | 5/21 | 255 | 5/27 |
| Chuncheon | 2019 | 37°45'16.8" N, 127°44'10.9" E | 338 | 5/20 | 142 | 5/20 |
| Seocheon | 2019 | 36°10'23.9" N, 126°46'28.0" E | 156 | 5/22 | 53 | 5/22 |
| Paju | 2019 | 37°57'00.8" N, 126°55'20.9" E | 171 | 5/21 | 29 | 5/27 |

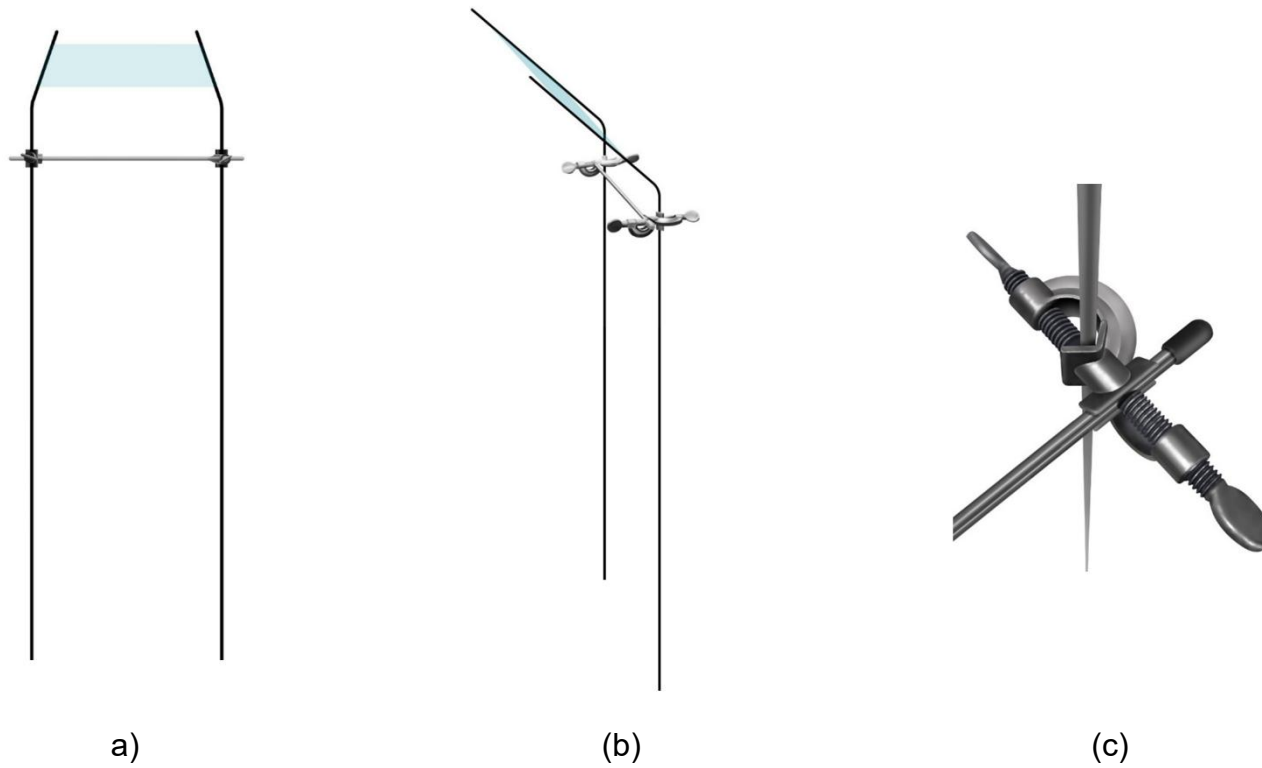


Fig. 1. Installation of clear sticky panel trap to capture the first instar nymphs falling from the trees (a) Front view; (b) Side view; (c) Connector to maintain the width of two rods as the trap width.

3-3-2. Starting point of degree-day models

Two starting dates for degree-day accumulation were examined to predict the phenology of first instar nymphs of *M. pruinosa*. One was January 1, commonly used in degree-day models from a practical standpoint (Jones et al., 2008), and the other was a starting date empirically determined from egg hatching data sets in this study. The latter starting date was estimated as the point producing the lowest variation of accumulative degree-days to the first egg hatch for synchronizing the first appearance of nymphs by degree-days (Rigamonti et al., 2011). A total of 89 dates from February 1 to April 30 were potentially considered, and variations in accumulative degree-days from the potential starting dates to the first egg hatch date of each monitoring site were compared. Because egg hatching was not observed daily, the first egg hatching date of each monitoring site was estimated by extrapolating the first and second appearance of nymphs from the egg hatching data (Fig. 2). The accumulative degree-days from each potential starting date were calculated, using temperature data and a LDT of 10.1 °C for the eggs. Among the potential 89 dates, a proper starting date was selected based on the coefficient of variation (CV) of the accumulative degree-days of eight data sets (two

years \times four sites). Finally, along with this empirically selected starting date, January 1 was examined as a starting point for the degree-day models.

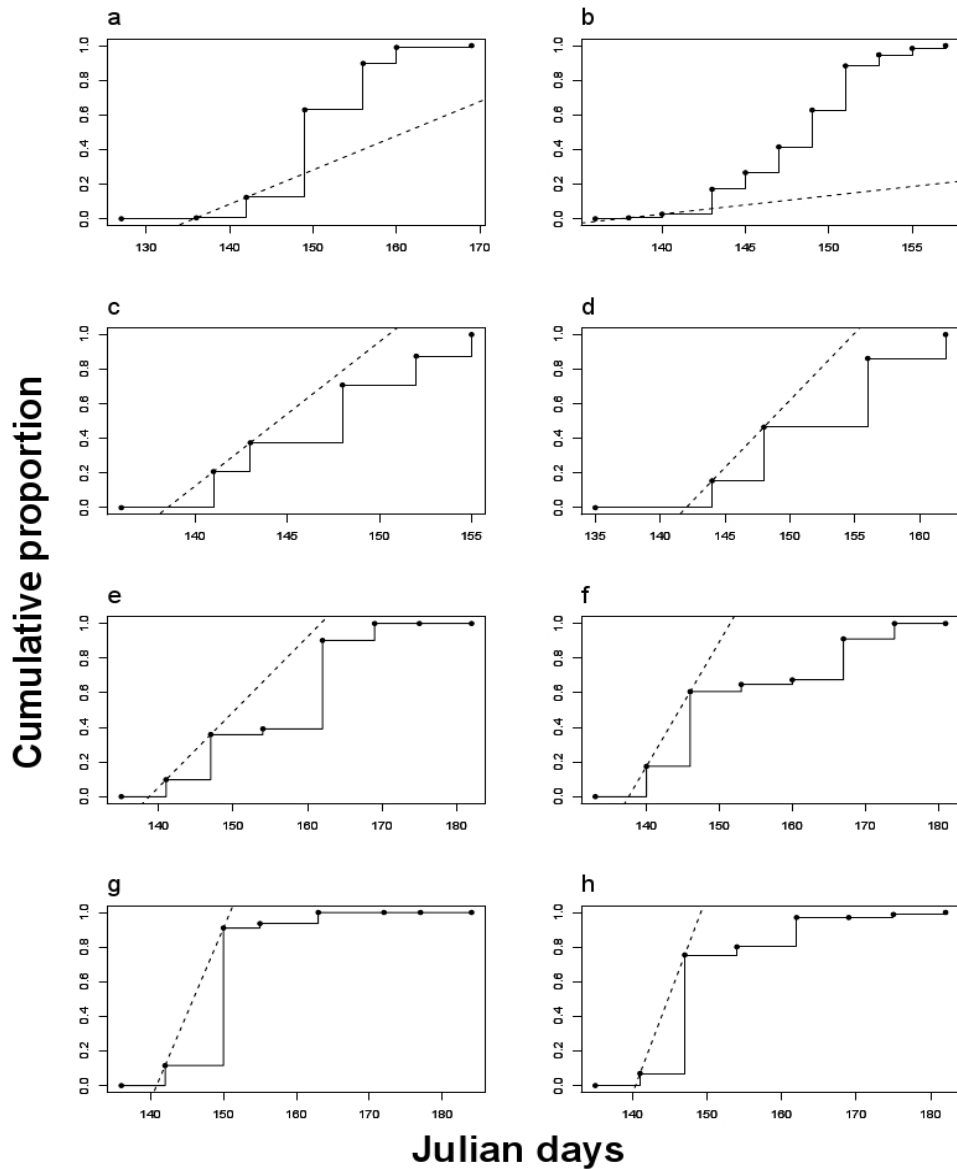


Fig. 2. Estimation of first egg hatching date in (a) Yeoncheon, (b) Seoul, (c) Suwon, and (d) Yesan in 2018, and (e) Yeoncheon, (f) Chuncheon, (g) Seocheon, and (h) Paju in 2019 (●, Observed points; ---, Extrapolation line).

3-3-3. Estimation of model parameters

The eight data sets from the egg hatching and nymphal trap catch studies in the fields were converted to cumulative percent proportions of the first instar occurrence and falling, respectively. Each cumulative proportion (%) was fitted against the time (degree-days) accumulated from the two candidate starting points (i.e., January 1 and the selected date with the smallest CV) by the two-parameter Weibull function.

$$F(x) = 100 \times [1 - \exp((-x/\alpha)^\beta)] \quad (\text{Eq. 1})$$

where $F(x)$ is the cumulative proportion (%) of the appearance or falling of the first instars, for the respective models; time x is the degree-days, and α and β are the scale and shape parameters of the Weibull function, respectively. The parameters were estimated by using function 'nls' in R 3.5.1 (R core team). Four models (egg hatching and first instar falling models with each of the two starting points) were finally constructed.

3-3-4. Validation and accuracy of models

Independent field monitoring data were constructed to validate the models apart from the data for model development. The egg hatching data were collected in Yeoncheon (38°04'47.7" N, 127°04'37.8" E), Chuncheon (37°45'16.1" N, 127°47'18.7" E), Paju (37°59'05.1" N, 126°58'59.5" E), and Seocheon (36°11'03.8" N, 126°46'20.1" E) in 2019. The trap catch data were collected in Yeoncheon (38°04'47.7" N, 127°04'37.8" E) in 2017 and Seoul (37°27'27.4" N, 126°56'54.4" E) in 2019. All validation data from the fields were obtained by the same method described previously at one-week intervals. In addition, the 50 % appearance times of the first instar nymphs in the three sites in Korea from the previous study were used (Lee et al., 2016).

To determine a starting date for the models that better described both the appearance and falling of the first instar nymphs, the models were grouped into two groups, one using January 1 and one with a potential date selected by CV comparison. Then, the two groups were compared. Whether the predictive performance differed according to different starting points was examined. For this, Julian dates corresponding to the cumulative proportion of validation data

were calculated by each model for the two groups. Linear regression analysis was then performed between the predicted dates of the two groups, and estimates of the parameters were calculated with 95% confidence intervals (CI). The closer the slope and intercept of the regression line are to one and zero, respectively, the closer the predictive ability is between the two groups of models (Mesplé et al. 1996). Then, the root mean square error (RMSE) of each group was calculated to select the starting point with better performance.

$$\text{RMSE} = \sqrt{\frac{\sum_{i=1}^n (D_{\text{predicted}} - D_{\text{observed}})^2}{n}} \quad (\text{Eq. 2})$$

where $D_{\text{predicted}}$ is the Julian date predicted by the models, D_{observed} is the actual Julian date of the validation data, and n is the number of observations. The models producing smaller RMSE were chosen to forecast the egg hatching and nymphal falling of *M. pruinosa*. However, if no significant difference in accuracy was found between the two groups (less than one day), the models created by degree-days accumulated from January 1 were selected for generality.

3-3-5. Change of nymphal density

After the *M. pruinosa* eggs are hatched, the first instar nymphs move to the ground from the trees. Thus, their relative population on the trees during the period of first instar stage can be estimated using the cumulative proportion of egg hatching and the cumulative proportion of the first instar nymphs moving from the trees to the ground. The relative population size of the *M. pruinosa* first instar nymphs on the trees at x degree days was simulated by the following model.

$$F_3(x) = F_1(x) - pF_2(x) \quad (\text{Eq. 3})$$

where $F_3(x)$ is the relative proportion (%) of first instar population on the tree over time, and $F_1(x)$ and $F_2(x)$ are the cumulative proportions estimated from the egg hatching model and the falling model of the first instar nymphs, respectively. The parameter p is the falling proportion of the first instar nymphs of the total population. The $F_3(x)$ was simulated with different values of p ranging from 0.1 to 0.9 because the proportion of falling nymphs is unknown. The time range of the relative maximum population density on the trees with

different values of p was calculated through this model.

In 2019, the actual density of *M. pruinosa* nymphs on herbaceous plants around the trees was observed in Yeoncheon and Chuncheon, where the hatching and falling of the first instar nymphs were monitored (Table 1). Five plant leaves were randomly selected within a meter from a tree trunk, and the number of nymphs on the leaves was counted by the naked eye. The sampled herbaceous plants were *Hosta* spp. in Yeoncheon and *Parthenocissus tricuspidata* in Chuncheon. A total of 30 plant leaves around six trees were examined on each sampling occasion. Nymph density monitoring on the ground plants was conducted every week from early May before the first emergence of adult *M. pruinosa*. Finally, whether changes in the nymph population on the ground could be described well by the constructed models was verified.

3-4. Results

3-4-1. Starting date of degree-day models

The CVs of degree-days accumulated from the potential starting date to the estimated first egg hatch date for eight occurrence data sets varied according to the starting dates (Fig. 3). The CV of the cumulative degree-days increased as the starting date of the degree-day accumulation and the first egg hatch date became closer. The CV was the smallest on March 18. Therefore, this date and January 1 were applied for model development and were compared for model performance.

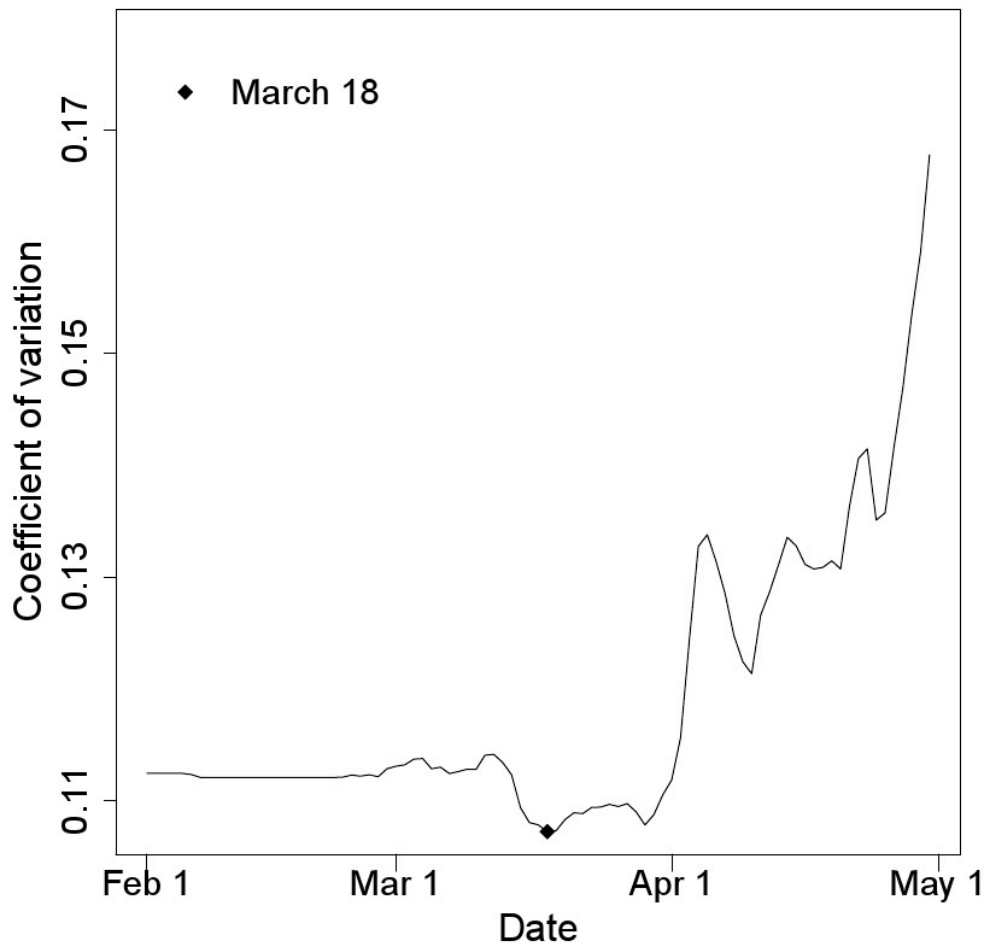


Fig. 3. Coefficient of variation (CV) of the cumulative degree-days (DD) from the potential starting date to the first hatch of *Metcalfa pruinosa*; March 18 (◆) produced the lowest CV.

3-4-2. Egg hatching and first instar falling models

All models with a starting date of January 1 or March 18 provided a good fit for egg hatching and the first instar falling of *M. pruinosa* (Table 2, 3). The Julian dates predicted by the models with January 1 or March 18 as start dates were almost identical. Neither the slope or intercept of the regression line was significantly different from one and zero, respectively (i.e., 1:1 line) ($P > 0.05$; Table 3). The models with January 1 as a start date were better because they were closer to the observed data (Table 3). Therefore, the models with a starting point of January 1 were selected for forecasting the appearance and falling time of the first instar nymphs of *M. pruinosa*. There was a long time gap between the appearance and falling of the first instar nymphs of *M. pruinosa* and this time gap gradually increased with increasing daily degree-day (Fig. 4 and 5). The time gap between 50% egg hatching and 50% first instar falling was 91.74 DD, which was about a week in Korea (Table 4).

Table 2. Estimated parameter values for the distribution model of egg hatching time and first instar falling time of *Metcalfa pruinosa*

| Model | Starting date ¹ | Parameter | |
|----------------------|----------------------------|---------------------------|--------------------------|
| | | α (Mean \pm SEM) | β (Mean \pm SEM) |
| Egg hatching | 01-Jan | 379.554 \pm | 7.115 \pm |
| | | 4.4365* | 0.7276* |
| | 18-Mar | 362.466 \pm | 6.907 \pm |
| | | 4.2109* | 0.6798* |
| First instar falling | 01-Jan | 476.119 \pm | 7.121 \pm |
| | | 5.2429* | 0.6990* |
| | 18-Mar | 460.282 \pm | 6.819 \pm |
| | | 5.3532* | 0.6776* |

¹ Starting date for degree-day (LDT = 10.1°C) accumulation in each model.

* All estimated parameter values significantly different from zero ($p < 0.001$).

Table 3. Parameter values of the regression line between the Julian dates predicted by the two groups of models with different starting points, and the accuracy of each group

| Starting date | n ¹ | Linear regression | | | RMSE ³ (days) |
|---------------|----------------|---------------------------------|-----------------------|---------------------|-----------------------------|
| | | Slope (95% CI ²) | Intercept (95% CI) | <i>P</i> - value | |
| 01-Jan | | 0.99 | 1.14 | | 6.0 |
| | 34 | (0.98, | (-1.72, | <0.001 | 0.997 |
| 18-Mar | | 1.01) | 4.00) | | 6.3 |

¹ number of observations

² confidence intervals for the parameter of the regression line.

³ root mean squared error of Julian dates between the model-predicted and observed.

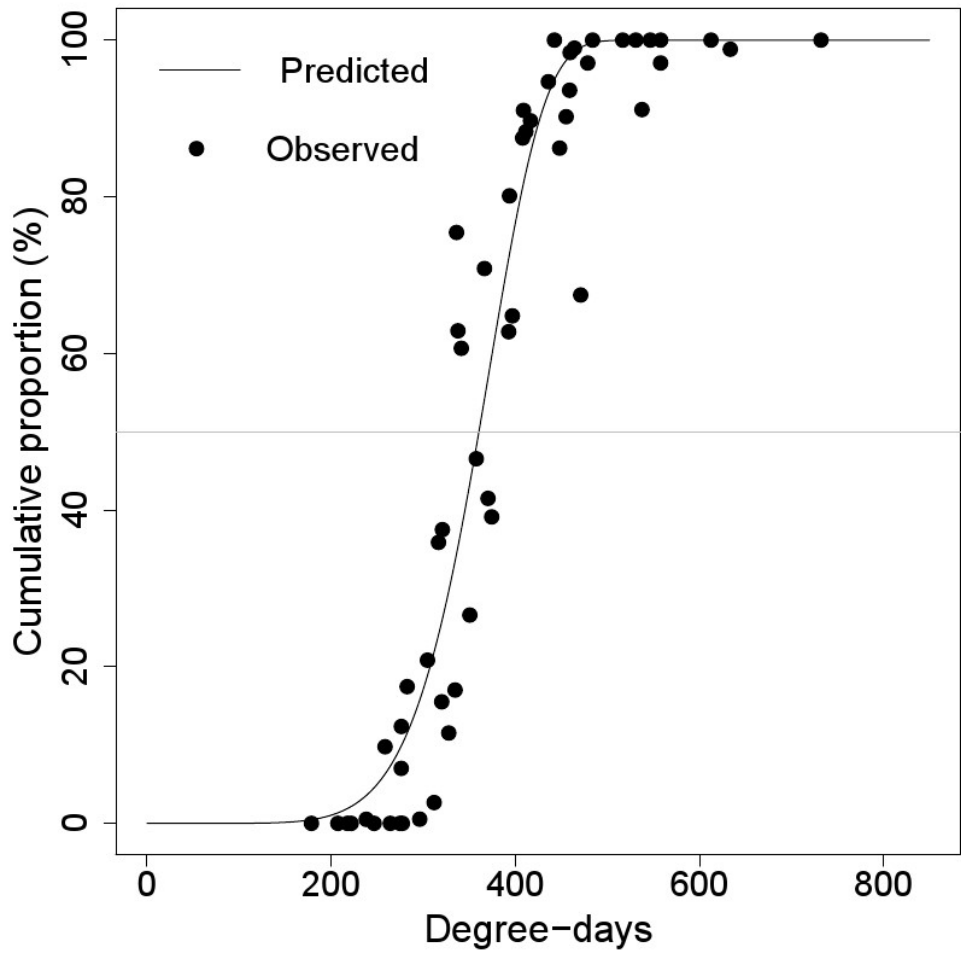


Fig. 4. Distribution model of *Metcalfa pruinosa* egg hatching time, (DD) from January 1.

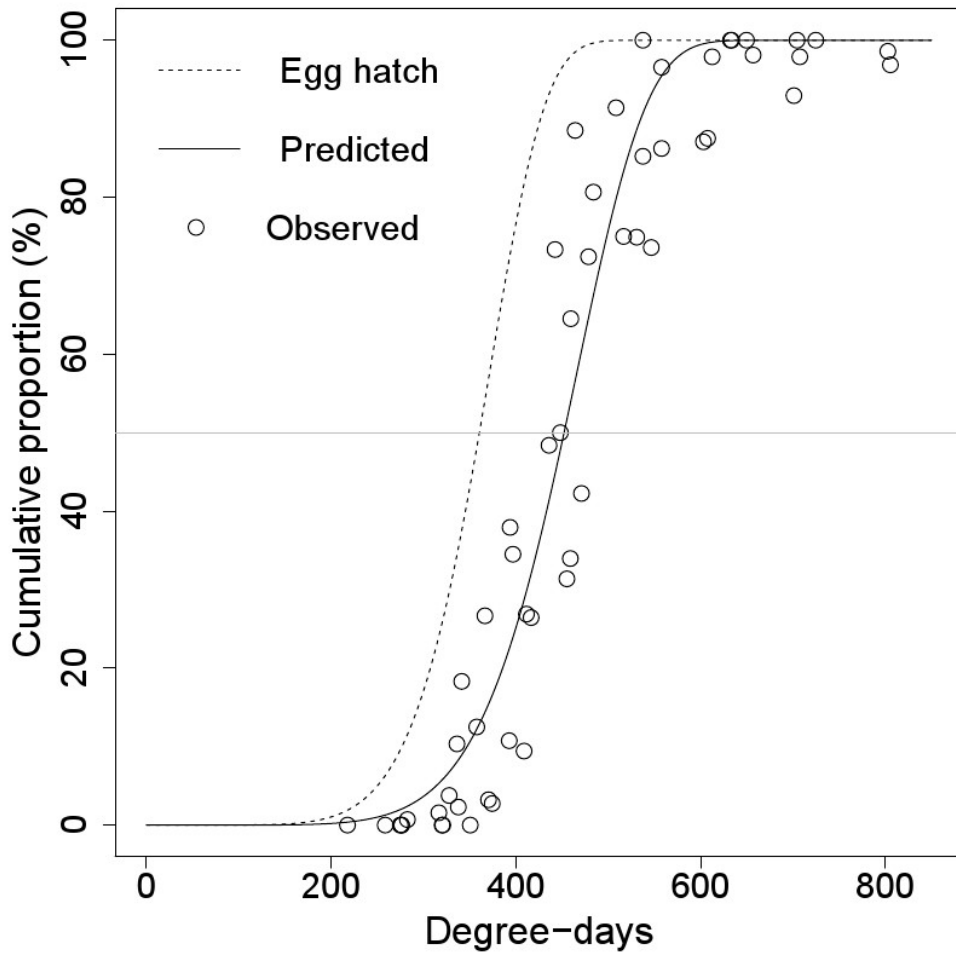


Fig. 5. Distribution model of falling time of the first instar nymphs of *Metcalfa pruinosa* from the trees, (DD) from January 1. The dashed line represents the egg hatching model of *Metcalfa pruinosa*.

Table 4. Predicted time (DD) of egg hatching and first instar falling of *Metcalfa pruinosa*

| Model | Cumulative proportion (%) | | | | |
|------------|---------------------------|--------|--------|--------|--------|
| | 10 | 30 | 50 | 70 | 90 |
| Hatching | 276.64 | 328.36 | 360.50 | 389.59 | 426.76 |
| Falling | 347.12 | 411.95 | 452.23 | 488.69 | 535.28 |
| Difference | 70.47 | 83.59 | 91.74 | 99.11 | 108.52 |

3-4-3. Change in nymphal density

The relative population size on the trees changed depending on p , the falling proportion of the first instar nymphs from the trees to the ground (Fig. 6). The maximum population density on the trees was estimated at 474 DD when $p = 0.1$, and 423 DD when $p = 0.9$. Therefore, the highest density of first instar nymphs of *M. pruinosa* on the trees would be from 423 DD to 474 DD. On the ground cover, the density of the nymphs reached a peak at ca. 530 DD, and then decreased (Fig. 7). This peak time coincided with the time of 90% proportion described by the falling model (Table 4) and did not overlap with the time of the highest density of first instar nymphs on the trees predicted by the simulation model (Fig. 6).

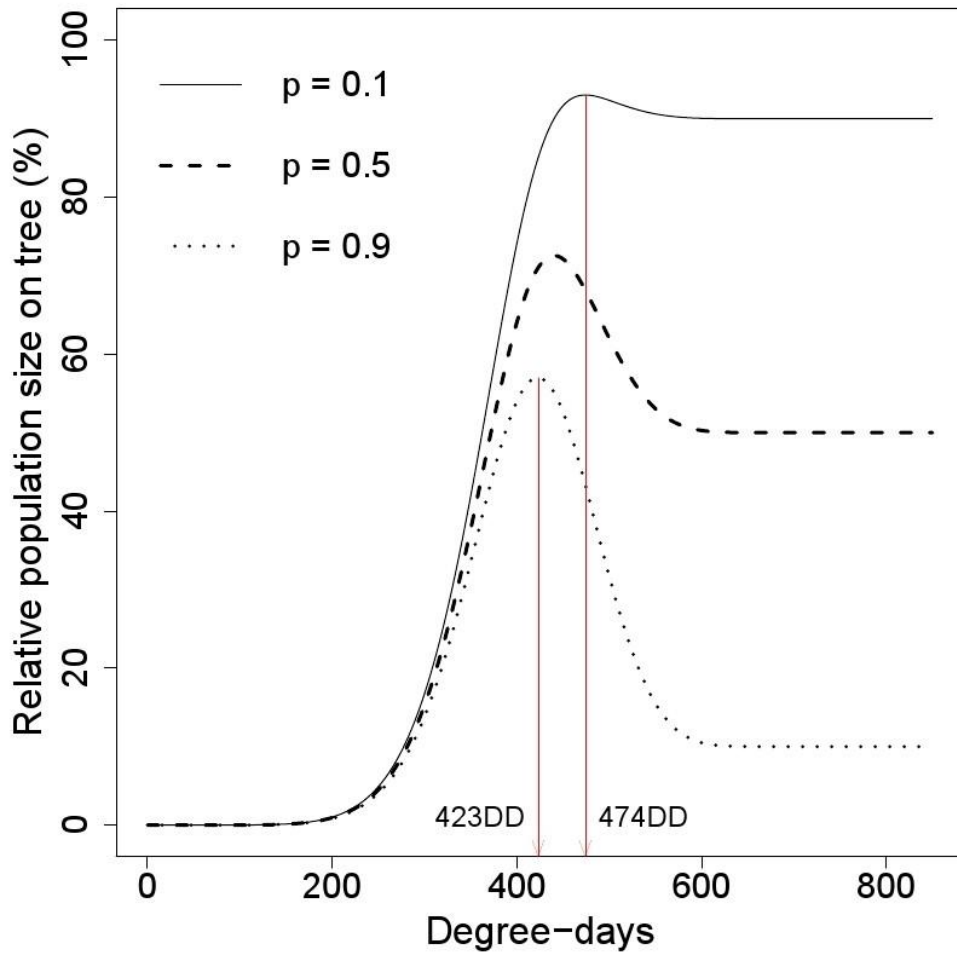


Fig. 6. Simulation model for estimating the relative population density of *Metcalfa pruinosa* on the trees. The population on the trees was calculated with different moving parameters (p) of the first instar nymph falling from the tree to the ground. The maximum density on the trees was estimated at 423 DD to 474 DD.

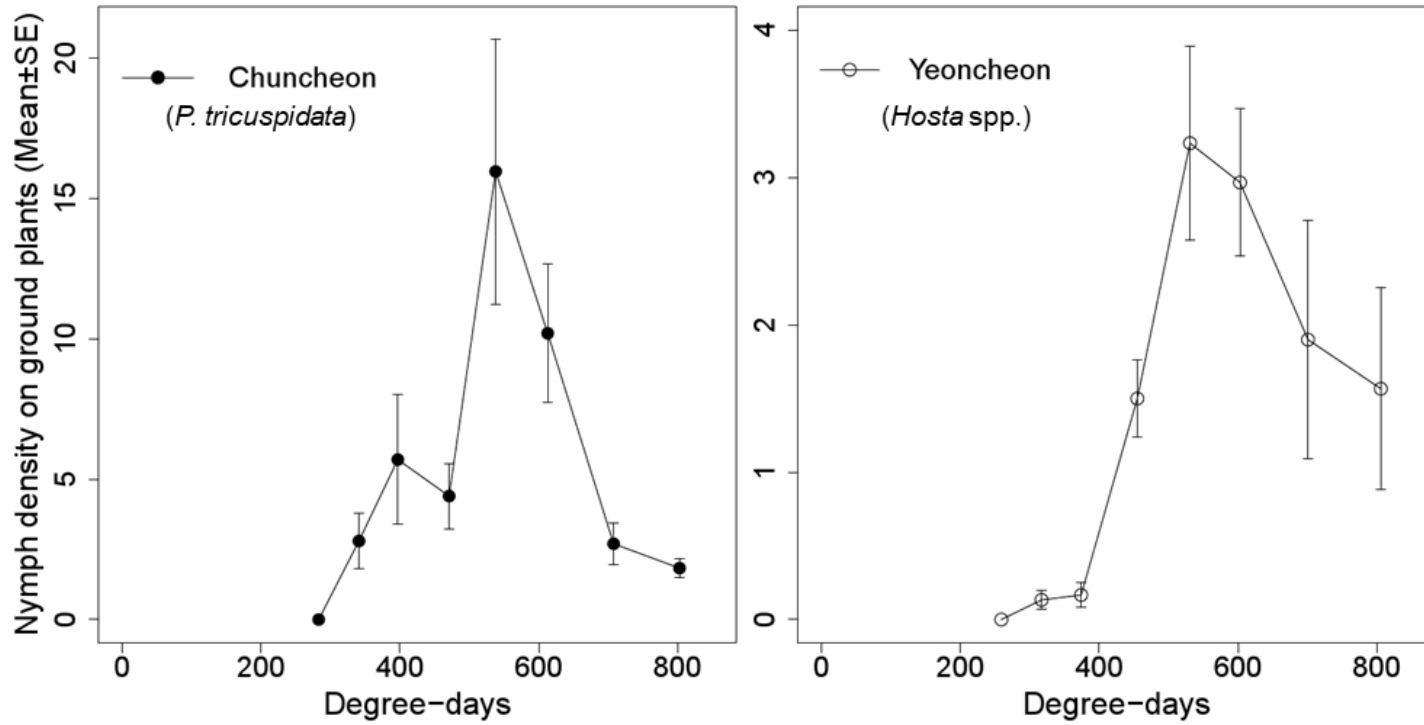


Fig. 7. Changes of *Metcalfa pruinosa* nymph densities on 30 leaves of ground plants relative to the degree days in Chuncheon and Yeoncheon.

3-5. Discussion

The starting point for degree-day accumulation is a critical component of a degree-day model for predicting insect phenology (Flint, 2012). Ideally, the starting point has to be established at a point on which the development of the target stage of the insect begins (Flint, 2012). However, in many cases, the actual time when the development of overwintered insects begins is very hard to know. Thus, many researchers have proposed different starting points, such as empirical fixed calendar date (e.g., the first date of a month such as January) or bio-fix date (e.g., the first trap catch, the first occurrence, or crop planting date) for the reliable prediction of target insect phenology (Flint, 2012). In this respect, I examined March 18 as a candidate point that showed the lowest variation in accumulative degree-days to the first hatch of *M. pruinosa*. However, the performance of models using January 1 appeared to be better than those using March 18 (Table 3), although both models well-explained the phenology of first instar nymphs of *M. pruinosa*. Therefore, models using January 1 were selected for general application to forecast the phenology of the first instar nymphs of *M. pruinosa*.

Even if the trees where overwintered eggs of *M. pruinosa* were hatching are their host plants, it was observed substantial amount of first instar nymphs were moved to other host plants by falling from trees. This behavior is thought to be a strategy for finding proper host plants that they are ease to ingest plant sap. Mouthpart of first instar nymphs of *M. pruinosa* are very short, less than 0.5 mm (RDA, 2015), thus they have to move to leaves or stems of host plants for sap feeding by piercing to plant tissue (Seo et al. 2016). For hatched nymphs, falling from trees could be an efficient way to find proper host plants. In fact, because of broad host range of *M. pruinosa*, it may be more efficient to fall down from trees than move to leaves of trees they are hatching.

The phenology models in this study showed that newly hatched nymphs of *M. pruinosa* did not fall immediately. Rather, most of the newly hatched nymphs stayed on the trees for a certain period and then fell to the ground. This delayed falling pattern of *M. pruinosa* nymphs matched field observed nymphal density on the ground cover (Fig. 7). In the predicted 90% hatching time of the eggs, 427 DD, the nymphal density on ground plants was relatively low, indicating that many nymphs still remained on the trees at that time. Therefore, if

control actions needed to be implemented, the time when the first instar nymphs of *M. pruinosa* are gathered on trees would be an effective timing to control them. Through a model of population changes induced by both the appearance and falling of nymphs, the control time to target nymphs on the trees was from 423 DD to 474 DD were estimated. During this time range, young nymphs would be present at high density on the trees, and 88.5 – 99.3 % of the *M. pruinosa* eggs would hatch to first instar nymphs that are no longer protected by eggshells or the bark of trees against chemical sprays. Therefore, chemical application during this time period would reduce the potential damage of *M. pruinosa*. This action will be applicable in various environments, such as orchards, unmanaged trees around crop fields, and roadside trees.

In the preliminary study, I found that the frequency of nymphs falling from trees was negatively correlated with the distance from the trees, i.e., within 10 m (unpublished data). This indicates that the chance of nymphs direct falling onto crops is very low in fields where they are located more than 10 m from trees with overwintering habitats of *M. pruinosa*, whereas crop damage by nymphs would be inevitable in crop fields closely bordering overwintering habitats of *M. pruinosa*.

Ciampolini et al. (1987) reported that an infestation of *M. pruinosa* nymphs begins from trees bordering the fields and expands toward the center in soybean fields. Likewise, the field observation in this study showed once the nymphs landed on the ground, they dispersed to other host plants gradually over time. The nymphal density on the ground plants around the trees peaked near the predicted time of 90% completion of first instars falling from the trees (535 DD), and then drastically decreased, probably due to the dispersal of the nymphs. Thus, control actions in the crop fields adjacent to trees around 535 DD may be another option. This action includes chemical application in the efficient timing and locations to control the fallen nymphs in crop fields before they spread over other crop plants. It is also applicable to ground plants in a variety of landscapes where *M. pruinosa* massively appeared. In crop fields sufficiently far from overwintering habitats where the nymphs cannot directly land, the immigration pattern of nymphs into the fields might vary depending on the distance from the source populations on the trees. If the fallen nymphs randomly immigrate into crop fields just after falling, the immigration pattern of the nymphs might be similar to their falling pattern, and chemical application on the edge of fields closest to the trees could be effective

at the time when falling of the first instar nymphs is nearly finished. In contrast, if fallen nymphs from the trees do not immediately move to crops due to their own dispersal ability or distance to the fields, the immigration time into the fields will be delayed. Therefore, an optimal control timing and range for *M. pruinosa* in field crops needs to be improved by coupling with observations of *M. pruinosa* in the fields.

In summary, two degree-day models to forecast the egg hatch and falling of first instar nymphs of *M. pruinosa* were developed in this study, and a model to describe the population change of *M. pruinosa* nymphs on trees and ground over time was presented by using these two phenology models. For the reliable prediction of phenological events related to *M. pruinosa*, January 1 was determined as a starting date of the degree-day models. Finally, two options to control the timing and target sites of *M. pruinosa* were discussed, using a simulation model and field observations in the ground cover. The results showed that between 423 DD and 474 DD in the trees and 535 DD in the ground plants bordering the trees were good control timing for *M. pruinosa* nymphs. This results would be applicable in most temperate regions where the seasonal occurrence of *M. pruinosa* appears to be similar (Wilson and McPherson, 1981; Duso, 1984;

Wilson and Lucchi, 2001; Souliotis et al, 2008; Balakhnina et al., 2014; Lee et al., 2016; Park et al., 2019), with a few adjustments after validation, if necessary.

Chapter IV.

**Immigration risk and population simulation
models for *Metcalfa pruinosa* nymphs within
crop fields**

4-1. Abstract

Immigration pattern and population dynamics of *Metcalfa pruinosa* nymphs in crop fields were studied to evaluate immigration risk of the nymphs and understand their occurrence pattern. Movement of *M. pruinosa* nymphs from one place to other place was regularly monitored using sticky traps in several regions of Korea, and the nymphal immigration model was developed based on degree-days with a lower development threshold of 10.1 °C. This model was transformed into the immigration risk model having specific starting point of the nymphal influx, and then validated. The starting date for the model was the beginning time of crop cultivating in each of the surveyed crop fields. In addition, survival rate of the nymphs until adult emergence was observed in field cages, and proportions of stage transition from the nymphs to the adults were modelled based on degree-days. Finally, a population simulation model based on degree-days was constructed by integrating following components: (1) beginning time of plants growing, (2) amount of immigrant nymphs, (3) survival rate in the crop fields, and (4) proportion of stage transition to the adults. There was a good agreement between the population

model output and nymphal abundance in various crop cultivation conditions. Among the components of simulation model, the beginning time of plants growing after 205.5 DD was evaluated to be important, because influx amount of nymphs was relatively high in the early part of nymphal occurrence time and then steadily decreased. The peak time of nymphal influx were predicted to be 475.3 DD, about the second week of June in Korea. However, even with the delayed starting point, the times of maximum density and ending of nymphal occurrence in crop fields did not change as much as delayed time. After 800 DD, the population of *M. pruinosa* within crop fields was predicted to gradually decrease due to emigration of the adults.

Keywords: *Metcalfa pruinosa*, Nymphs, Immigration risk, Stage transition model, Population model, Planting time, Field validation

4-2. Introduction

Since an invasive species, *Metcalfa pruinosa* (Say) was first reported in Korea, it has become a major pest of various field crops such as soybean, sesame, ginseng, perilla and corn (Seo et al., 2016; Seo et al., 2019). This pest cause damage to crops via sucking sap, leading to shoot stunting and a reduction in plant vitality, and subsequent yield losses (Ciampolini et al., 1987; Wilson and Lucchi, 2007; Strauss, 2010). The necessity for management of *M. pruinosa* in crop fields has been exponentially increasing in Korea due to its mass occurrence with rapid expansion (Kim et al., 2019).

Population of *M. pruinosa* in crop fields entirely originate from outside of the fields, because this pest lay eggs in only tree hosts not herb plants (Dean and Baily, 1961; Lucchi, 1994). After overwintered eggs hatched in the spring, nymphs consistently disperse into surrounding vegetation including crop plants by directly falling from the trees and moving on after falling (Park et al, 2019; Kim et al., 2020). Adults start to emerge through five nymphal stages approximately two months after egg hatching (Wilson and McPherson, 1981; Wilson and Lucchi, 2001; Mead, 2004), and soon leave to the tree hosts for mating

and laying overwintering eggs (Yoon et al., 2012; Park et al, 2019). Thus, *M. pruinosa* damages in crop plants are mainly caused by immigrant nymphs from the overwintering hosts. The damage could potentially occur in most of crop fields where trees are present around there, because *M. pruinosa* can use more than 300 plant species and a variety of tree hosts for oviposition (Ciampolini et al., 1987; Strauss, 2010; Kim et al., 2020). To understand population dynamics of the nymphs within the crop fields is helpful to reduce nymphal damage in field crops with various cultivation conditions.

Population dynamics of *M. pruinosa* nymphs in the crop fields can be characterized by several factors. The first factor is the immigration of nymphs from the crop-field surroundings. This is a major factor driving the occurrence of nymphs in crop fields. The second factor is the survivorship of nymphs in the field. Third, the transition from nymphs to adults reduces the population of *M. pruinosa* nymphs. Finally, the crop-growing period could significantly affect the amount of the immigrating nymphs in crop fields. For example, if crops are planted later or harvested earlier than the time of the nymphal occurrence would be delayed or shortened.

Because the factors mentioned above have a complex effect on

the population dynamics of *M. pruinosa* nymphs in the crop fields, it is challenging to describe their dynamics by considering all factors together. In particular, the crop-planting period is hard to incorporate in defining the nymphal occurrence pattern because it is not a natural characteristic of *M. pruinosa* but varies with the cultivation environment. An alternative way to describe the nymphal population dynamics might be to integrate the controlling factors after the variation of each factor over time has been examined deterministically by sub-models (Kim and Lee, 2010). Therefore, the objectives of this study were (1) to develop an immigration model of *M. pruinosa* nymphs in crop fields, (2) to validate variation in the influx of *M. pruinosa* nymphs depending on the length of crop growing period in the fields, (3) to estimate survival rate of *M. pruinosa* nymphs per unit time, (4) to develop a stage transition model from nymphs to adults of *M. pruinosa*. The final goal was to construct a complete population model for *M. pruinosa* nymphs within the crop fields by integrating the sub-models of these factors to clarify their occurrence pattern.

4-3. Materials and methods

4-3-1. Nymphal immigration model

The immigration patterns of *M. pruinosa* nymphs were monitored in several regions in Korea from 2017 to 2019 (Table 1). At each site, the monitoring was conducted by clear sticky panel traps (25 cm × 15 cm, Greenagrotech, Gyeongsan, Korea) in open fields where overwintering habitats (i.e., the trees infested by *M. pruinosa* eggs) were present on one side. The influx amount of the nymphs was estimated by the number of nymphs caught at specific locations by traps. For this, the traps were installed at two heights, 1m above the ground and on the ground. The traps at the higher level were designed to capture nymphs falling from the trees, and the bottom level traps were for sampling nymphs moving on the ground after falling from the trees (Fig. 1). To fix the traps, two rods (5.2 mm diameter × 160 cm height, Eden Plant Support, Gimhae, Korea) which the 50 cm tips were bent at 45° angles were embedded vertically into the ground at a position more than 5 m away from five trees. The top-level traps were fixed on tilted parts of the rods on the opposite side to the trees to increase the capacity for the capture of falling nymphs (Kim et al, 2020).

The nymphs moving on the ground were sampled by the traps fixed closely to the ground (Fig. 1). A roof made of clear plastic was installed above the bottom traps so that nymphs falling directly from the trees and dirt brought by the rain would not stick on the bottom traps (Fig. 1). Five sets of traps with top and bottom levels were placed at each monitoring site to estimate the number of immigrating nymphs. In addition to observing nymphal immigration, the number of adults caught in traps were also counted. The traps were changed at one-week intervals from late April, when the nymphs did not yet appear, until adults were no longer caught.

Air temperature data from the weather station closest to each experiment site were obtained from the Korea Meteorological Administration website (<http://web.kma.go.kr/>). The daily maximum and minimum temperature data were used to calculate daily degree-day using the sine wave method with 10.1 °C of lower development threshold (LDT) of *M. pruinosa* eggs (Lee et al. 2016). Then, accumulative degree-days from January 1 to each monitoring date were calculated and paired with observation data (Kim et al, 2020).

The influx amount of the nymphs between observation dates were estimated by summing trap catches of top and bottom heights

from the five sets of traps at each monitoring site. The trap-catch data from the open fields were then converted to cumulative percent proportion of the immigration of nymphs. Each cumulative proportion (%) according to accumulative degree-days was fitted by a three-parameter Weibull cumulative function:

$$F(x) = 100 \times [1 - \exp(-(x - \gamma)/\alpha)^\beta] \quad (\text{Eq. 1})$$

where $F(x)$ is the cumulative proportion of immigration of the nymphs passing through specific borders between two areas at time x degree-days (DD), and α , β , and γ are the scale, shape, and location parameters of the Weibull function, respectively. The location parameter γ represents the starting point of the Weibull function, i.e., the time at which nymphal immigration begins in the open fields. The immigration model was fitted by using PROC NLIN in SAS 9.4 (SAS Institute 1999).

Table 1. Description of the study sites and sampling information for the development of a nymphal immigration model of *Metcalfa pruinosa* in open fields and adult transition model

| Site | Latitude and longitude (°, min, sec.) | Year | No. observation | Date of first catch | | No. catches | |
|-----------|--|------|--------------------|---------------------|---------|-------------|-------|
| | | | | Nymph | Adult | Nymph | Adult |
| Yeoncheon | 38°04'59.0" N, 127°04'36.7" E | 2017 | 22 | May 18 | July 13 | 2634 | 72 |
| Yeoncheon | 38°04'59.0" N, 127°04'36.7" E | 2018 | 19 | May 22 | July 16 | 654 | 20 |
| Suwon | 37°15'57.8" N, 126°59'11.1" E | 2018 | 20 | May 28 | July 18 | 78 | 32 |
| Yesan | 36°44'11.9" N, 126°49'17.9" E | 2018 | 19 | May 24 | July 18 | 118 | 25 |
| Yeoncheon | 38°04'59.0" N, 127°04'36.7" E | 2019 | 21 | May 27 | July 23 | 2575 | 48 |
| Paju | 37°57'00.8" N, 126°55'20.9" E | 2019 | 21 | May 27 | July 24 | 412 | 37 |
| Chuncheon | 37°45'16.8" N, 127°44'10.9" E | 2019 | 21 | May 20 | July 21 | 890 | 52 |

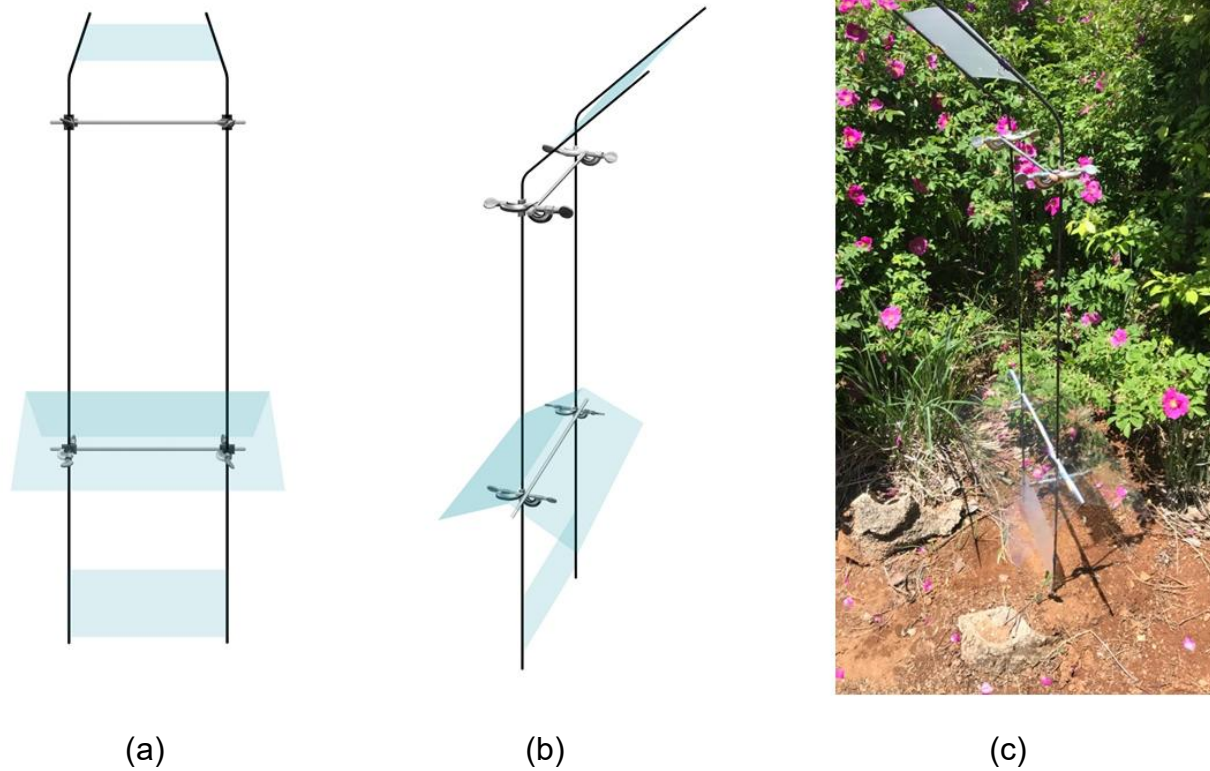


Fig. 1. Sets of traps with top and bottom heights to capture the immigrant nymphs of *Metcalfa pruinosa* in open fields and on the border of crop fields. (a) Front view; (b) Side view; (c) Photo of a set of traps.

4-3-2. Immigration risk of nymphs in crop fields

The immigration pattern of *M. pruinosa* nymphs were also monitored in soybean fields in Anseong, Jincheon, and Yeoncheon in Korea in 2017, and in Yesan and Yeoncheon in Korea in 2018 (Table 2). The monitoring was conducted in the same manner, using the two heights of trap described above. However, trap sampling started after seedlings were transplanted or seeds sprouted. This is because nymphs that cause crop damage virtually begin to invade the fields from when crops are beginning to grow. In all experiment sites, except for Anseong, the traps were installed the day after the farmer transplanted the seedlings in the fields. In the Anseong field in 2017, because the farmer seeded soybean, the traps were in place when most of the seeds sprouted. A total of 20 sets of traps was installed at regular distance intervals along the border of each crop field. When the sets of traps were installed in each experiment field, there were no host plants on which *M. pruinosa* nymphs could develop except for the soybean plants. The traps were changed at one-week intervals from trap installation date until no further immigration of nymphs occurred. Thus, the trap catches in the border of soybean fields could describe the amount of nymphal influx into each field during different plant-

growing periods.

The trap catches in soybean fields are censored data without information prior to their own starting points, and cannot be described as $F(x)$, representing the cumulative amount of immigration in open field until time x DD. Thus, the following immigration risk model was introduced to validate the proportion of immigration in crop fields.

$$R(x) = 100 - F(x) \quad (\text{Eq. 2})$$

where $R(x)$ is the immigration risk (%), representing the cumulative proportion of nymphal inflow from time x DD. Thus, the immigration could be described as $R(x)$, regardless of starting points. The immigration risk $R(x)$ was then transformed to evaluate immigration risk of the nymphs in soybean fields by the same percent proportional scale.

$$R_{t_0}(x) = R(x) \times \frac{100}{R(t_0)} \quad (\text{Eq. 3})$$

where $x \geq t_0$, $R_{t_0}(x)$ is the immigration risk model with a specific starting point t_0 (DD) in each soybean field, and $100/R(t_0)$

is a normalization term that makes $R_{t_0}(x)$ a percent proportion (%) between 0 and 100. The field-specific immigration risk models were compared to inverse cumulative proportion (%) calculated by trap catches sampled in the border of each soybean field. For this comparison, linear regression analysis was performed between the predicted (X) and observed proportions (Y) corresponding to observation times (DD). If the model perfectly predicts the observed proportions, the regression line is $Y = X$ (Mesplé et al. 1996).

Table 2. Description of the crop fields and sampling information for validation of immigration risk model for the nymphs

| Site | Latitude and longitude (°, min, sec.) | Year | Planting method | Starting point | | No. observation | No. catches (Nymph) |
|-----------|--|------|-----------------|----------------|--------------------------|-----------------|------------------------|
| | | | | Date | Degree days ¹ | | |
| Yeoncheon | 38°04'58.5" N, 127°04'27.9" E | 2017 | Trans-planting | June 15 | 500 | 8 | 475 |
| Anseong | 37°04'25.5" N, 127°25'32.4" E | 2017 | Sowing | June 9 | 489 | 7 | 198 |
| Jincheon | 36°49'39.5" N, 127°23'28.0" E | 2017 | Trans-planting | June 30 | 780 | 6 | 67 |
| Yeoncheon | 38°04'58.5" N, 127°04'27.9" E | 2018 | Trans-planting | June 9 | 464 | 7 | 70 |
| Yesan | 36°44'13.0" N, 126°49'17.1" E | 2018 | Trans-planting | June 11 | 517 | 7 | 61 |

¹ The degree-days were calculated with lower development threshold of 10.1°C for *Metcalfa pruinosa* eggs

4-3-3. Survival rate and development time of the nymphs

The survival and development of *M. pruinosa* nymphs until adult emergence were observed in two host plants, *Hosta* sp. and soybean. The nymphal cohorts for the experiments were prepared by collecting nymphs hatching from eggs which were collected in Chuncheon on April 26, 2019, in a growth chamber (23.8 ± 0.76 [mean \pm SD] °C, a photoperiod of 16:8 [L:D] h, and 70-80% RH). On June 1, 2019, the first instar nymphs that hatched in the chamber were collected and individually transferred into each insect-rearing tents (75 × 75 × 115 cm, 160 μ m aperture, BugDorm, Talchung, Taiwan) with pots of two different host plants. A total of 30 nymphs on *Hosta* sp. and 25 nymphs on soybean were prepared. The tents were placed outdoors on the Seoul National University campus, and the emerging adults were counted and removed from the tent every day. The temperature data of the weather station nearest to the campus were used to calculate degree-days with the sine wave method using a Microsoft Excel application, DegDay version 1.01 (Copyright © 2002 Regents of the University of California).

Since there were no significant differences in survival rate ($X = 0.197$; $df = 1$; $p > 0.05$) and nymphal development time ($t = -1.230$; df

= 24; $p > 0.05$) between two host plants, these data were pooled for further analysis. It is assumed that the survival rate over time in the nymphal stage of *M. pruinosa* was constant, and the survival probability per unit time was estimated by exponential function:

$$S(x) = \exp(-\theta x) \quad (\text{Eq. 4})$$

where $S(x)$ is the survival rate of *M. pruinosa* at adult emergence time x DD (LDT = 10.1 °C). The survival rate $S(x)$ was obtained by dividing the total number of emerged adults by the number of total transferred nymphs, and time x was taken as the accumulative degree-days corresponding to median development time (days) of the nymphs to adults.

Table 3. Developmental time and emergence rate of *Metcalfa pruinosa* nymphs in semi-field condition, observed in insect rearing tents placed on Seoul National University campus in 2019

| Host plant | No. nymphs | Emergence rate | Development time (dyas) | |
|------------------|------------|----------------|-------------------------|--------|
| | | | Mean+SE | Median |
| <i>Hosta</i> sp. | 30 | 0.5 | 48.6+2.26 | 48 |
| Soybean | 25 | 0.44 | 49.9+3.18 | 49 |
| Total | 55 | 0.473 | 48.9+2.64 | 48.5* |

* The accumulated degree-days corresponding to median development time (days) for adult was calculated to be 644.2 DD (LDT = 10.1 °C).

4-3-4. Stage transition model from the nymph to the adult

The transition proportion from the nymphs to the adults over time was estimated by using trap-catch data sampled from populations of nymphs and adults in open fields (Table 1). The trap capture rate between two development stages is not identical, because of the different behavioral characteristics of the two stages of *M. pruinosa* (e.g., flight activity of adults). Thus, the ratio of trap capture rates between nymphs and adults was estimated for calibration of the relative population size represented by trap catch-counts. First of all, the expected number of adult catch was estimated when the population sizes of the two stages were the same. For this estimation, it was strictly assumed that nymphs all emerge at one time and that their deaths occur only at the emergence time. The sum of the total number of adult catch from all the experiment fields was divided by the survival rate of nymphs, $S(x)$, to calculate the total expected adult catch in conditions of the same population size. Then, the ratio of total expected adult catch to the sum of the total nymph catch from all experiment fields was applied to the original trap catches of the adults as a weight in the observation data of all fields. Through this process, calibrated estimates of adult population sizes were obtained, reflecting

the possibility of adults being caught in traps.

The proportion of adults was calculated using corrected counts of adults and original counts of nymphs caught in the traps on each field sampling occasion. If nymphs of *M. pruinosa* had not been captured on one occasion, the proportion would have been calculated as 1. The calculated proportions were fitted against the time (DD) by the sigmoid function (Nematollahi et al., 2016):

$$T(x) = \frac{1}{1 + \exp[-\varepsilon(x - \delta)]} \quad (\text{Eq. 5})$$

where $T(x)$ is the transition proportion from the nymphs to the adults at time x DD, ε is a shape parameter determining the steepness of Eq 5, and δ is a parameter representing median transition time of the nymphs to the adults, i.e., the time when the $T(x)$ is 0.5. The parameters of sigmoid function were estimated using function 'nls' in *stata* package in R.3.5.1 (R core team, 2018).

4-3-5. Population simulation model for the nymphs within the crop fields

By applying the developed sub-models (immigration, survival rate, and stage transition), the population changes of the nymphs within the crop field were simulated by 1 DD interval. For the simulation, the nymphal influx during 1 DD was assumed to be a single cohort and the following equation was used:

$$P(t) = \left[\sum_{x=t_0+1}^t \{F(x) - F(x-1)\} \times \exp(-\theta(t-x+1)) \right] \times 1 - T(t)$$

(Eq. 6)

In Eq. 6, the relative population size of nymphs $P(t)$ at time t DD was described for four components: 1) field-specific starting point of nymphal immigration, t_0 ; 2) the relative population size of immigrant cohort between $x-1$ DD to x DD; 3) survival rate of each immigrant cohort at time t ; and 4) transition proportion from nymphs to adults, $T(t)$. The population size of the immigrant cohort during 1 DD was estimated as the difference between values of the immigration model of consecutive degree-days (1 DD interval). The survival rates of each

cohort at time t were calculated as the power of staying time in the crop fields of the cohort ($t - x + 1$) for the survival rate per unit time ($\exp(-\theta)$). Finally, the $P(t)$ was calculated by multiplying the total surviving population size of all cohorts by the proportion of nymphs that had not yet emerged as adults. Here, if there is neither nymphal death nor adult emergence, $P(t)$ is the same as $F(t)$, and the value would be 100 % when nymph immigration completed. To evaluate the effect of the starting point, the population models were simulated with three different t_0 of 0 DD, 400 DD, and 800 DD.

The population simulation model was finally evaluated by comparing the model output with the population density sampled in the same soybean fields where nymphal immigration into the fields was monitored (Table 2). In addition, a sesame field (37°59'03.5" N, 126°59'01.9" E) and a soybean field (37°59'02.4" N, 126°58'55.4" E) were investigated in Paju in 2019. In the soybean field in Anseong and the sesame field in Paju, insecticides were applied on June 28, 2017 and July 6, 2019, respectively. For surveys of nymph population size in crop fields, the fields were divided into more than 100 quadrats of the same size, and the plants in the center of each quadrat were marked by sticks. After crops were transplanted (Yeoncheon,

Jincheon, Yesan, and Paju) or seeds sprouted (Anseong), the numbers of nymphs on the marked plants were counted by the naked eye from the first sighting until no further nymphs occurred. At all sites except Paju, in 2019, the survey was conducted at one-week intervals. The surveys at Paju, in 2019, were conducted at two-week intervals. To compare the population model with the field population density, the model output and the number of observed nymphs were scaled to a ratio against the respective maximum peak. In the simulation processes, if insecticides were treated, it was assumed that all the nymphs that had been established in the fields were dead. The time of each sampling occasion and the simulation was presented as accumulative degree-days calculated from weather station data and LDT of 10.1 °C (Lee et al. 2016).

4-4. Results

4-4-1. Nymphal immigration model

The cumulative percent capture of *M. purinosa* nymphs in open fields was well described by a Weibull function (Fig. 2, Table 4). The estimate of parameter γ was 202.5; thus, no influx of nymphs was expected before 202.5 DD (10.1 °C of LDT) (Table 4). The peak and median times of nymphal immigration were predicted to be 475.3 DD and 537.9 DD, respectively, about the second week of June in Korea.

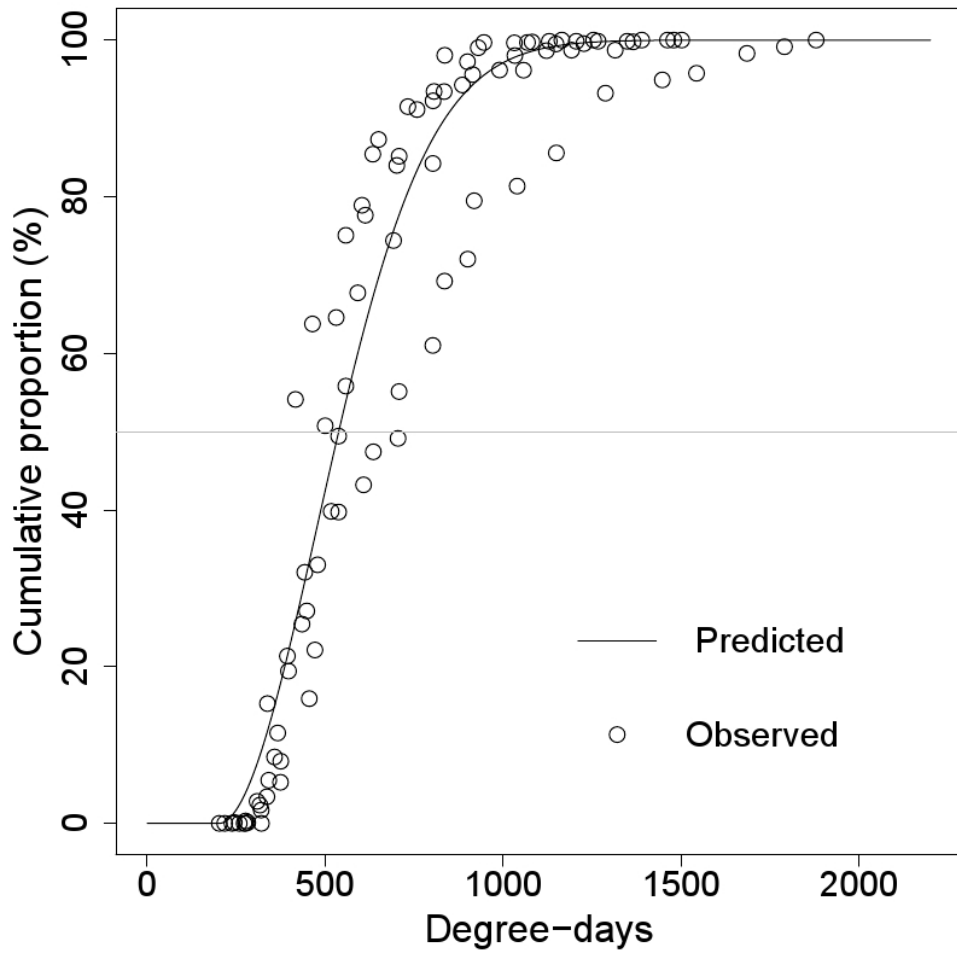


Fig. 2. Distribution model of *Metcalfa pruinosa* nymph immigration time (DD)

4-4-2. Immigration risk of nymphs in crops fields

The field-specific immigration risk models soundly predicted the immigration pattern of nymphs overall (Fig. 3). The slope and intercept of the regression line ($F = 412.6$; $df = 1, 33$; $P < 0.001$; $r^2 = 0.93$) between the predicted and observed proportion were 1.04 ± 0.051 (Mean \pm SEM) and -0.75 ± 2.492 (Mean \pm SEM) respectively, and this line very closed to 1:1 line (Fig. 3). The greater t_0 , the shorter period in which the nymphs inflow, and the immigration risk was decreased more sharply over time (Fig. 4).

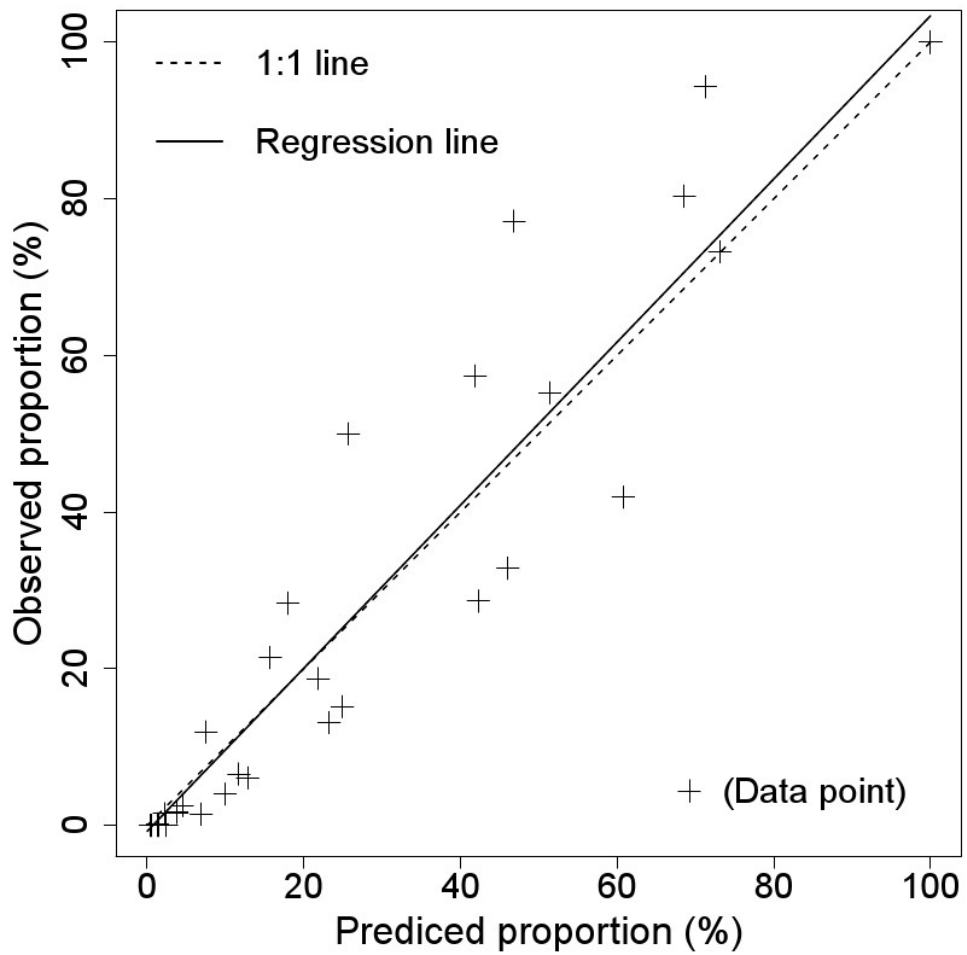


Fig. 3. Validation of *Metcalfa pruinosa* nymph immigration risk (%) in crop field. The regression line was created to compare 1:1 line, using observed proportions and predicted proportions of field specific immigration risk model.

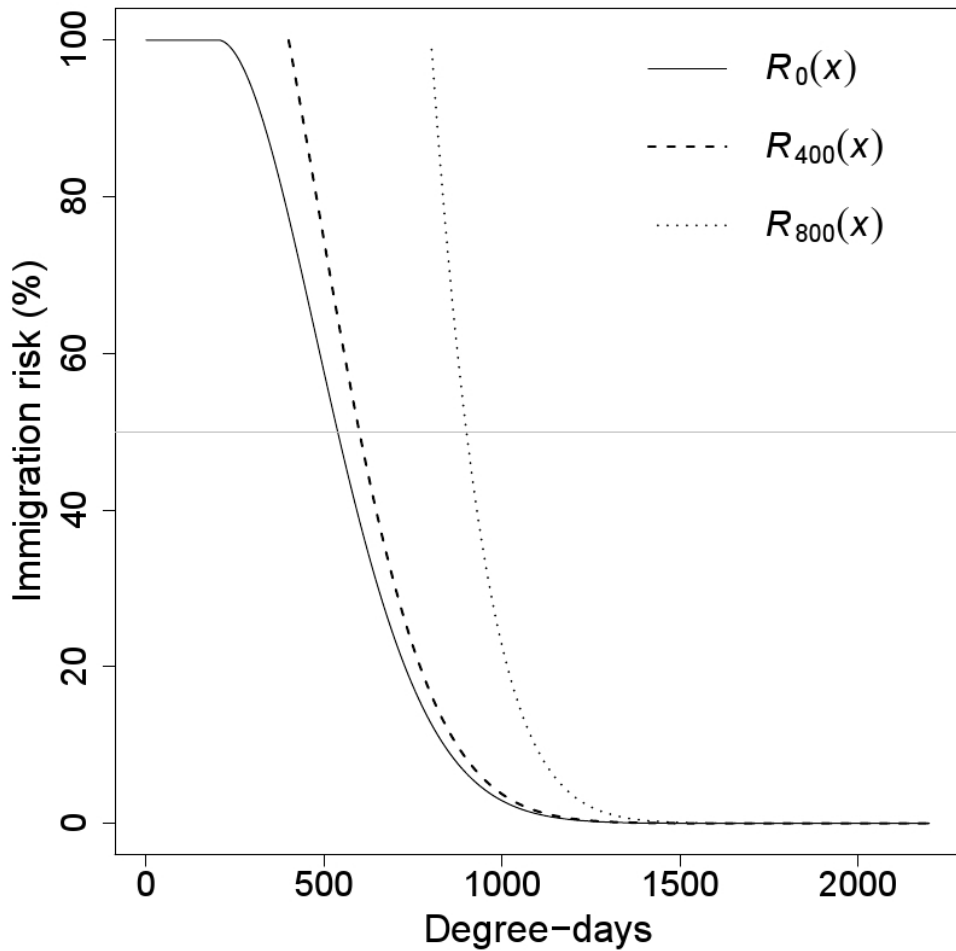


Fig. 4. Normalized immigration risk (%) models for *Metcalfa pruinosa* nymphs with field specific starting point. Each nymph immigration risk model was created with different parameters t_0 representing the time of the start of plant growing.

4-4-3. Survival rate and development time of the nymphs

Among 55 nymphs transferred to *Hosta* sp. and soybean (*Glycine max* (L.) Merr.) pots, 26 nymphs emerged to adults (Table 3). The survival rate $S(x)$ was 0.473 in the semi-field condition without the natural enemy of *M. pruinosa* (Table 3). Accumulative degree-days of median development time (days) of nymphs until adult emergence was 644.2 DD (LDT = 10.1 °C). The survival rate per unit time $\exp(-\theta)$ was estimated from these results (Table 4).

4-4-4. Stage transition model from the nymph to the adults

A total of 286 adults of *M. pruinosa* were captured in all experiment sites during whole monitoring period (Table 1). The expected number of adult catches, assuming all nymphs develop to adults without dying, was calculated to be 604.7. The ratio of expected values compared to the sum of total nymphs catches from all experiment fields (7361 catches, Table 1) was 0.082. This calculated ratio was applied as a weight to the original trap-catch data for adults in each observation. The proportions of the adults calculated by calibrated trap-catch data in fields were well fitted to a sigmoid function (Fig. 5, Table 4). The estimate of parameter δ was 1019 in the transition model, and it was predicted that 50% of total population of *M. pruinosa* would have completed the transition to adults at this time.

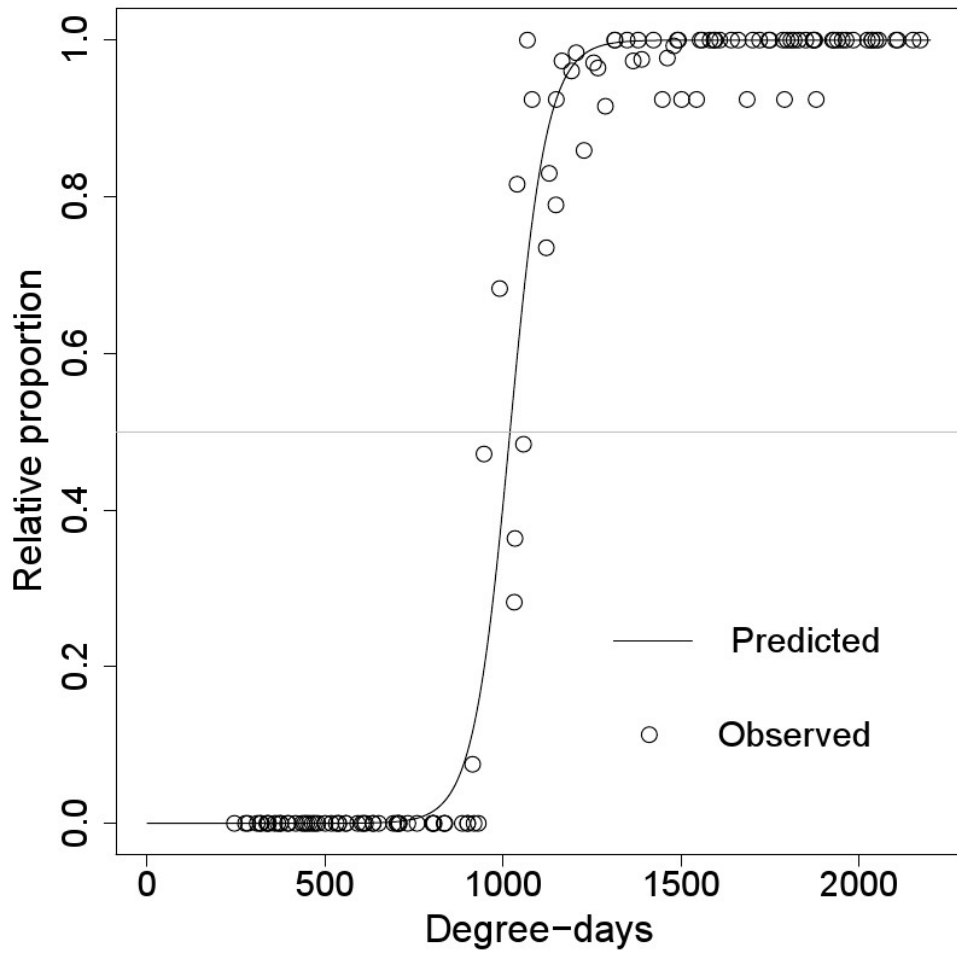


Fig. 5. Stage transition model from nymphs to adults of *Metcalfa pruinosa*. The ratio of trap catch rates between nymphs and adults was reflected as a weight for obtaining observed points.

Table 4. Estimated parameter values used by each sub-model for population model for *Metcalfa pruinosa* nymphs within crop fields

| Models | Function | Parameter | Estimated value | SEM |
|-------------|------------------------|---------------|-----------------|---------|
| Immigration | Weibull (Eq. 1) | α | 407.3 | 69.68 |
| | | β | 1.885 | 0.4072 |
| | | γ | 202.5 | 63.82 |
| Survival | Exponential (Eq. 4) | θ | 0.0016 | - |
| Transition | Sigmoid (Eq. 5) | δ | 1019 | 5.42 |
| | | ε | 0.0192 | 0.00168 |

4-4-5. Population simulation model for the nymphs within the crop fields

The nymph population size within crop fields changed sensitively depending on t_0 , the starting point of field specific nymphal immigration (Fig. 6). The maximum relative population within crop fields was estimated 62.3 % at 789 DD when $t_0 = 0$, 49.4 % at 814 DD when $t_0 = 400$, and 6.0 % at 943 DD when $t_0 = 800$. Thus the time of maximum density was from early July to mid-July in Korea, which showed relatively small variations compared to difference of t_0 .

The prediction performances by population simulation model before the peak density of *M. pruinosa* nymphs were variable for each experiment field (Fig. 7). However, the model closely predicted the observed peak density and the density after each field's peak, except for the case of the soybean field in Yeoncheon (Fig. 7a and 7d). The model well described the effect of insecticide sprays (Fig. 7c and 7g), especially in case of Anseong field, the second peak and density change after insecticide treatment was very well predicted by the model (Fig. 7c).

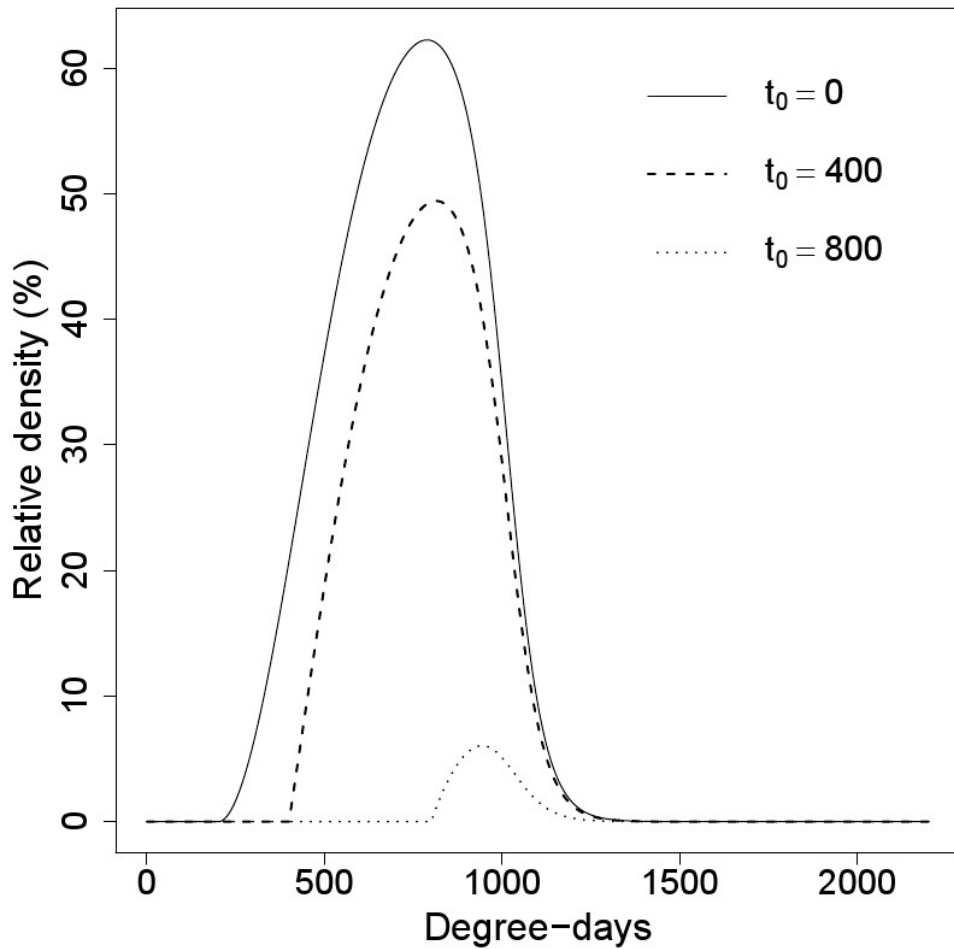


Fig. 6. Population simulation model for estimating relative population density of *Metcalfa pruinosa* nymphs within crop fields. Each population model was created with different parameters t_0 representing the time of the start of plant growing.

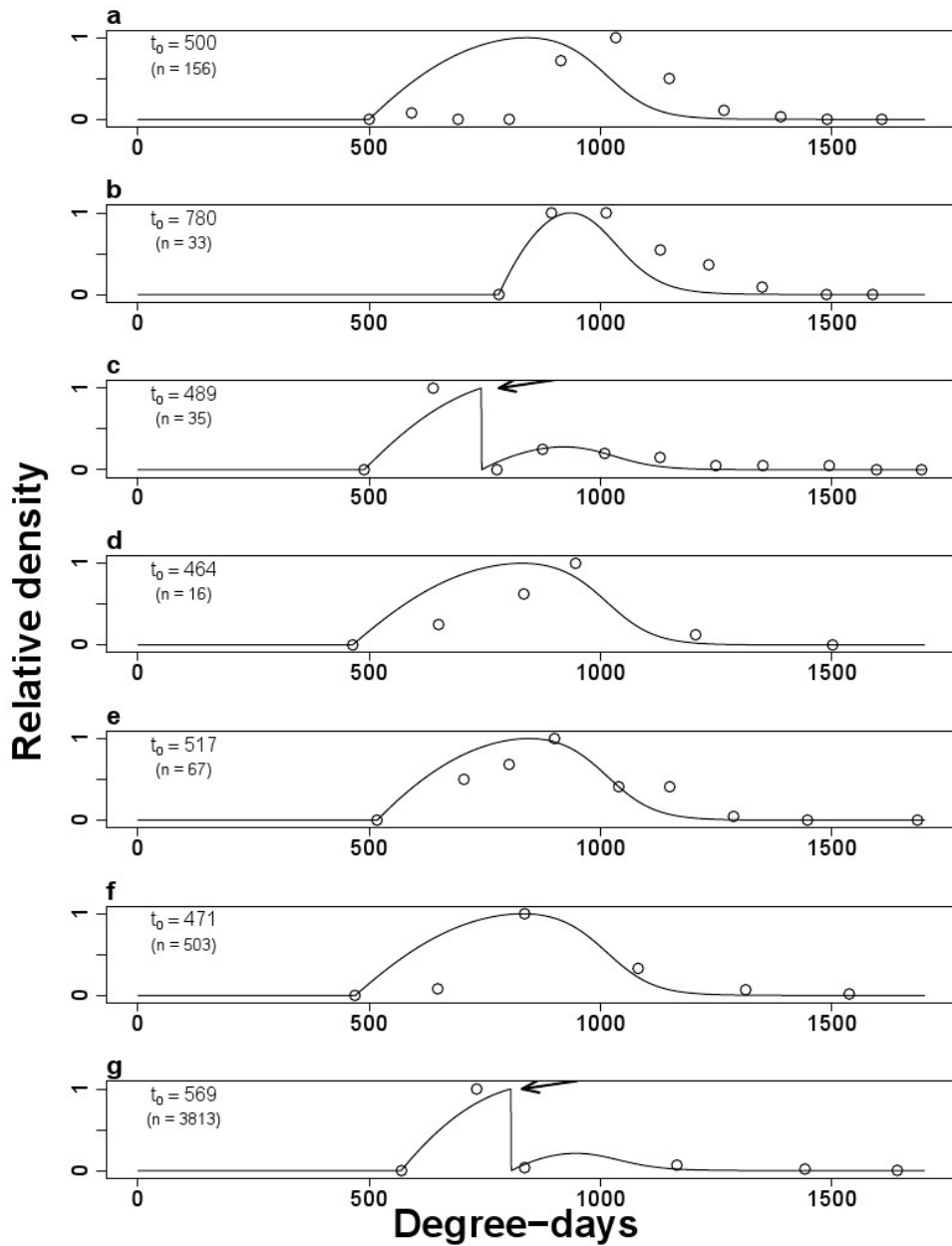


Fig. 7. Variations of *Metcalfa pruinosa* nymphal density predicted by population simulation model and observed density in soybean fields in

(a) Yencheon in 2017, (b) Jincheon in 2017, (c) Anseong in 2017, (d) Yeoncheon in 2018, (e) Yesan in 2018, (f) Paju in 2019, and in a sesame field in (g) Paju in 2019. The predicted and observed values were scaled against respective peak density of each crop field. In the case of insecticide treatment (✓), the survival rate of the immigrant nymphs until the treatment in the fields was assumed to be zero at this time.

4-5. Discussion

In this study, the LDT (10.1 °C) estimated from egg development model by Lee et al (2016) was used to develop all sub-models and the population model, because there was no information related to temperature-dependent development for *M. pruinosa* nymphs. Although it is rather unclear whether the degree-days of the models can represent true thermal requirement for the nymphal development, the developed models in this study are still useful because of following reasons. First, the parameter δ of stage transition model, representing median transition time of the nymphs to the adults, is almost consistent with the sum of the time of the 50 % cumulative appearance of first instar nymphs (Kim et al, 2020) and median development time of just hatched nymphs to the adults in semi-field condition. Moreover, the adult emergence time predicted by the stage transition model matched with approximate emergence time in most temperate regions (Duso, 1984; Wilson and McPherson, 1981; Wilson and Lucchi, 2001; Lauterer and Malenovsky, 2002; Souliotis et al., 2008; Park et al., 2019). The second reason is that the nymphal immigration pattern naturally arises from the distribution of egg

hatching time of *M. pruinosa* rather than the distribution of nymphal development time (Kim et al., 2020). If the degree-days for the nymphal development were used to the immigration model, the model might fail to explain the immigration pattern originated from different egg hatching times in various climate conditions. Therefore, to develop more realistic models, it would be useful to predict a series of phenological events of *M. pruinosa* as degree-days simply calculated by the LDT of the egg.

The degree-day based nymphal immigration model was able to predict the influx amount of nymphs in crop fields with different starting points by transforming the model to immigration risk. The normalized immigration risk (%) decreased more sharply as field crop cultivation was delayed (Fig. 4). These patterns arise from not only the starting point of nymphal immigration but also adult emergence time. This time would operate as the ending point in the immigration risk model. Thus, the starting point would be a determinant the exposure time of the nymphal immigration because adult emergence time is relatively stable in Korea, as seen from Table 1. On the other hand, before 205.5 DD (Table 4), which is the estimated location parameter of the Weibull function for the immigration model, the risk would remain at 100 %, so

there would be no reduction of exposure time of immigration by moving the starting point. Therefore, the immigration risk in perennial crops such as ginseng, or crops generally planted before about 202.5 DD (middle of May in Korea) would be even greater.

The immigration pattern after 202.5 DD could have been influenced by factors such as survival rate and adult emergence, which have already been reflected in trap-catch data for the developing immigration model. These factors will reduce the number of nymphs that can inflow over time. However, the main drive determining the immigration pattern would be dispersal from the source population of nymphs, because the adults only lay eggs in trees. This naturally causes the highest initial nymph density at the source, and will cause density gradient around the source over time. In particular, this change of nymphal density was found to be more active during relatively young nymphal periods (Park et al. 2019, Kim et al. 2020). Kim et al. (2020) reported that the peak time for first instar nymphs falling from the trees to the ground was 466.2 DD. They also reported a sharp decrease of the nymphal density on plants under the trees from about 530 DD, indicating that the nymphal dispersal on the ground actively occurred around that time. After this time, new immigrant nymphs into the given

area (scale of typical agricultural field) would decrease continually because of the reduction of nymphal density around the sources. Likewise, in the immigration model in this study, the immigration time of the nymphs showed a positively skewed distribution because the shape parameter of the model is $1 < \beta < 2.6$ (Table 4) (Stapelberg, 2009). It indicates that the peak (475.3 DD) and median (537.9 DD) are located on left side of mean in distribution of immigration time. In other words, the nymphal influx from one place to another is more likely to occur in the early part of their occurrence time. Thus, the chemical application or sampling during this time period (about the second week of June) in boundary of crop field bordering the trees could be an effective option for management of *M. pruinosa* nymphs, if the crop plants are growing in this time.

As mentioned above, the survival rate of nymphs affects the amount of the nymphs that can inflow into crop fields, while also reducing population size of the nymphs that have already established into fields. The estimated natural survival rate of the nymphs until adult emergence was 47.3% in semi-field, which suggested that *M. pruinosa* could establish sufficiently in invaded regions, when considering egg production of the adult (about 90) (Bozsik, 2012). However, the

estimated survival rate in this study might be significantly different in invaded regions where natural enemy had been introduced (Wilson and Lucchi, 2001). Since a natural enemy, *N. typhlocybae*, is not parasitic on first and second instar nymphs of *M. pruinosa* and prefers older nymphs (Favaro et al, 2018), it may reduce the number of viable nymphs faster over time. This could change the immigration pattern and population density in crop fields estimated in this study. Therefore, in the region where natural enemy of *M. pruinosa* is present, it would be necessary to validate the immigration and population models developed in this study, along with re-estimation of survival rates.

In population simulation model, the density of nymphs within the crop fields sharply decreased as the starting point of the immigration was delayed (Fig. 6). This is due to reduction of exposure time and influx amount of the nymphs. However, even with the delayed starting point, the times of maximum density and ending of nymphs' occurrence did not change as much as delayed time. (Fig. 6). This is because *M. pruinosa* adult naturally emerges irrespective of beginning time of plants growing. The proportion of adult emergence over time will have a great impact on the population dynamics of nymphs in the crop fields by reducing both inflowing and immigrant nymphs after

approximately 800 DD. This characteristic of nymph population dynamics suggested that the relatively late-planting crops after 800 DD were expected to suffer much less damage from *M. pruinosa*.

The population simulation results well described the general patterns and peak time of the nymphal occurrence in each crop field (Fig. 7). In particular, the model could explain the change of the nymphs' density before and after insecticide treatment. In Fig. 7c and 7g, the second peak of the nymphal density was lower than the first peak in both fields. This is probably because the effects of reduction of immigrant nymphs and stage transition to adult have been reflected in the size of nymph population after the sprays. However, the predictions of model did not match the nymphal density before peak and the peak density of nymphs observed in a soybean field in Yeoncheon in 2017 and 2018 (Fig. 7a and 7d). The soybean field in Yeoncheon was an experimental field for selecting resistance the varieties of soybean against a pest, *Leguminivora glycinivorella* (Matsumura), that emerges from the ground soil in early August (Paik et al., 2007). Thus, there was no insecticide sprays in the field during the nymphal density observation, but weeds in the field and its surrounding were removed by man-power periodically. Also, there was

a paved road with three-meter-wide between the source trees of *M. pruinosa* nymphs in near the field and the soybean field. This cultivation environment in Yeoncheon field would have caused discontinuous density gradient of nymphs from sources due to absence of host plants in road and surroundings, which might have altered the pattern of their occurrence.

In summary, this study described the immigration risk and population dynamics of *M. pruinosa* nymphs in crop fields by parameterizing their immigration, survivorship, and stage transition based on degree-days calculated by LDT of 10.1 °C. As a result, nymphal immigration begins at 205.5 DD, peaked at 475.3 DD and the amount of nymphs' influx declined sharply after the peak time. Because of this pattern, the immigration risk of nymphs in crop fields was expected to vary depending on when crop plants begin to exist. It was estimated that the *M. pruinosa* damage in crops would be significantly decreased as the adult emergence after approximately 800 DD. This result would be applicable in countries where the *M. pruinosa* have invaded. However, in regions natural enemy was introduced, the survival rate of *M. pruinosa* nymphs and the developed models may need to be reviewed.

Chapter V.
General conclusion

5-1. National management plan

This study confirmed a distinct possibility that long distance spread of *M. pruinosa* in Korea may have been facilitated by vehicle traffic and consequent its fast expansion. However, this factor is not proper to explain current distribution of *M. pruinosa*. Therefore, management policy for mitigation of the *M. pruinosa* damages will be established based on current potential distribution (2017 Climate only model). For example, control materials and costs may be preferentially distributed to areas with high presence probability of *M. pruinosa*.

The current distribution model for *M. pruinosa* may give another foreknowledge in that average climate data for 10 years was used to develop it. Based on the difference of the weather conditions between the certain year and the average year, the approximate increase or decrease in the density of *M. pruinosa* may be estimated. For example, in 2018, the summer temperature, related to Bio 10 variable (mean temperature of warmest quarter) was unusually high in Korea (<http://web.kma.go.kr/>), since then, the population density of *M. pruinosa* was significantly decreased in following year, 2019 (<http://www.rda.go.kr/>).

The future habitat suitability of *M. pruinosa* have innate uncertainty derived from the RCP 8.5 scenario. Since the scenario is a prediction result based on modelling of current climate changing patterns (<http://web.kma.go.kr/>), there is no guarantee that the future climate will change according to the RCP 8.5 scenario. In this regard, the future habitat suitability of *M. pruinosa* should be used as a reference information for preparing long-term management policy in Korea.

5-2. Optimal control timing in various landscape

The phenology models for first instar nymphs of *M. pruinosa* would be applicable to decide its optimal control timing in a variety of landscapes everywhere oviposition hosts are present. The time suggested by a population model for the first instar in trees would be a first timing to effectively control them. Secondly, control timing of the nymphs around the host trees could be decided using a first instar falling model. These actions implemented around the host trees are able to substantially reduce immigration risk of the nymphs into crop field in advance. It is believed that the suggested timing would help decision making for comprehensive pest control considering occurrence times of other pests.

5-3. Management in crop fields

As stated above, the control actions against the *M. pruinosa* nymphs in the source trees and its surrounding is a useful option which is able to reduce immigration amounts. This strategy deserves special consideration in agricultural fields where perennial plants produce new shoots or annual plants exist before mid-May, and also viable in other crop cultivation systems. Meanwhile, if the nymphs' density was observed in the crop fields in early part of crop growing time, change of their density from the observation time could be predicted by the immigration model and population simulation model (Shaffer and Gold, 1985). Thus, the models can be directly used as the management tools for deciding application time of existing control options. After mid-July in Korea, it is estimated that the necessity for controlling the nymphs in crop fields would greatly reduce due to emigration of emerging adults.

Literatures cited

- Ahn, K.-S., Lee, G.-S., Lee, K.-H., Song, M.-K., Lim, S.-C., Kim, G.-H., **2011**. Susceptibility of North America planthopper, *Metcalfa pruinosa* to commercially registered insecticides in Korea. *Korean J. Pestic. Sci.* 15, 329-334.
- Alma, A., Ferracini, C., Burgio, G., **2005**. Development of a sequential plan to evaluate *Neodryinus typhlocybae* (Ashmead) (Hymenoptera: Dryinidae) population associated with *Metcalfa pruinosa* (Say) (Homoptera: Flatidae) infestation in northwestern Italy. *Environ. Entomol.* 34, 819-824.
- Austin, M., **2007**. Species distribution models and ecological theory: A critical assessment and some possible new approaches. *Ecol. Modell.* 200, 1-19.
- Balakhnina, I.V., Pastarnak, I.N., Gnezdilov, V.M., **2014**. Monitoring and control of *Metcalfa pruinosa* (Say) (Hemiptera; Auchenorrhyncha: Flatidae) in Krasnodar territory. *Entomol. Rev.* 94, 1067-1072.
- Blackburn, T.M., Pyšek, P., Bacher, S., Carlton, J.T., Duncan, R.P., Jarošík, V., Wilson, J.R.U., Richardson, D.M., **2011**. A proposed

- unified framework for biological invasions. *Trends. Ecol. Evol.* 26, 333-339.
- Bozsik A., **2012**. Mass occurrence of the citrus flatid planthopper (*Metcalfa pruinosa* [Say, 1830]) (Hemiptera: Flatidae) in an agricultural hedgerow at Gödöllő (Hungary). *J. Agri. Sci, Debrecen*, 50 (Supplement), 115-118.
- Bradie, J., Leung, B., **2016**. A quantitative synthesis of the variables used in MaxEnt species distribution models. *J. Biogeogr.* 44, 1344-1361.
- Brown, J.L., **2014**. SDMtoolbox: a python-based GIS toolkit for landscape genetic, biogeographic and species distribution model analyses. *Methods. Ecol. Evol.* 5, 694-700.
- Byeon, D.-H., Jung, J.-M., Lohumi, S., Cho, B.-K., Jung, S., Lee, W.-H., **2017**. Predictive analysis of *Metcalfa pruinosa* (Hemiptera: Flatidae) distribution in South Korea using CLIMEX software. *J. Asia Pac. Biodivers.* 10, 379-384.
- Chapman, R. F., **1982**. The insects: structure and function, third ed. Harvard university press, Cambridge, MA.
- Choi, D.S., Kim, D.I., Ko, S.J., Kang, B.Y., **2013**. Reports of current occurrence and eco-friendly management for sporadic and main

- pests in Jeonnam. Proceedings: *Fall meeting of Korea Society of Applied Entomology*. pp. 443.
- Choi, Y.S., Seo, J.H., Jo, H.R., Hwang, I.S., Jung, S.H., Choi, G.R., **2014**. Reports of current occurrence for major pests in Chungnam. Proceedings: *Spring meeting of Korea Society of Applied Entomology*. pp. 264.
- Choi, Y.-S., Whang, I.-S., Na, M.-S., Park, D.-G., Seo, H.-Y., **2018**. Monitoring methods for *Metcalfa pruinosa* (Say) (Hemiptera: Flatidae) eggs on acacia branches. *Korean. J. Appl. Entomol.* 57, 297-302.
- Ciampolini, M., Grossi, A., Zottarelli, G., **1987**. Damage to soyabean through attack by *Metcalfa pruinosa*. *L'Inf. Agrar.* 43, 101-103.
- Colewill, R.K., Rangel, T.F., **2009**. Hutchinson's duality: The once and future niche. *Proc. Natl. Acad. Sci. USA.* 106, 19651-19658.
- Dean, H.A., Bailey, J.C., **1961**. A flatid planthopper; *Metcalfa pruinosa*. *J. Econ. Entomol.* 54, 1104-1106.
- Della Giustina, W., Navarro, E., **1993**. *Metcalfa pruinosa*, un nouvel envahisseur? *Phytoma.* 451, 30-32.
- Donati, I., Mauri, S., Buriani, G., Cellini, A., Spinelli, F., **2017**. Role of *Metcalfa pruinosa* as a vector for *Pseudomonas syringae* pv.

- actinidae. *Plant. Pathol. J.* 33, 554-560.
- Dormann, C.F., Elith, J., Bacher, S., Buchman, C., Carl, G., Carré, G., García Marquéz, J.R., Gruber, B., Lafourcade, B., Leitão, P.J., Münkemüller, T., McClean, C., Osborne, P.E., Reineking, B., Schröder, B., Skidmore, A.K., Zurell, D., Lautenbach, S., **2013**. Collinearity: a review of methods to deal with it and a simulation study evaluating their performance. *Ecography*. 36, 27-46.
- Duso, C., **1984**. Infestations by *Metcalfa pruinosa* in the Venice district. *Inf. Fitopatol.* 34, 11-14.
- Elith, J., **2002**. Quantitative methods for modelling species habitat: Comparative performance and an application to Australian plants, in: Ferson, S., Burgman, M. (Eds.), Quantitative methods for conservation biology. New York Springer-Verlag., New York, pp. 39-58.
- Elith, J., **2016**. Predicting distributions of invasive species, in: Andrew, P.R., Terry, W., Mark, A.B., Mike, N. (Eds.), Invasive species: Risk assessment and management. Cambridge university press., United Kingdom, pp. 93-129.
- Elith, J., Graham, C.H., Anderson, R.P., Dudik, M., Ferrier, S., Guisan, A., Hijmans, R.J., Huettmann, F., Leathwick, J.R., Lehmann, A.,

- Li, J., Lohmann, L.G., Loisel, B.A., Manion, G., Moritz, C., Nakamura, M., Nakazawa, Y., Overton, J.M., Peterson, A.T., Phillips, S.J., Richardson, K., Scachetti-Pereira, R., Schapire, R.E., Soberón, J., Williams, S., Wisz, M.S., Zimmermann, N.E., **2006**. Novel methods improve prediction of species' distributions from occurrence data. *Ecography*. 29, 129-151.
- Elith, J., Leathwick, J.R., **2009**. Species distribution models: ecological explanation and prediction across space and time. *Ann. Rev. Ecol. Evol. Syst.* 40, 677-697.
- Elith, J., Phillips, S.J., Hastie, T., Dudík, M., Chee, Y.E., Yates, C.J., **2010**. A statistical explanation of MaxEnt for ecologists. *Divers. Distrib.* 17, 43-57.
- ESRI. **2012**. ArcGIS Desktop 10.1. ESRI. Redlands, California. USA.
- Favaro, R., Roved, J., Girolami, V., Martinez-Sañudo, I., Mazzon, L., **2018**. Host instar influence on offspring sex ratio and female preference of *Neodryinus typhlocybae* (Ashmead) (Hymenoptera, Dryinidae) parasitoid of *Metcalfa pruinosa* (Say) (Homoptera, Flatidae). *Biol. Control*. 125, 113-120.
- Flint, M.L., **2012**. IPM in practice: principles and methods of integrated pest management. 2nd ed.; University of California Agriculture

- and Natural Resources: Oakland, CA, USA, pp. 182-187.
- Girolami, V., Conte, L., **1999**. Possibilità di controllo chimico e biologico di *Metcalfa pruinosa*. *Informatore fitopatologico*. 49, 20-25.
- Grozea, I., Gogan, A., Virteiu, A.M., Grozea, A., Stef, R., Molnar, L., Carabet, A., Dinnesen, S., **2011**. *Metcalfa pruinosa* Say (Insecta: Homoptera: Flatidae): a new pest in Romania. *Afr. J. Agric. Res.* 6, 5870-5877.
- Hanley, J.A., McNeil, B.J., **1982**. The meaning and use of the area under a receiver operation characteristic (ROC) Curve. *Radiology*. 143, 29-36.
- Hijmans, R.J., Guarion, L., Mathur, P., **2012**. DIVA-GIS. Free GIS for biodiversity research, version 7.5. <http://www.diva-gis.org/>
- Johnson, J.B., Omland, K.S., **2004**. Model selection in ecology and evolution. *Trends. Ecol. Evol.* 19, 101-108.
- Jones, V.P., Doerr, M.D., Brunner, J.F., **2008**. Is biofix necessary for predicting codling moth (Lepidoptera: Tortricidae) emergence in Washington State apple orchards? *J. Econ. Entomol.* 101, 1651-1657.
- Jung, T.S., Moon, Y.G., Lee, J.H., Lee, N.G., Kwon, S.B., Hwang, M.R.,

- Kim, J.R., **2015**. Reports of current occurrence for invasive and sporadic pests in Gangwon. Proceedings: *Spring meeting of Korea Society of Applied Entomology*. pp. 193.
- Kahrer, A., Strauss, G., Stolz, M., Moosbeckhofer, R., **2009**. Beobachtungen zu Faunistik und Biologie der vor kurzem nach Österreich eingeschleppten Bläulingszikade (*Metcalfa pruinosa*). *Beitr. Entomofaunistik*. 10, 17-30.
- Keane, R.M., Crawley, M.J., **2002**. Exotic plant invasions and the enemy release hypothesis. *Trends. Ecol. Evol.* 17, 164–170.
- Kim, D.-E., Kil, J., **2014**. Occurrence and host plant of *Metcalfa pruinosa* (Say) (Hemiptera: Flatidae) in Korea. *J. Environ. Sci. Int.* 23, 1385-1394.
- Kim, D.-S., Lee, J.-H., **2010**. A population model for the peach fruit moth, *Carposina sasakii* Matsumura (Lepidoptera: Carposinidae), in a Korean orchard system. *Ecol. Model.* 221, 268-280.
- Kim, H., Lee, J.-H., **2008**. Phenology Simulation Model of *Scotinophara lurida* (Hemiptera: Pentatomidae). *Environ. Entomol.* 37, 660-669.
- Kim, M.-J., Baek, S., Lee, S.-B., Park, B., Lee, S.-K., Lee, Y.S., Ahn, K.-S., Choi, Y.-S., Seo, H.-Y., Lee, J.-H., **2019**. Current and future

- distribution of *Metcalfa pruinosa* (Say) (Hemiptera: Flatidae) in Korea: Reasoning of fast spreading. *J. Asia Pac. Entomol.* 22, 933-940.
- Kim, M.-J., Baek, S., Lee, J.-H., **2020**. Egg hatching and first instar falling models of *Metcalfa pruinosa* (Hemiptera: Flatidae). *Insect.* 11, 345.
- Kim, Y., Kim, M., Hong, K.-J., Lee, S., **2011**. Outbreak of an exotic flatid, *Metcalfa pruinosa* (Say) (Hemiptera: Flatidae), in the capital region of Korea. *J. Asia Pac. Entomol.* 14, 473-478.
- Kwon, D. H., Kim, M., Kim, H., Lee, Y., Hong, K.-J., Lee, S. H., Lee, S., **2015**. Estimation of genetic divergence based on mitochondrial DNA variation for an invasive alien species, *Metcalfa pruinosa* (Say), in Korea. *J. Asia Pac. Entomol.* 18, 447-451.
- Lauterer, P., **2002**. Citrus flatid planthopper - *Metcalfa pruinosa* (Hemiptera: Flatidae), a new pest of ornamental horticulture in the Czech Republic. *Plant. Prot. Sci.* 38, 145-148.
- Lauterer, P., Malenovsky, I., **2002**. *Metcalfa pruinosa* (Say; 1830) introduced into the Czech Republic (Hemiptera: Flatidae). *Beitr. Zikadenkunde.* 5, 10-13.

- Lee, D.-S., Bae, Y.-S., Byun, B.-K., Lee, S., Park, J., Park, Y.-S., **2019a**. Occurrence prediction of the citrus flatid planthopper (*Metcalfa pruinosa* (Say; 1830)) in South Korea using a random forest model. *Forests*. 10, 583.
- Lee, G.-S., Lee, S.-M., Ahn, K.-S., **2011**. Spreading of *Metcalfa pruinosa* and possibility of dispersal by vehicle attachment in Korea. Proceedings: *Fall meeting of Korea Society of Applied Entomology*. pp. 59.
- Lee, G.-S., Lee, S.-M., Lee, W., **2013a**. Spreading of invasive species, *Metcalfa pruinosa* (Say) (Hemiptera: Flatidae). Proceedings: *Spring meeting of Korea Society of Applied Entomology*. pp. 189.
- Lee, H.S., Han, I.Y., Kang, D.W., Lee, B.J., Kim, K.H., **2017**. Reports of current occurrence for sporadic and southern pests in Kyongsang-do. Proceedings: *Fall meeting of Korea Society of Applied Entomology*. pp. 171.
- Lee, H.-S., Wilson, S. W., **2010**. First report of the Nearctic flatid planthopper *Metcalfa Pruinosa* (Say) in the republic of Korea (Hemiptera: Fulgoridea). *Entomol. News*. 121, 506-513.
- Lee, J.-R., Choi, H.-S., Park, C.-G., Byeon, Y., **2014**. Development of management technology of problematic disease, pests and

weeds in Korea agriculture. Research report of National institute of agricultural science and technology.

Lee, W., Park, C.-G., Seo, B.Y., Lee, S.-K., **2016**. Development of an emergence model for overwintering eggs of *Metcalfa pruinosa* (Hemiptera: Flatidae). *Korean J. Appl. Entomol.* 55, 35-43.

Lee, Y.S., Lee, H.A., Lee, H.J., Choi, J.Y., Lee, S.-W., Lee, Y.S., **2019b**. Control effect of plant extracts mixture on *Metcalfa pruinosa* (Say) (Hemiptera: Flatidae). *Korean J. Appl. Entomol.* 58, 281-282.

Lee, Y.S., Lee, H.J., Jang, M. J., Jung, K.H., **2013b**. Reports of current occurrence for major pests in Kyeonggi-do. Proceedings: *Fall meeting of Korea Society of Applied Entomology*. pp. 263.

Liebholt, A.M., Bascompte, J., **2003**. The Allee effect, stochastic dynamics and the eradication of alien species. *Ecol. Lett.* 6, 133-140.

Liebholt, A.M., Tobin, P.C., **2008**. Population ecology of insect invasions and their management. *Annu. Rev. Entomol.* 53, 387-408.

Liebholt, A.M., Berec, L., Brockerhoff, E.G., Epanchin-Niell, R.S., Hastings, A., Herms, D.A., Kean, J.M., McCullough, D.G.,

- Suckling D.M., Tobin, P.C., Yamanaka T., **2016**. Eradication of invading insect populations: from concepts to applications. *Annu. Rev. Entomol.* 61, 335-352.
- Lockwood, J.L., Hoopes, M.F., Marchetti, M.P., **2013**. Propagules, in: Lockwood, J.L., Hoopes, M.F., Marchetti, M.P. (Eds.), *Invasion ecology*. Blackwell publishing., United Kingdom, pp. 59-75.
- Lucchi, A., **1994**. The egg-burster of the flatid planthopper *Metcalfa pruinosa* (Say) (Homoptera, Fulgoroidea). *Proceedings: Entomological Society of Washington.* 96, 548-552.
- Lucchi, A., Mazzoni, E., **2004**, Wax production in adults of planthoppers (Homoptera: Fulgoroidea) with particular reference to *Metcalfa pruinosa* (Flatidae). *Ann. Entomol. Soc. Am.* 97, 1294-1298.
- Lucchi, A., L. Santini., **2001**. Aspetti fisiologici e morfofunzionali in *Metcalfa pruinosa* (Hom. Fulgoroidea) con riferimento agli effetti prodotti sulle produzioni agricole e sulle alberature ornamentali. *Atti Accad. Naz. Ital. Entomol. Rend. Anno.* 49, 131-147.
- Mead, F.W., **2004**. Citrus flatid planthopper, *Metcalfa pruinosa* (Say) (Insecta: Hemiptera: Flatidae). Original published as DPI Entomology Circular 85, 1-2, University of Florida, 1969.

- Mergenthaler, E., Fodor, J., Kiss, E., Bodnár, D., Kiss, B., Viczián, O., **2020**. Biological and molecular evidence for the transmission of aster yellows phytoplasma to French marigold (*Tagetes patula*) by the flatid planthopper *Metcalfa pruinosa*. *Ann. Appl. Biol.* 176, 249-256.
- Mesplé, F., Trousselier, M., Casellas, C., Legendre, P., **1996**. Evaluation of simple statistical criteria to qualify a simulation. *Ecol. Model.* 88, 9-18.
- Metcalf, Z.P., Bruner, S.C., **1948**. Cuban flatidae with new species from adjacent regions. *Ann. Entomol. Soc. Am.* 41, 63-118.
- Mikhajlovic, L., **2007**. *Metcalfa pruinosa* (Say) (Homoptera: Auchenorrhyncha) a new harmful species for entomo-fauna of Serbia, *Glasnik. Sumarskogo. Fakulteta.* 95, 127-134.
- Nematollahi, M.R., Fathipour, Y., Talebi, A.A., Karimzadeh, J., **2016**. Comparison of degree-day distribution models for predicting emergence of the cabbage aphid on canola. *Crop. Prot.* 80, 138-143.
- Ortega-Huerta, M.A., Peterson, A.T., **2008**. Modelling ecological niches and predicting geographic distributions: a test of six presence-only methods. *Rev. Mex. Biodivers.* 79, 205-216.

- Park, B., Kim, M.-J., Lee, S.-K., Kim, G.-H., **2019**. Analysis for dispersal and spatial pattern of *Metcalfa pruinosa* (Hemiptera: Flatidae) in southern sweet persimmon orchard. *Korean. J. Appl. Entomol.* 58, 291-297.
- Park, C.-G., Seo, B.Y., Lee, S.-K., Min, S.J., Lee, S.G., Jung, J.-K., Kim, J.R., **2016**. Development of the environment-friendly pest management techniques against an exotic citrus flatid planthopper, *Metcalfa pruinosa* and its basic ecological and physiological study. Research report of National institute of agricultural science and technology.
- Park, S.H., Woo, J.H., Kim, S.H., Choi, S.Y., **2013**. Reports of current occurrence for sporadic pests in Kyungbuk. Proceedings: *Fall meeting of Korea Society of Applied Entomology*. pp. 445.
- Pearson, R.G., **2010**. Species' distribution modelling for conservation educators and practitioners, in: Sterling, E., Bynam, N. (Eds.), *Lessons in conservation*. American museum of natural history., New York, pp. 54-89.
- Pénczes, B., Hári, K., **2016**. Az amerikai lepkekabóca (*Metcalfa pruinosa* Say). *Agrofórum*. 27, 56-60.
- Phillips, S.J., Anderson, R.P., Dudík, M., Schapire, R.E., Blair, M.E.,

- 2017.** Opening the black box: an open-source release of Maxent. *Ecography*. 40, 887-893.
- Phillips, S.J., Anderson, R.P., Schapire, R.E., **2006.** Maximum entropy modelling of species geographic distributions. *Ecol. Modell.* 190, 231-259.
- Phillips, S.J., Dudík, M., **2008.** Modelling of species distributions with Maxent: new extensions and a comprehensive evaluation. *Ecography*. 31, 161-175.
- Popova, L.V., Bondareva, L.M., Polozhenets, V.M., Nemeritskaya, L.V., **2019.** Formation of persistent population of invasive species *Metcalfa pruinosa* (Say, 1830) (Auchenorrhyncha: Flatidae) in the South of Ukraine. *Russ. J. Biol. Invasions*. 10, 48-51.
- Preda, C., Skolka, M., **2011.** Range expansion of *Metcalfa pruinosa* (Homoptera: Fulgoroidea) in southeastern Europe. *Ecol. Balk.* 3, 79-87.
- Ramirez-Villegas, J., Bueno-Cabrera, A., **2009.** Working with climate data and niche modelling: Creation of bioclimatic variables. International Center for Tropical Agriculture, Cali, Colombia.
- R Core Team. R: A language and environment for statistical computing. R Foundation for Statistical Computing, Vienna, Austria. Available

- online: <https://www.R-project.org/>.
- Rebek, E.J., Herms, D.A., Smitley, D.R., **2008**. Interspecific variation in resistance to emerald ash borer (Coleoptera: Buprestidae) among North American and Asian ash (*Fraxinus* spp.). *Environ. Entomol.* 37, 242-246.
- Reji, G., Chander, S., **2008**. A degree-day simulation model for the population dynamics of the rice bug, *Leptocorisa acuta* (Thunb.). *J. Appl. Entomol.* 132, 646-653.
- Rigamonti, I.E., Jermini, M., Fuog, D., Baumgärtner, J., **2011**. Toward an improved understanding of the dynamics of vineyard-infesting *Scaphoideus titanus* leafhopper populations for better timing of management activities. *Pest. Manag. Sci.* 67, 1222-1229.
- SAS Institute, **2011**. SAS/STAT user's guide, version 9.3. SAS Institute, Cary.
- Seo, B.Y., Jung, J.K., Park, C.-G., Lee, S.-G., Park, Y.-L., **2016**. Plant penetration activities by the flatid planthopper *Metcalfa pruinosa* (Hemiptera: Fulgoroidea): an electrical penetration graph-histology analysis. *J. Appl. Entomol.* 140, 706-714.
- Seo, H.-Y., Park, D.-K., Hwang, I.-S., Choi, Y.-S., **2019**. Host plants of *Metcalfa pruinosa* (Say) (Hemiptera: Flatidae) nymphs and adult.

- Korean. J. Appl. Entomol.* 58, 363-380.
- Shaffer, P.L., Gold, H.J., **1985**. A simulation model of population dynamics of the codling moth, *Cydia pomonella*. *Ecol. Model.* 30, 247–274.
- Shigesada, N., Kawasaki, K., **2002**. Invasion and the range expansion of species: effects of long-distance dispersal, in: Bullock, J., Kenward, R., Hails, R. (Eds.), *Dispersal ecology*. Blackwell publishing., United Kingdom, pp. 350-373.
- Souliotis, C., Papanikolaou, N.E., Papachristos, D., Fatouros, N., **2008**. Host plants of the planthopper *Metcalfa pruinosa* (Say) (Hemiptera: Flatidae) and observations on its phenology in Greece. *Hell. Plant. Protect. J.* 1, 39-41.
- Strauss, G., **2009**. Host range testing of the Nearctic beneficial parasitoid *Neodryinus typhlocybae*. *Biocontrol.* 54, 163-171.
- Strauss, G., **2010**. Pest risk analysis of *Metcalfa pruinosa* in Austria. *J. Pest. Sci.* 83, 381-390.
- Sutherst, R.W., Maywald, G.F., **1985**. A computerized system for matching climates in ecology. *Agric. Ecosyst. Environ.* 13, 281-299.
- Tobin, P. C., Liebhold, A. M., Roberts, E. A., **2007**. Comparison of

- methods for estimating the spread of a non-indigenous species. *J. Biogeogr.* 34, 305-312.
- Veloz, S.D., **2009**. Spatially autocorrelated sampling falsely inflates measures of accuracy for presence-only niche models. *J. Biogeogr.* 36, 2290-2299.
- Vétek, G., Korányi, D., Mezőfi, L., Bodor, J., Péntzes, B., Olmi, M., **2019**. *Neodryinus typhlocybae*, a biological control agent of *Metcalfa pruinosa*, spreading in Hungary and reaching Slovakia. *Bull. Insectol.* 72, 1-11.
- Virant-Doberlet, M., Žežlina, I., **2007**. Vibrational communication of *Metcalfa pruinosa* (Hemiptera: Fulgoroidea: Flatidae). *Ann. Entomol. Soc. Am.* 100, 73-82.
- Warren, D.L., Glor, R.E., Turelli, M., **2010**. ENMTools: a toolbox for comparative studies of environmental niche models. *Ecography.* 33, 607-611.
- Warren, D.L., Seifert, S.N., **2011**. Ecological niche modelling in Maxent: the importance of model complexity and the performance of model selection criteria. *Ecol. Appl.* 21, 335-342.
- Wilson, S.W., Lucchi, A., **2001**. Distribution and ecology of *Metcalfa pruinosa* and associated planthoppers in North America

- (Hemiptera: Fulgoroidea). *Atti. Accad. Naz. Ital. Entomol. Rend. Anno.* 49, 121-130.
- Wilson, S.W., McPherson, J.E., **1981**. Life histories of *Anormenis septentrionalis*; *Metcalfa pruinosa*; and *Ormenoides venusta* with descriptions of immature stages. *Ann. Entomol. Soc. Am.* 74, 299-311.
- Wilson, S.W., Lucchi, A., **2007**. Feeding activity of the feeding activity of the flatid planthopper *Metcalfa pruinosa* (Hemiptera: Fulgoroidea). *J. Kans. Entomol. Soc.* 80, 175-178.
- Yoon, Y.-W., Son, J.-Y., Ahn, G.-H., Choi, T.-M., Lee, H.-S., Park, D.-S., Hong, K.-P., **2012**. Seasonal occurrence of citrus flatid planthopper (*Metcalfa pruinosa*) in persimmon orchard. Research report of Gyeongnam agricultural research and extension services.
- Zangheri, S., Donadini, P., **1980**. Comparsa nel veneto di un omottero neartico: *Metcalfa pruinosa* Say (Homoptera; Flatidae). *Redia.* 63, 301-305.

Abstract in Korean

미국선녀벌레의 분포 및 분산 이동시기 모델링

서울대학교 대학원

농생명공학부

김민중

외래 매미충류인 미국선녀벌레 (노린재목: 선녀벌레과)는 2009년 국내에서 최초로 보고된 이후 다양한 식물에 피해를 주며 국내 전 지역으로 빠르게 정착 및 확산하였다. 따라서 국내에서 미국선녀벌레를 해충으로 관리해야 할 필요성이 증대되고 있다. 이 연구는 미국선녀벌레의 효율적 관리에 도움을 줄 수 있는 생태적 정보를 제공하고자 수행되었다. 연구의 목표는 (1) 국내에서 미국선녀벌레의 빠른 확산 원인을 규명하고, (2) 미국선녀벌레의 현재 잠재적 분포 및 미래 서식지 적합성을 예측하고, (3) 어린 미국선녀벌레 약충들의 계절 발생 및 이동 시기를 예측하고, (4) 마지막으로 작물 경작지로 유입되는 미국선녀벌레 약충들의 개체군 동태를 이해하는 것이다.

국내에서 미국선녀벌레의 빠른 확산과 관련하여, 인위적 요소 중 하나인 차량에 의한 확산 가능성과 이들의 잠재적 분포를 연구하였다. 확산

패턴 분석을 위해, 국내에서 미국선녀벌레의 시공간적 발생 정보들을 활용하여 이들의 확산 속도와 정착한 지역들 간의 군집 거리를 추정하였다. 또한 교통량 요소를 포함한 몇 가지 환경변수들을 이용하여 최대 엔트로피 방법(MaxEnt)으로 미국선녀벌레의 분포 모델들을 작성하고 비교하였다. 그 결과 국내에서 미국선녀벌레의 분포 확대는 초기 침입 집단의 점진적 확산이 아닌 정착한 개체군들의 장거리 운반에 의해 촉진되어왔음을 확인하였다. 2013년의 초기 확산 단계에서는 교통량 변수를 사용하였을 때 MaxEnt 모델이 미국선녀벌레의 분포를 더 잘 설명하였고, 가장 중요한 변수인 것으로 나타났다. 이 결과로부터 교통량 요소는 침입종의 징검다리 확산 메커니즘에서 이들의 장거리 확산을 가능케 하는 중요한 요소로 추정되었고, 미국선녀벌레의 확산을 촉진해왔을 것으로 예측되었다. 하지만 현재 침입 상태로 가정한 2017년 미국선녀벌레 분포 모델에서는 교통 요소의 기여도는 크게 감소하였고, 오히려 모델에서 제외하였을 때 분포를 더 잘 설명하였다. 따라서 미국선녀벌레의 현재 분포 모델은 교통량 변수를 제외한 가장 따뜻한 분기의 평균 온도, 가장 추운 분기의 평균 온도, 연간 강수량을 이용하여 작성되었다. 작성된 현재 분포 모델을 통해 미래 기후 시나리오(RCP 8.5)에 따른 서식지 적합성이 예측되었다. 그 결과 가까운 미래 (2030년대 및 2050년대)에는 산악지역과 남부지방을 제외한 국내 전역이 미국선녀벌레가 정착하기에 적합할 것으로 추정되었다.

유효적산온도에 따른 미국선녀벌레의 월동 알 부화 시기와 부화한 1령

약충이 월동 기주(나무)로부터 낙하하는 시간에 대한 분포 모델을 작성하였다. 모델 개발을 위해, 1월 1일과 관찰된 데이터를 통해 추정된 경험적 날짜인 3월 18일이 유효적산온도의 누적 시작일로 검토되었으며, 10.1 °C의 발육영점온도가 사용되었다. 월동 알 부화 모델과 1령 낙하 모델 모두 1월 1일의 적산온도 누적 시작일이 사용되었을 때 예측 성능이 더 우수하였다. 이 두 모델을 이용한 시뮬레이션을 통해, 나무 기주에서의 미국선녀벌레 약충을 대상으로 한 최적의 방제 시간은 423DD에서 474DD까지로 추정되었다. 또한 1령 낙하 모델과 나무 주변의 약충 밀도 자료를 통해, 월동처 주변 초본 식물에서의 미국선녀벌레 방제 및 예찰 시기가 제안되었다.

미국선녀벌레 약충이 작물 경작지로 유입되는 시간의 분포가 유효적산온도를 기반으로 예측되었다. 유효적산온도 계산에는 10.1 °C의 발육영점온도가 사용되었다. 또한 준 야외조건에서 미국선녀벌레 약충의 성충 우화까지 생존율이 조사되었으며, 야외에서 약충 및 성충의 트랩 포획 비율을 바탕으로 발육 단계 전이 모델을 개발하였다. 최종적으로 농경지 내에서 미국선녀벌레 약충의 개체군 시뮬레이션 모델은 (1) 작물을 재배하기 시작하는 시간, (2) 약충의 유입량, (3) 성충 우화까지 약충의 생존율, (4) 약충이 성충으로 우화한 비율을 이용하여 구축되었다. 구축한 시뮬레이션 모델과 실제 작물 재배지에서 밀도 변화는 다양한 작물 재배조건에서 비교적 잘 일치하였다. 205.5 DD 이후에는 작물이 재배되는 시작 시간이 경작지 내 약충 밀도를 결정하는 중요한 요소인 것으로 판단되었다. 하지만 유입 시작 시점이

지연된다 하더라도, 작물 재배지 내에서의 약충의 최대 밀도 시기는 유입 시작 시점의 차이만큼 지연되지 않았다. 800 DD 이후에는 경작지 내에서 우화한 성충들의 이탈로 인해 미국선녀벌레 밀도가 점점 감소할 것으로 예측되었다.

검색어: 미국선녀벌레, 서식 적합성, 징검다리 확산, 알 부화, 1령 낙하, 유입 위험, 개체군 시뮬레이션, 최적 방제 시기

학번: 2017-24294